# Bikini and Nearby Atolls

## Part 3. Geophysics

Seismic Studies of Bikini Atoll

Seismic-Refraction Studies of Bikini and Kwajalein Atolls and Sylvania Guyot

Magnetic Structure of Bikini Atoll

---

GEOLOGICAL SURVEY PROFESSIONAL PAPER 260-J, K, L

# Bikini and Nearby Atolls

## Part 3. Geophysics

### Seismic Studies of Bikini Atoll

*By* M. B. DOBRIN *and* BEAUREGARD PERKINS, Jr.

### Seismic Refraction Studies of Bikini and Kwajalein Atolls

*By* RUSSELL W. RAITT

### Magnetic Structure of Bikini Atoll

*By* L. R. ALLDREDGE, FRED KELLER, Jr., *and* W. J. DICHTEL

---

GEOLOGICAL SURVEY PROFESSIONAL PAPER 260-J, K, L


---

UNITED STATES GOVERNMENT PRINTING OFFICE, WASHINGTON : 1954

UNITED STATES DEPARTMENT OF THE INTERIOR

**Douglas McKay, *Secretary***

GEOLOGICAL SURVEY

**W. E. Wrather, *Director***

For sale by the Superintendent of Documents, U. S. Government Printing Office
Washington 25, D. C. - Price 45 cents (paper cover)

# CONTENTS

# Seismic Studies of Bikini Atoll

*By* M. B. DOBRIN *and* BEAUREGARD PERKINS, Jr.

## Bikini and Nearby Atolls, Marshall Islands

GEOLOGICAL SURVEY PROFESSIONAL PAPER 260-J


UNITED STATES GOVERNMENT PRINTING OFFICE, WASHINGTON : 1954

# CONTENTS



# ILLUSTRATIONS



# TABLE

# BIKINI AND NEARBY ATOLLS, MARSHALL ISLANDS

## SEISMIC STUDIES OF BIKINI ATOLL

By M. B. Dobrin and Beauregard Perkins


### ABSTRACT

During Operation Crossroads in July 1946 a seismic refraction survey of Bikini Atoll was made by Joint Task Force I to determine stratification of the subsurface and if possible the thickness of the calcareous sediments. One hundred twenty-six depth charges were exploded during the survey along 4 profiles extending across the lagoon. One year later a hole was drilled to 2,556 feet below sea level on Bikini island, and vertical velocities were measured from a depth of 1,800 feet to the surface.

The time-distance curves indicate the existence of a surface zone with a seismic velocity of 7,000 fps. Below this at a depth of about 2,500 feet lies a zone with a velocity of 11,000 fps. A third zone in which the seismic velocity is 17,000 fps ranges in depth from 7,000 to 13,000 feet below sea level. The vertical velocity measurements indicate that the velocity increases with depth from the surface velocity to 11,000 fps at about 2,000 feet. Thus the calcareous material at the surface extends down to two or three thousand feet and may extend to the top of the 17,000 fps zone. However, since Emery, Tracey, and Ladd have reported dredging basalt and pyroclastics at 1,000 and 1,150 fathoms, respectively, it is more likely that the base of surface calcareous sediments rests on pyroclastics of lower seismic velocity which in turn rest on the 17,000 fps zone. This last zone is believed to be igneous rock.

These findings would indicate a minimum subsidence of about 3,000 feet and a maximum of about 13,000 feet.


### INTRODUCTION

In the summer of 1946, during the tests of the A-bomb, while the geologic and oceanographic data were being gathered at Bikini Atoll, seismic surveys were undertaken to determine the stratification and if possible, the thickness of the calcareous sediments which lay beneath the lagoon. A reconnaissance refraction survey was conducted by the Oceanographic Section of Joint Task Force 1 and the Low Frequency Group of the Naval Ordnance Laboratory (Dobrin and others, 1949). A reflection survey was attempted by another group at the same time, but it was unsuccessful. In the summer of 1947 an expedition was sent to Bikini Atoll to study the after effects of the explosion of the A-bombs. Advantage was taken of this opportunity to drill several holes on Bikini island in one of which vertical velocities were measured to a depth of 1,800 feet. The measurements were made by Joseph Chernock of the Geotechnical Corp. In the summer of 1950 geological studies and seismic refraction studies were made by Roger R. Revelle and Russell Raitt in an expedition sponsored by the Office of Naval Research and Scripps Institution of Oceanography. The results of these studies are reported elsewhere in this volume (chap. K).

### VERTICAL VELOCITIES

Since the vertical velocities from the hole on Bikini island have influenced the interpretation of the survey data they will be discussed first. The hole (No. 2*B* in figure 123) was drilled to a depth of 2,556 feet on the lagoon side of Bikini island. In measuring the velocity a geophone was placed in hole 2*B* at intervals varying from 50 to 300 feet between the depths of 1,820 feet and 150 feet below the surface. Charges were exploded in the shallow hole (No. 2*A*), 178 feet to the west of the deep hole. A total of 74 charges were fired, of which 47 produced usable records. (See table 1.) The depth of the shots varied from 35 feet to 16 feet. Each charge

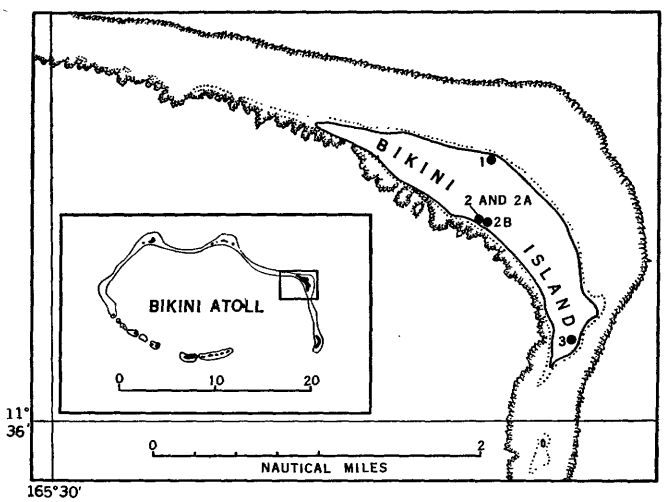


FIGURE 123.—Bikini island showing location of drill holes. Hole 2B was drilled to 2,556 feet. The others ranged from 150 to 300 feet in depth.

| Shot No. | Dg | Ds | Dgd | $\tan_i$ | T | $\cos_i$ | Tgd | Dgd Avg | Tgd Avg | Va (fps) | Dgd | Tgd | $V_i$ (fps) |
|---|---|---|---|---|---|---|---|---|---|---|---|---|---|
| 73 | 150' | 16' | 126' | 1.4126 | .032 | .5779 | .0185 | | | | | | |
| 74 | 150' | 17' | 125' | 1.4240 | .034 | .5748 | .0195 | 126' | .0190 | 6630' | 48' | .0076 | 6320' |
| 69 | 200' | 18' | 174' | 1.0229 | .037 | .6990 | .0259 | | | | | | |
| 70 | 200' | 18' | 174' | 1.0229 | .039 | .6990 | .0273 | 174' | .0266 | 6540' | 101' | .0133 | 7590' |
| 71 | 300' | 17' | 275' | .6472 | .049 | .8395 | .0411 | | | | | | |
| 72 | 300' | 17' | 275' | .6472 | .046 | .8395 | .0386 | 275' | .0399 | 6890' | 99' | .0098 | 10,100' |
| 59 | 400' | 18' | 374' | .4759 | .055 | .9030 | .0497 | | | | | | |
| 60 | 400' | 18' | 374' | .4759 | .055 | .9030 | .0497 | 374' | .0497 | 7520' | 49' | .0042 | 11,670' |
| 61 | 400' | 18' | 374' | .4759 | .055 | .9030 | .0497 | | | | | | |
| 57 | 450' | 20' | 422' | .4218 | .059 | .9214 | .0544 | | | | | | |
| 58 | 450' | 19' | 423' | .4208 | .058 | .9218 | .0535 | 423' | .0539 | 7850' | 49' | .0069 | 7100' |
| 55 | 500' | 20' | 472' | .3771 | .065 | .9357 | .0608 | | | | | | |
| 56 | 500' | 20' | 472' | .3771 | .065 | .9357 | .0608 | 472' | .0608 | 7760' | 50' | .0055 | 9090' |
| 53 | 550' | 21' | 521' | .3416 | .070 | .9463 | .0662 | | | | | | |
| 54 | 550' | 20' | 522' | .3409 | .070 | .9465 | .0663 | 522' | .0663 | 7870' | 48' | .0063 | 7620' |
| 50 | 600' | 25' | 567' | .3139 | .075 | .9541 | .0716 | | | | | | |
| 51 | 600' | 21' | 571' | .3117 | .077 | .9547 | .0735 | 570' | .0726 | 7850' | 47' | .0033 | 14,240' |
| 52 | 600' | 21' | 571' | .3117 | .076 | .9547 | .0726 | | | | | | |
| 47 | 650' | 25' | 617' | .2884 | .079 | .9609 | .0759 | | | | | | |
| 48 | 650' | 25' | 617' | .2884 | .079 | .9609 | .0759 | 617' | .0759 | 8130' | 48' | .0065 | 7380' |
| 49 | 650' | 25' | 617' | .2884 | .079 | .9609 | .0759 | | | | | | |
| 44 | 700' | 29' | 663' | .2684 | .086 | .9658 | .0831 | | | | | | |
| 45 | 700' | 29' | 663' | .2684 | .086 | .9658 | .0831 | 665' | .0824 | 8070' | 46' | .0044 | 10,450' |
| 46 | 700' | 25' | 667' | .2668 | .085 | .9662 | .0821 | | | | | | |
| 42 | 750' | 32' | 710' | .2507 | .089 | .9699 | .0863 | | | | | | |
| 43 | 750' | 30' | 712' | .2500 | .090 | .9702 | .0873 | 711' | .0868 | 8190' | 48' | .0048 | 10,000' |
| 41 | 800' | 32' | 760' | .2342 | .093 | .9737 | .0906 | | | | | | |
| 39 | 800' | 34' | 758' | .2348 | .095 | .9735 | .0925 | 759' | .0916 | 8290' | 114' | .0178 | 6400' |
| 36 | 900' | 20' | 872' | .2041 | .110 | .9798 | .1078 | | | | | | |
| 37 | 900' | 19' | 873' | .2038 | .112 | .9799 | .1097 | 873' | .1094 | 7980' | 197' | .0223 | 8430' |
| 38 | 900' | 19' | 873' | .2038 | .113 | .9799 | .1107 | | | | | | |
| 33 | 1100' | 23' | 1069' | .1665 | .133 | .9864 | .1312 | | | | | | |
| 34 | 1100' | 22' | 1070' | .1663 | .134 | .9864 | .1322 | 1070' | .1317 | 8130' | 296' | .0408 | 7250' |
| 27 | 1400' | 26' | 1366' | .1303 | .174 | .9916 | .1725 | | | | | | |
| 28 | 1400' | 26' | 1366' | .1303 | .175 | .9916 | .1735 | | | | | | |
| 29 | 1400' | 26' | 1366' | .1303 | .174 | .9916 | .1725 | 1366' | .1725 | 7920' | | | |
| 30 | 1400' | 26' | 1366' | .1303 | .174 | .9916 | .1725 | | | | 198' | .0218 | 9080' |
| 32 | 1400' | 26' | 1366' | .1303 | .173 | .9916 | .1715 | | | | | | |
| 25 | 1600' | 28' | 1564' | .1138 | .195 | .9936 | .1938 | | | | | | |
| 24 | 1600' | 28' | 1564' | .1138 | .196 | .9936 | .1947 | 1564' | .1943 | 8050' | | | |
| 7 | 1800' | 20' | 1772' | .1004 | .216 | .9950 | .2149 | | | | | | |
| 10 | 1800' | 20' | 1772' | .1004 | .215 | .9950 | .2139 | | | | | | |
| 11 | 1800' | 20' | 1772' | .1004 | .214 | .9950 | .2129 | 1768' | .2143 | 8250' | 204' | .0200 | 10,200' |
| 12 | 1800' | 34' | 1758' | .1012 | .215 | .9949 | .2139 | | | | | | |
| 14 | 1800' | 35' | 1757' | .1013 | .218 | .9949 | .2169 | | | | | | |
| 15 | 1800' | 35' | 1757' | .1013 | .216 | .9949 | .2149 | | | | | | |
| 1 | 1820' | 25' | 1787' | .0996 | .214 | .9951 | .2130 | | | | | | |

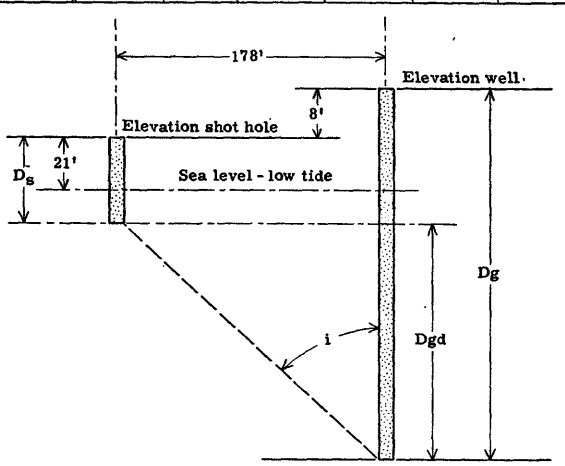


Data by
The Geotechnical Corp.

Dg = Geophone depth measured from well elevation

$D_s$ = Depth of shot

$D_{gd}$ = Geophone measured from shot depth.

$T_{gd}$ = Vertical travel time from shot depth to geophone.

T = Observed time from shotpoint to geophone.

$V_a$ = Average velocity from shot depth to geophone depth.

$V_i$ = Interval velocity.

i = Angle between seismic ray and vertical.

TABLE 1.—Vertical-velocity computations. The travel time for a pulse generated by an explosion at the surface to a geophone located at various depths in the hole was measured. The difference in times to the various depths permits the interval velocity to be determined.

consisted of one-eighth pound of 60 percent gelatin. The charges were tamped with sea water.

In positioning the detector, an attempt was made to choose points near the top and the bottom of the various cemented layers which had been logged during the drilling of the hole. If successful this would permit the determination of the velocities in the cemented material separately from those of the unconsolidated sediments.

The velocities are presented in table 1 and are shown graphically in figure 126. In the first 1,000 feet below the surface the velocity was found to vary widely from approximately 6,000 fps in the unconsolidated material to about 14,000 fps in the well-cemented layers. From a depth of 1,000 feet to 1,800 feet, the velocity increased steadily from about 7,000 fps to 10,000 fps. The average vertical velocity through the first 1,800 feet was approximately 8,000 fps.

The seismic-refraction survey indicates only the horizontal seismic velocities in the subsurface and those discontinuities where the velocity is greater than in any overlying strata. Thus, decreases in velocity are completely obscured, and a gradual increase in velocity could be marked by a high-speed zone at the base of the section in which the increase takes place.

## PLAN AND PROCEDURE OF THE REFRACTION SURVEY

The principles of seismic refraction surveying have been discussed briefly in Dobrin and others (1949) and in more detail in textbooks on geophysical prospecting (see Nettleton, 1940; Heiland, 1940; or Dobrin, 1952).

The seismic survey in 1946 was a reconnaissance. It consisted of four profiles as shown in figure 124. These profiles are designated by the names of the islands at each end of the various profiles. All shots were fired

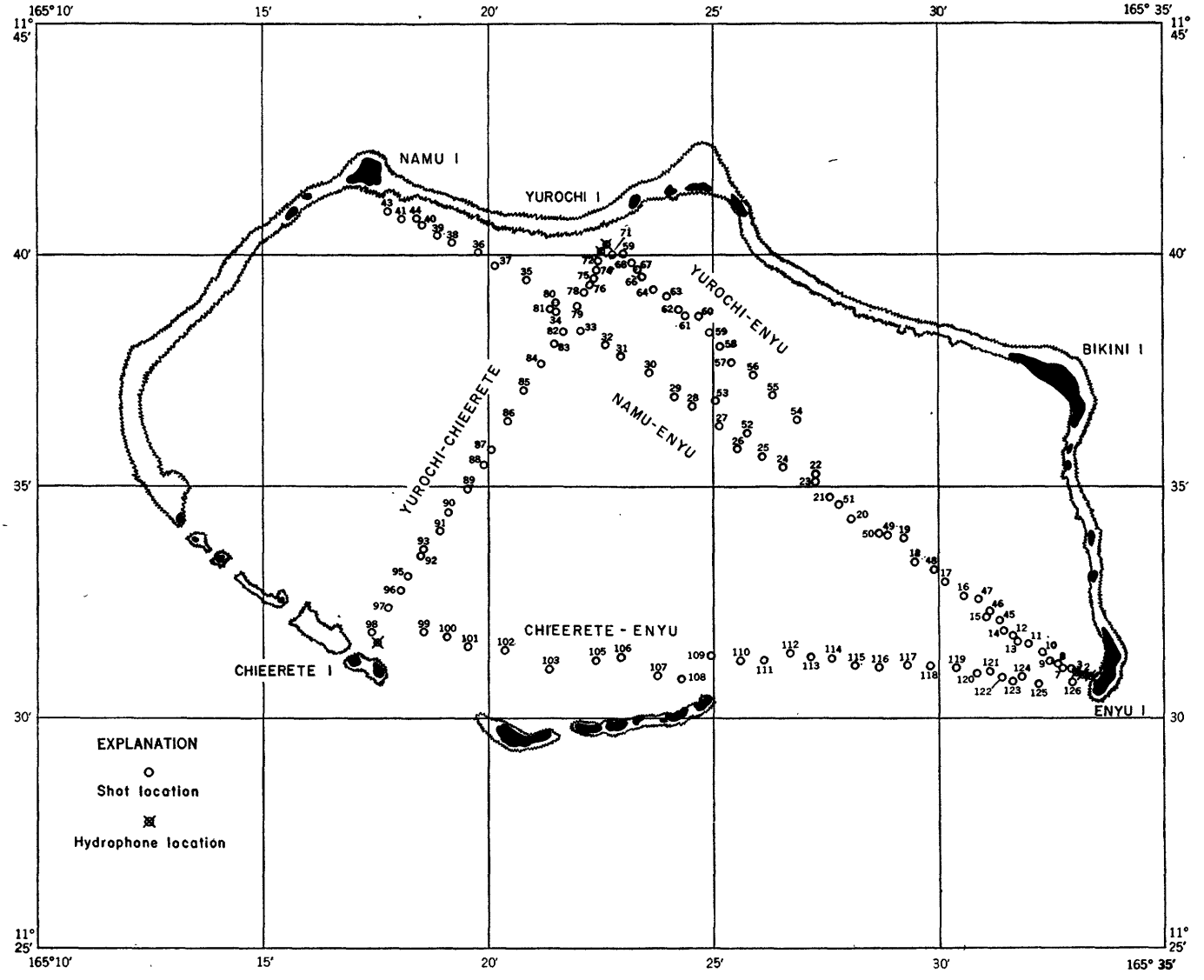


FIGURE 124.—Bikini Atoll showing profiles. Hydrophones were resting on the bottom off Enyu island, Yurochi island, and Chieerete island.

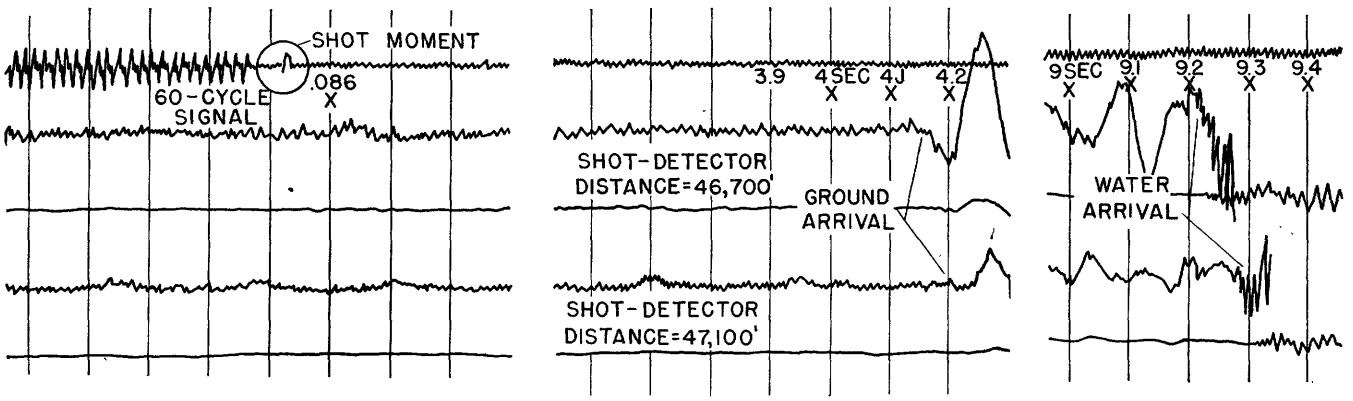


RECORD OF SHOT 92 MADE BY SHELL
OSCILLOGRAPH ON USS GILLIS ANCHORED OFF YUROCHI ISLAND

The two high-sensitivity traces appear to break shortly after the water-wave arrivals. The water waves on the record were weak and were intensified by pencil as far as they could be followed

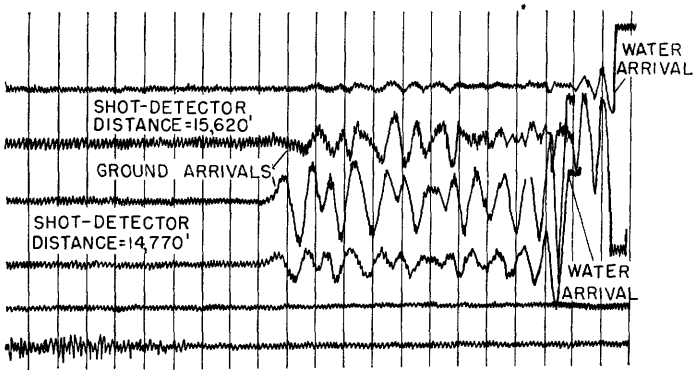


RECORD OF SHOT 120 MADE BY
HATHAWAY OSCILLOGRAPH ON ENYU ISLAND
(Time break not shown)

FIGURE 125.—Sample records. Typical recordings of pulses which had been transmitted through the ground (ground arrival) and of those which were transmitted directly through the water (water arrival). The shot moment indicates zero time or the time explosive was fired.

on the bottom of the lagoon in water 100 to 180 feet deep, on lines between two receiving stations. One receiving station (at Enyu island) was stationary. The hydrophones were on the lagoon bottom in about 40 feet of water with cables connecting them to the recording systems on the island about 1 mile distant. A second station was established aboard the U. S. S. *Gilliss* which anchored first off the island of Yurochi to record the Enyu-Yurochi and the Yurochi-Chieerete profiles and which later anchored off Chieerete to record a portion of the shots on the Chieerete-Enyu profile. At both locations hydrophones were lowered to the lagoon bottom and connected by cable to the recording equipment aboard the ship. The shot-detector distances ranged from 2,000 to 98,000 feet.

The hydrophones and the associated recording systems responded both to the low-frequency pressure changes induced in the water by ground waves as well as to the higher frequencies transmitted directly through the water from the explosion. The pressure variations were recorded photographically by a Hathaway oscillograph at the Enyu station and by a Shell Oil Co. oscillograph on the U. S. S. *Gilliss*.

The seismic pulses were generated by detonating standard depth charges. The Mark 10 depth charges (25 pounds) were used when within about 4,000 feet of any of the geophones. The Mark 6 charges (300 pounds) were used for the more distant shots. The charges were lowered to the bottom from a small ship which would then back off approximately 1,000 feet. The charge was fired by means of a demolition cable and an electric detonator which had been inserted in place of the usual hydrostatic firing device. A special radio time-break transmitter permitted the accurate recording of the shot moment on the oscillograph records.

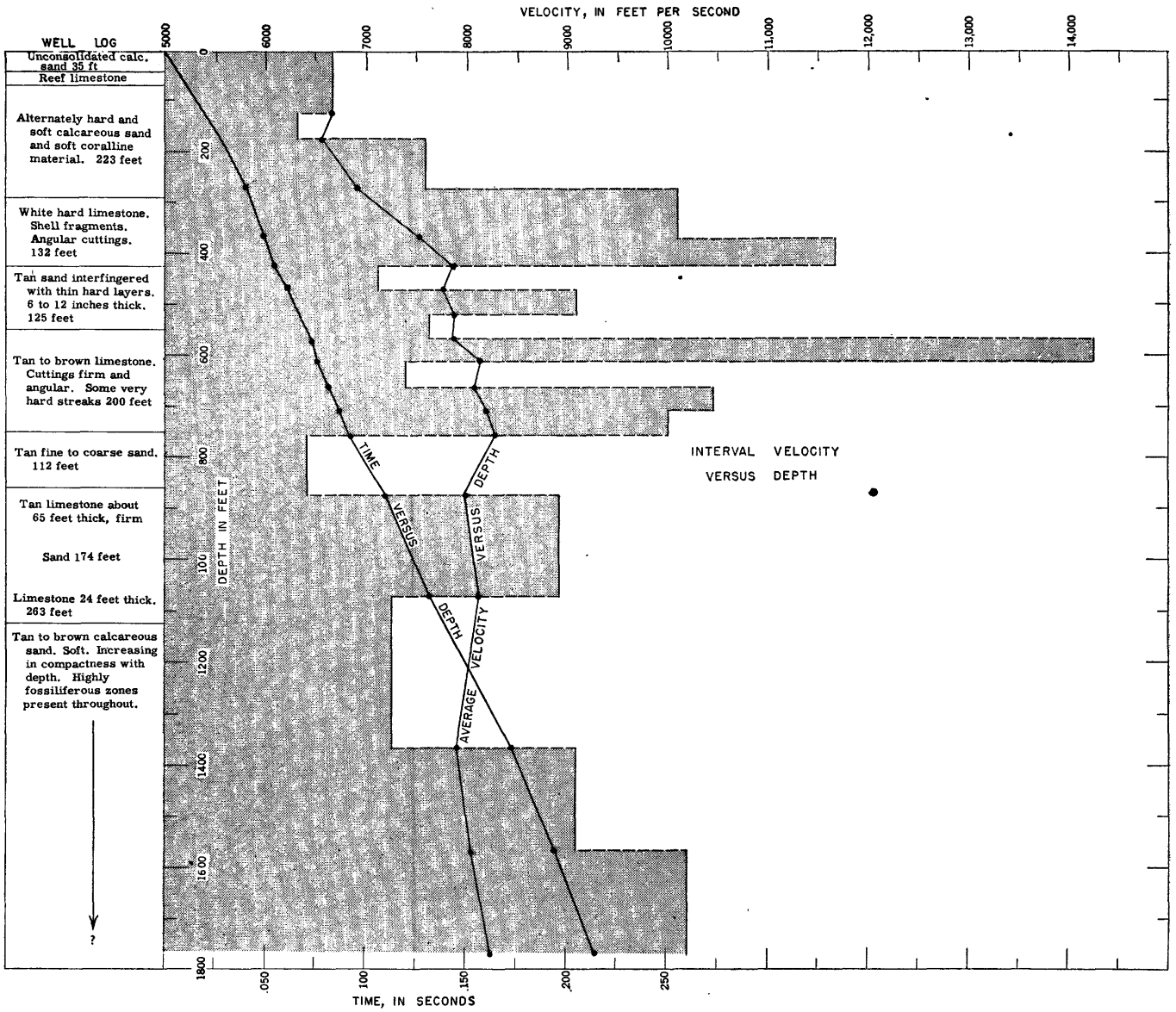


FIGURE 126.—Graphic chart of vertical velocities from surface to a depth of 1,800 feet. The relation of the velocity to compaction and cementation is shown by the table of geologic formations derived from the cores.

The sample records (fig. 125) show the shot-moment signal and the ground-wave and water-wave arrivals. The output of each detector was recorded through two channels: one of high sensitivity, the other of low sensitivity. This assured both sharper time breaks and clearer records showing details of the recorded wave motions. The water-wave arrival time could usually be read to within 0.001 second. The ground wave that had traveled a short distance could be timed to within 0.002 second, while the more distant shots, because of the more gradual break, could not be timed to better than within 0.010 second.

The hydrophones from the U. S. S. *Gilliss* were separated by a few hundred feet while those from the land station at Enyu island were 1,000 feet apart. All these phones responded to frequencies from 1 to 200 cycles per second. At the Enyu station in addition there was for most of the shots a sonic frequency hydrophone responsive to frequencies from 50 to 10,000 cycles per second. This was useful in locating the water-wave arrivals from the more distant shots.

The hydrophone and shot locations were determined by means of sextant bearings on beacons and buoys and tangents to islands. Precise locations were not necessary since the distance from shot to hydrophone was determined from the travel time of the sound wave through the water from the explosion to the phone. The temperature and salinity of the lagoon water had been determined by the oceanographers of the Operation Crossroads expedition at many stations preceding and

during the seismic survey. Using the average values of temperature 83°±0.5° F. and of salinity 34.45 ±0.35 °/₀₀ the theoretical speed of sound is 5,047 fps according to tables by Kuwahara (1939). The speed of sound was determined experimentally along the eastern portion of the profile from Namu to Enyu (fig. 124). Here the shot and hydrophone locations had been ascertained accurately by the many beacons whose coordinates were known to within a few feet. The measured speed was 4,980 fps. The discrepancy between these values may indicate that Kuwahara's tables do not apply to shallow water or that the tables are not correct; however, there is the possibility that the tuning fork used for timing may have been fast, so that the measured speed should not be considered definitive. In computing the distances, a sound velocity of 5,000 fps was assumed. This is within 1 percent of either of the above values and will introduce an error of less than 1 percent in the calculated seismic velocities or in the depth of the observed velocity discontinuities.

### SEQUENCE OF SHOTS

Of the four profiles across the lagoon the profile from Namu to Enyu was shot prior to the first A-bomb test. Shots out to 98,000 feet from Enyu island were recorded by the Enyu station. The shots fired in the northwest end of the profile within 40,000 feet of Namu island were recorded by geophones (on the island) operated by engineers of the Geotechnical Corp.

The three remaining profiles were shot in the period between the two A-bomb tests. The profile from Enyu to Yurochi was recorded by the Enyu station and by the U. S. S. *Gilliss* anchored off Yurochi island. The eastern two-thirds of this profile could not be shot owing to the presence of target vessels and personnel working in the water preparing for the next bomb test.

The Yurochi-Chieerete shots were recorded by the U. S. S. *Gilliss* at Chieerete island and by the Enyu hydrophones. The profile from Chieerete to Enyu was started while the *Gilliss* was moving from Yurochi to a point off Chieerete island. All the shots of this profile were recorded by the Enyu station but only the shots in the eastern half (shots 111 to 126) were recorded by the hydrophones of the U. S. S. *Gilliss*.

## RESULTS

### DETERMINATION OF VELOCITIES

The time-distance curves (figs. 127 to 130) show the arrival times of the ground waves plotted against the corresponding shot-detector distances on the four profiles. The reciprocal of the slope of these lines at any point indicates the velocity at which the ground wave is travelling in the lower portion of its path. The points on the various curves thus appear to indicate three zones of different velocities in the first few miles below the lagoon floor. The velocities indicated are 7,000, 11,000 and 17,000 fps. The first of these velocities is very consistent over all four profiles, the deviation not exceeding 200 fps. However a study of the well log would indicate that the velocity in the first zone increases gradually from a little over 6,000 fps at the surface to 10,000 fps at about 1,800 feet. It is therefore reasonable to expect the velocity of the near-surface material to continue to increase with compression of greater depth to the velocity of 11,000 fps shown in the time-distance curves. The 7,000 fps horizontal velocity can be accounted for as the average velocity of the near-surface material since the hard high-velocity material is in layers too thin to transmit much energy.

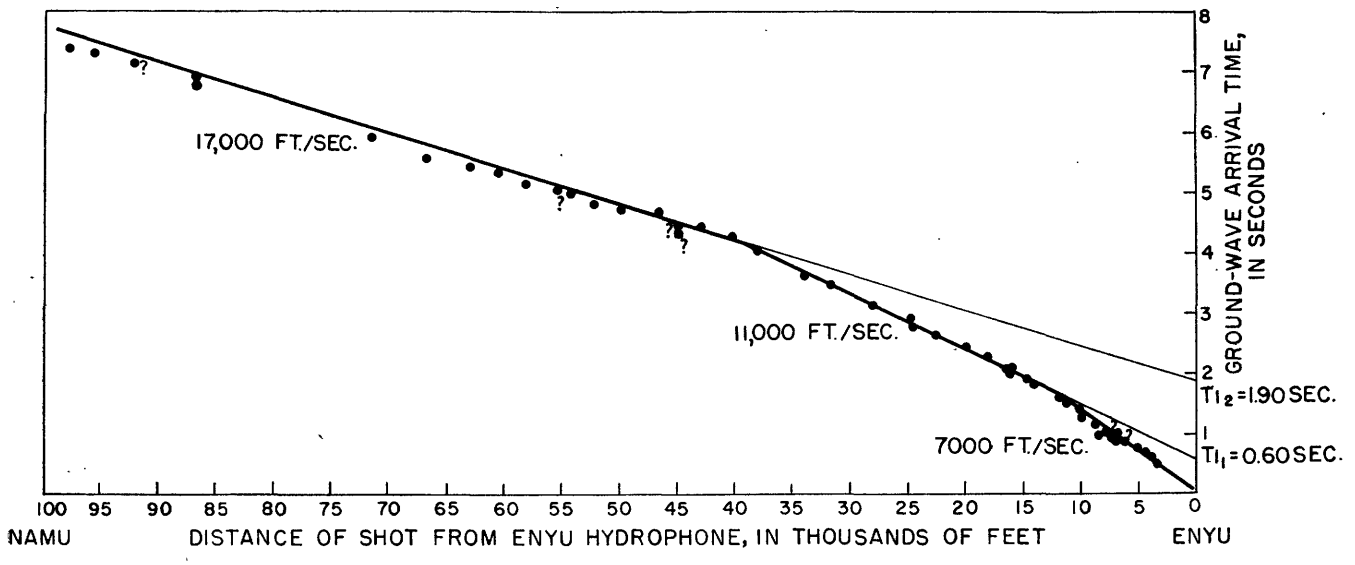


FIGURE 127.—Time-distance curve for Enyu-Namu profile. Hydrophones off Enyu island.

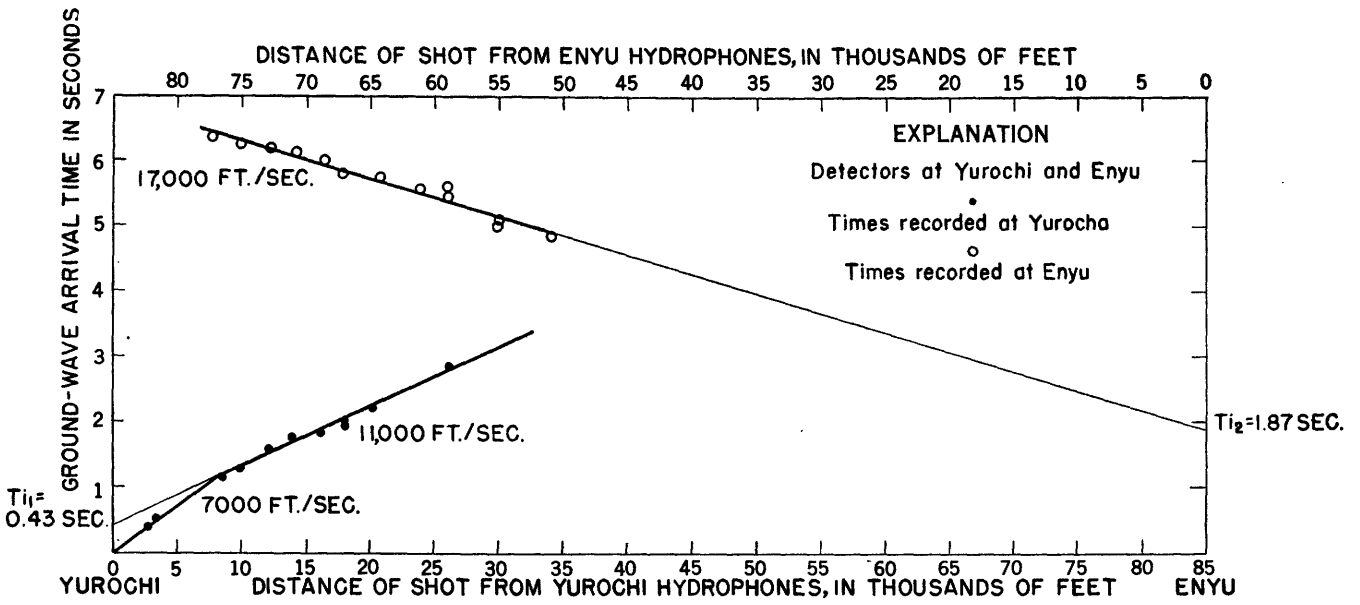


FIGURE 128.—Time-distance curves for Enyu-Yurochi profile. Hydrophones off Enyu and Yurochi islands. No shooting was permitted along east part of profile because of target vessels.

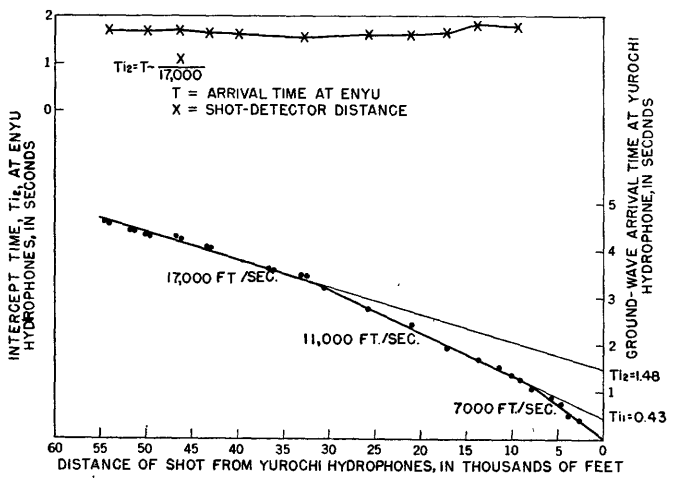


FIGURE 129.—Time-distance curves for Yurochi-Chieerete profile. Hydrophones off Enyu and Yurochi islands. At top is plotted intercept times for arrivals at Enyu from shots along the profile.

The 11,000 fps may represent the velocity of maximum compression. The velocity of 11,000 fps was consistent throughout the profiles except for a portion of the profile from Enyu to Chieerete near the southeastern edge of the lagoon where it changes to 9,000 fps (fig. 130). This anomaly will be discussed later. The apparent velocity indicated by the third segment of the curves ranges from 16,500 to 18,500 fps but reverse control in the profile from Enyu to Chieerete and the distant shots on the Enyu-Yurochi and the profiles from Yurochi to Chieerete indicate a true velocity of 17,000 fps. This value has been used in the calculations of the depth of the third layer. Most of the shots fired along the Yurochi-Chieerete profile were also received by the Enyu hydrophones through paths which were approximately at right angles to the profile. The variations in depth of the third layer are indicated by the intercept times, as observed for the respective shots at Enyu, which are plotted on the upper portion of figure 129.

The apparent decrease in slope at the west end of the Enyu-Chieerete time-distance curve suggested the possibility of a fourth and higher velocity zone below the 17,000 fps, layer. Such a zone, with its apparent velocity of 25,000 fps, would have a depth of 25,000 feet. It was decided, however, that the bend in the curve could more reasonably be explained as a rise to the west, since the difference between intercept times observed at the two ends of the profile from Enyu to Chieerete indicated that the western end of the third zone was higher than the eastern end.

## DETERMINATION OF DEPTHS AND THICKNESSES OF LAYERS

To compute the depths of the various beds a method was employed which was based on one described by Jones (1934) and Gardner (1939). Three of the four profiles form a triangle at the vertices of which were detectors receiving impulses from shots fired along each of the adjacent sides. These stations, as indicated previously, were at Enyu (*E*), Yurochi (*Y*) and Chieerete (*C*) islands. The intercept times are composed of two delay times corresponding, respectively, to the shot and detector ends of the least-time trajectory for each shot. Since the stations at the vertices are common to two trajectories, equations can be set up, for the arrivals from the 17,000 fps marker, that permit

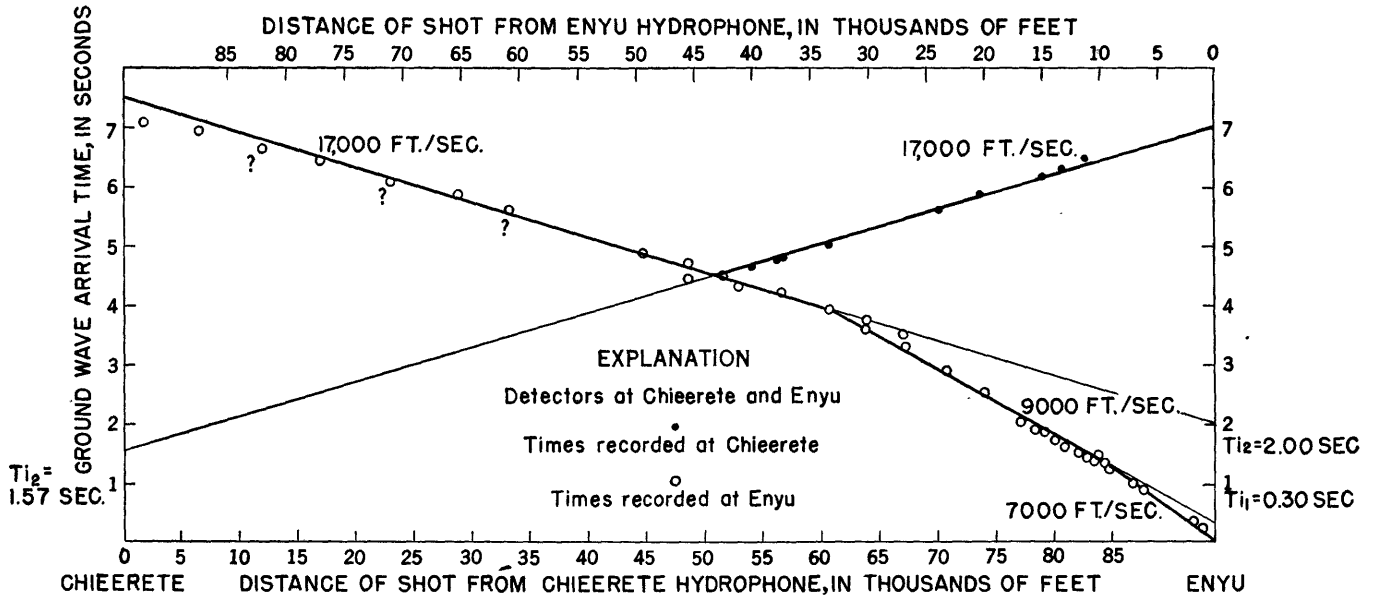


FIGURE 130.—Time-distance curves for Chieerete-Enyu profile. Detectors off Chieerete and Enyu islands. Note anomalous arrival times recorded at Enyu from shots 20,000 to 35,000 feet away.

solving for the separate delay times. Let $T_E$, $T_C$, and $T_Y$ be the delay times at the respective vertices and $T_{iEC}$ be the intercept time for a shot fired at $E$ and received at $C$; similarly, let $T_{iCY}$ and $T_{iEY}$ be the intercept times for shots fired at $C$ and $E$, respectively, and received at $Y$. Then

$$T_E+T_C=T_{iEC}=1.64,$$

$$T_C+T_Y=T_{iCY}=1.46,$$

$$T_E+T_Y=T_{iEY}=1.90,$$

the numerical values being obtained from the time-distance curves. Solving, we obtain

$$T_E=1.04$$

$$T_C=0.60$$

$$T_Y=0.86.$$

Since on the profile from Enyu to Chieerete, arrivals were received from the 17,000 fps marker on both stations for some of the shots, the delay times can be calculated. Thus, for shot at Station 114 we have

$$T_E+T_{114}=T_{iE114}=2.00$$

$$T_C+T_{114}=T_{iC114}=1.54$$

$$T_C+T_E=T_{iCE}=1.64.$$

Solving these, we have $T_E=1.06$ sec. and $T_C=0.58$ sec., which are in good agreement with the preceding values.

The delay times at each shot position in which the arrivals traversed the deeper interface can now be ascertained by subtracting the computed delay times at the receiver from the intercept time for the particular shot.

Since arrivals from the 11,000 fps zone were not received at two of the receiving stations from any one shot position, it was not possible to determine the delay times under the shots. These times were approximated by halving the average intercept time for each line. For the delay times under the Enyu receivers intercept times were available from the profile from Enyu to Namu profile and the profile from Enyu to Chieerete. The average value calculated from these is 0.26 second. At the Yurochi station, also, two profiles converged, each having an intercept time of 0.44 second, which gave a delay time of 0.22 second for that station. At the Chiereete station no arrivals from the 11,000 fps horizon were received, so the delay time could not be computed, but was assumed to be 0.25 second.

The thickness of the layers was computed by the following formulae:

$$Z_0=T_{d1}[V_1V_0/(V_1^2-V_0^2)^{1/2}]$$

and

$$Z_1=[T_{d2}-Z_0(V_2^2-V_0^2)^{1/2}/V_0V_2][V_1V_2/(V_2^2-V_1^2)^{1/2}].$$

The total depth to the second interface is

$$Z=Z_0+Z_1.$$

In the above $T_{d1}$ is the delay time associated with the depth $Z_0$ to the first interface below some point on any of the profiles where arrivals were received after refraction along the first interface. Similarly, $T_{d2}$ is the delay

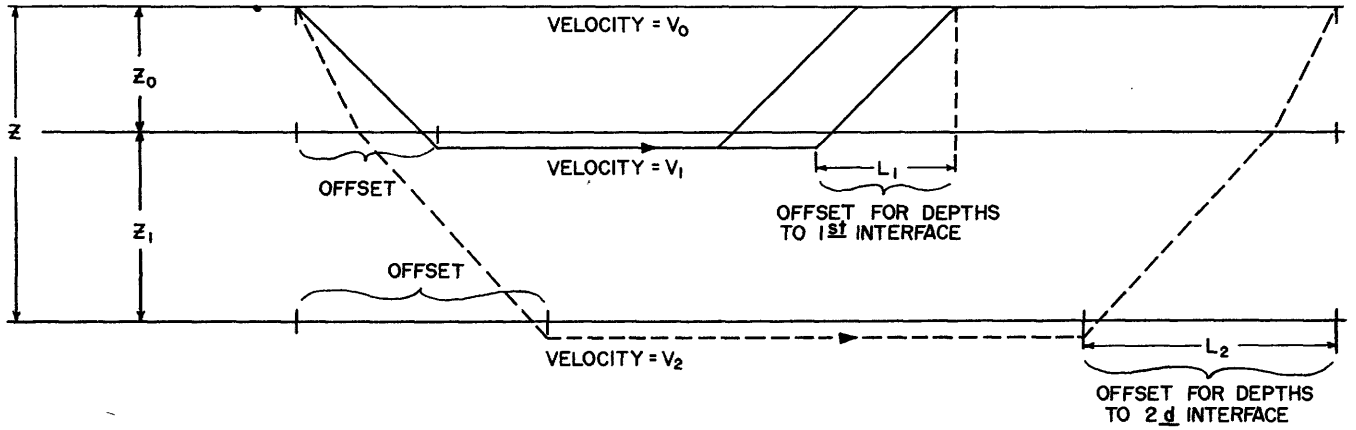


FIGURE 131.—Geometry of wave paths from shot to detectors. The elastic pulses leaving the shot may travel horizontally to the detectors at velocity $V_0$ or may travel downward and be refracted horizontally thru the second or third zone and travel at a velocity of $V_1$ or $V_2$, respectively. $V_0<V_1<V_2$.

time associated with the depth $Z$ to the second interface below some point on any of the profiles where arrivals were received after refraction along the second interface. The meaning of the other symbols are illustrated in figure 131, which shows the geometry of the wave paths from the shot to the detectors.

The depths calculated were actually the depths at the offset position in each case. The offset distances for the two interfaces are indicated in figure 131 and are calculated from the following formulae; for the first interface

$$L_1=Z_0V_0/(V_1^2-V_0^2)^{1/2},$$

and for the second interface

$$L_2=Z_0V_0/(V_2^2-V_0^2)^{1/2}+Z_1V_1/(V_1^2-V_0^2)^{1/2}.$$

Substituting numerical values for the velocities, the formulae for the depths and offsets reduce to

$$Z_0=9080\ T_{d1}$$

$$Z_1=14{,}400\ T_{d2}-17{,}200\ T_{d1}$$

$$L_1=0.83\ Z_0$$

$$L_2=0.45\ Z_0+0.85\ Z_1.$$

In using the above formulae to compute the thickness of $Z_1$ of the second layer beneath any surface location, one must know the thickness $Z_0$ of the uppermost layer at the same location. With the type of shooting done here there will be no arrivals from the first interface along the portions of the profile where there are arrivals from the second one. That is, the thickness $Z_0$ cannot be calculated for the locations where there are arrivals from the second interface, and it therefore must be assumed. This assumption will probably be responsible for some error.

A more serious source of error lies in the incomplete control over the velocity of any given layer within the area of the survey. Any local variation of speed along the wave trajectory would effect the apparent depth. With reverse control on the 17,000 fps bed available along only a limited portion of a single profile and with numerous gaps even in the one way control, there is no assurance that such variations do not occur.

Because of these uncertainties, as well as those inherent in the seismic refraction technique even under optimum conditions of control (Nettleton, 1940, p. 255), the depths indicated in the cross section and contours given below are not exact but represent what is thought to be the most reasonable of several possible ways in which one can account for the observed time data. The depths to the upper interface are probably reliable to the nearest 200 feet (except along the anomalous zone of the profie from Enyu to Chieerete), whereas those to the lower interface may be in error by 1,000 to 1,500 feet. These uncertainties are not sufficient to affect the fundamental conclusions one can draw from the results regarding the internal constitution and geological history of the atoll.

Figures 132 and 133 show vertical cross sections of the subsurface below the four shooting profiles and also along a synthetic profile *A–B* which extends almost directly south from Romuk island (fig. 134). The last profile was chosen mainly as a mode of representing the depth data afforded by two shots (107 and 108), displaced somewhat southward from the line from Enyu to Chieerete, which indicate a sharp falling off in the depth to the 17,000 fps zone as the edge of the reef is approached.

It is observed from the sections that the depth to the first interface averages about 2,500 feet, whereas that to the second is in the neighborhood of 10,000 feet.

The top surface of the 17,000 fps zone is characterized (fig. 134) by a prominent nose plunging to the southeast through the center of the atoll. The highest observed portion of this surface is under the south-

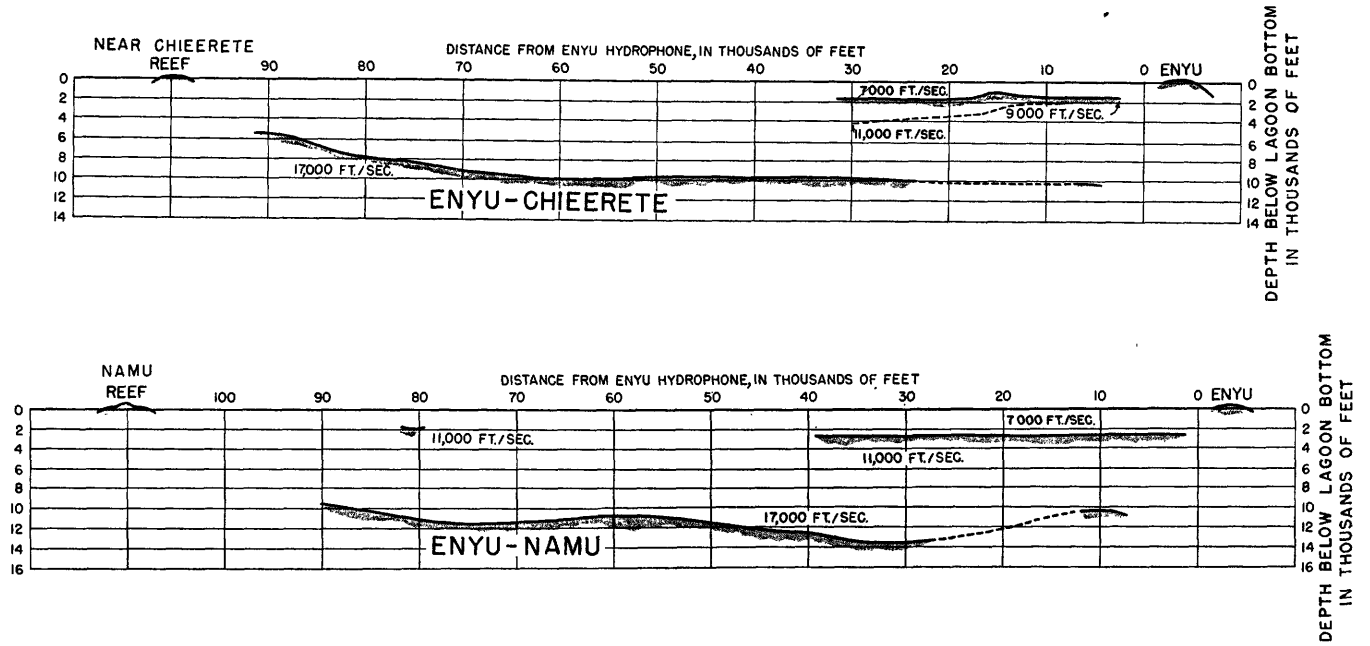


FIGURE 132.—Cross sections showing subsurface structure indicated by seismic data along Enyu-Chieerete and Enyu-Namu profiles. Interfaces are between the media having seismic velocities as indicated.

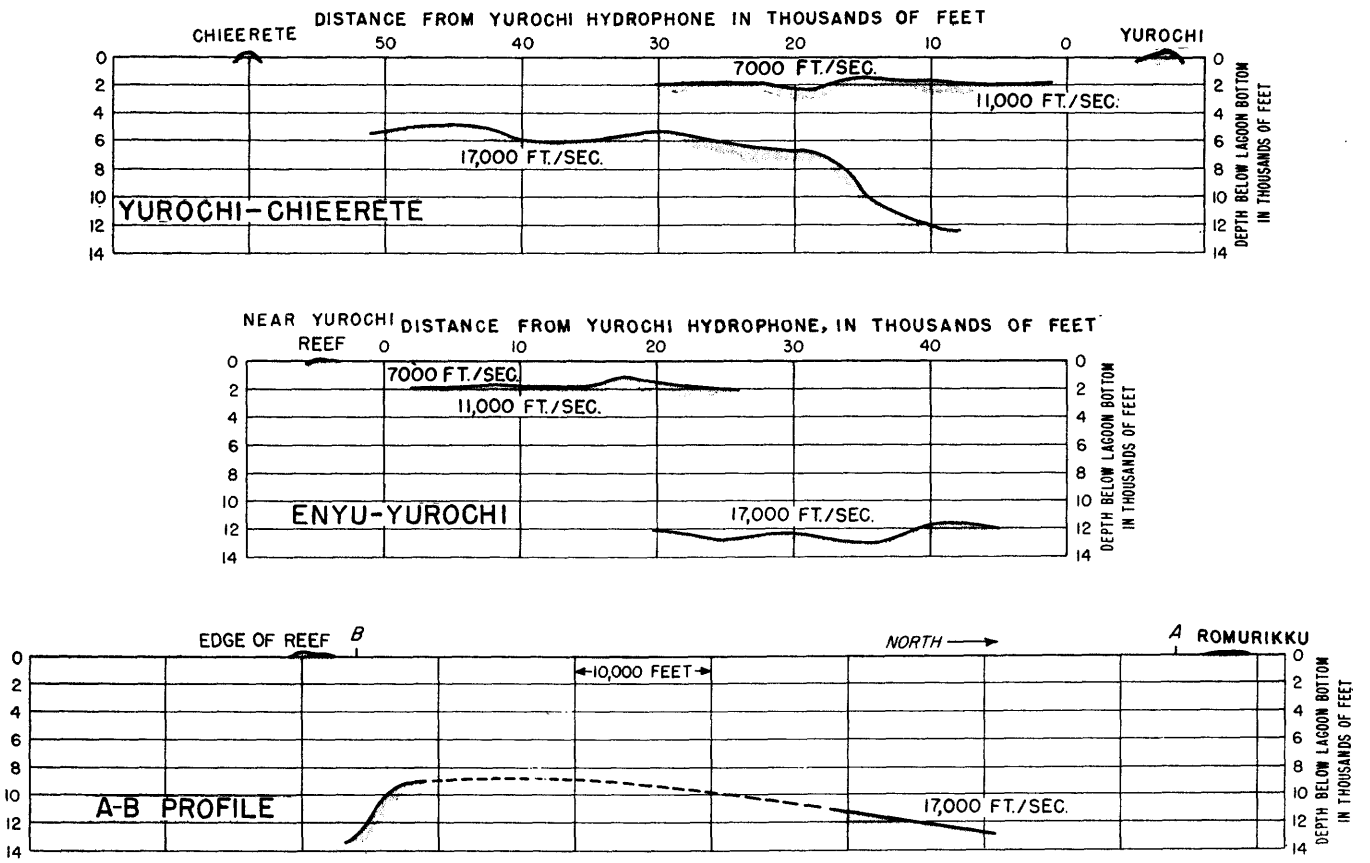


FIGURE 133.—Cross sections showing subsurface structure indicated by seismic data along Yurochi-Chieerete, Enyu-Yurochi, and *A–B* profiles. Interfaces are between media having seismic velocities as indicated.

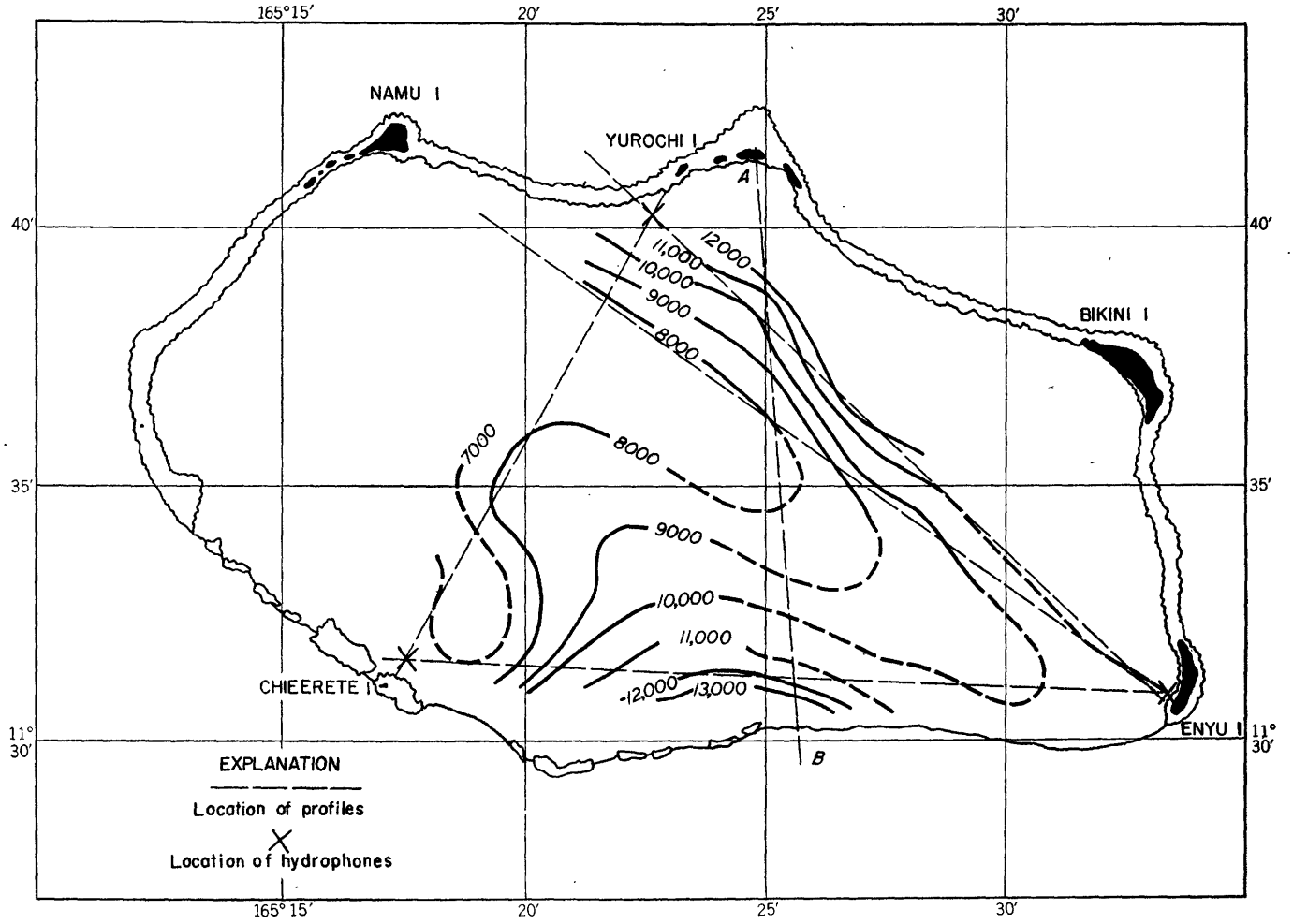


FIGURE 134.—Contour map of depths to top surface of 17,000 fps zone. Depths are in feet below sea level.

western portion of the atoll, although there is insufficient control to be certain that the depth does not continue to decrease as the western edge of the atoll is approached. Low regions are observed under the northeast and south central parts of the atoll. It should be borne in mind, however, that the greatest depth observed on this interface is about a mile higher than the ocean floor in the areas between the atolls of the Marshall Islands.

The top of the 11,000 fps layer (fig. 135) has a more uniform depth, except for the anomalous plunge observed near the southern border of the lagoon beginning about 3 miles west of Enyu. The cross section of the profile from Enyu to Chieerete and the contour map (fig. 135) show only one of three assumptions which were made. With such a paucity of data, many assumptions were possible. The three that seemed most reasonable were:

1. The velocity of 11,000 fps is constant throughout the zone, and at about 3 miles west of Enyu there is a sharply cut valley or a fault, downthrown to the west, in the 11,000 fps material. The increase in depth is about 3,000 feet. Two or three miles farther west (where there is no control on this horizon) the top of this zone must rise by the same amount.

2. The velocity throughout the zone ($V_1$) changes from 11,000 fps to 9,000 fps at the point along the profile corresponding to the apparent break in slope on the time-distance curve. Farther west, at an undetermined point, the velocity changes back to 11,000 fps.

3. The velocity in the first zone increases with depth from a value of 7,000 fps to a maximum of 11,000 fps. Everywhere beneath the atoll the base of the first zone rests on a second in which the velocity is lower. Along the southern edge of the atoll the second zone rises to such an elevation that below a portion of the profile from Chieerete to Enyu the thickness of the first zone is such that velocity increases only to 9,000 fps.

The sections resulting from all three assumptions are shown schematically in figure 136. The Enyu-Chieerete time-distance curves show that there is no anomaly in the arrival times from the deepest interface

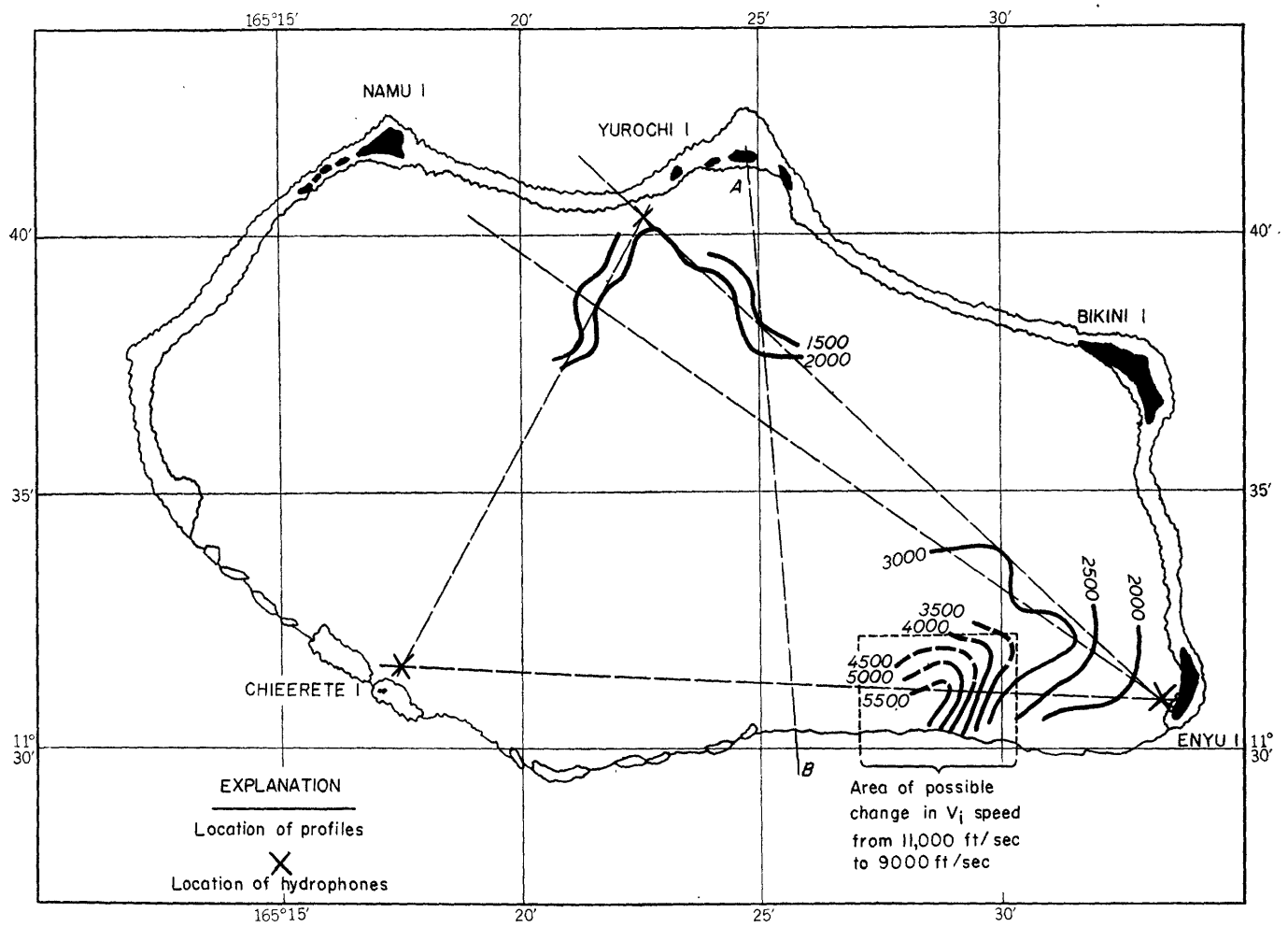


FIGURE 135.—Contour map of depths to top surface of 11,000 fps zone. Depths are in feet below sea level. These contours are based on the assumption that seismic velocity in second zone is uniformly 11,000 fps everywhere under the lagoon. Figure 136 shows alternative possibilities.

which corresponds to that in the intermediate speed zone above. If the lower interface were horizontal, one would expect that any change either in the speed or thickness of the intermediate zone should, according to the depth-intercept time relations, give rise to some anomaly in the arrival times observed from the 17,000 fps marker. Since there is none, one must postulate that a rise in the lower interface just compensates either for the depression in the top surface of the intermediate zone or for the change in its velocity, which might explain the anomaly in the arrivals from the upper interface. The upper and middle diagrams of figure 136 illustrate this. The third assumption does not require such a conveniently coincidental rise in the surface of the 17,000 fps zone, but positive evidence for a low-speed intermediate zone is of course lacking.

The arrival times in the refraction survey was for points too widely separated to permit determination of the velocity of the material within a few hundred feet of the surface by refraction methods. However, by applying Pekeris' dispersion theory, Dobrin (1950, 1951) has deduced the velocities in the first 400 feet of sediments.

A brief qualitative summary of the dispersion theory as given by Dobrin (1950) is quoted below to facilitate the discussion to follow.

When an explosion is detonated under water, the initial pressure pulse traveling away from the source can be resolved by Fourier analysis into sinusoidal components having all frequencies from zero to infinity. For wave lengths no shorter than about one-tenth the water depth, dispersion will be observed, and each frequency will travel through the water at a different speed. The initial pulse will now spread out into a train of almost sinusoidal waves having frequencies continually varying with their position in the train.

In such a train, any given wave cycle will change in length as the wave moves away from its source. If an observer follows the crest of such a wave he finds it has, at any point, an instaneous velocity, $c$, which varies with the frequency. This is defined as the *phase velocity* (fig. 1 [fig. 137, this report]). If, at each distance, he selects a pair of crests separated by a given interval—that is, constant wave length—he finds that this wave length is

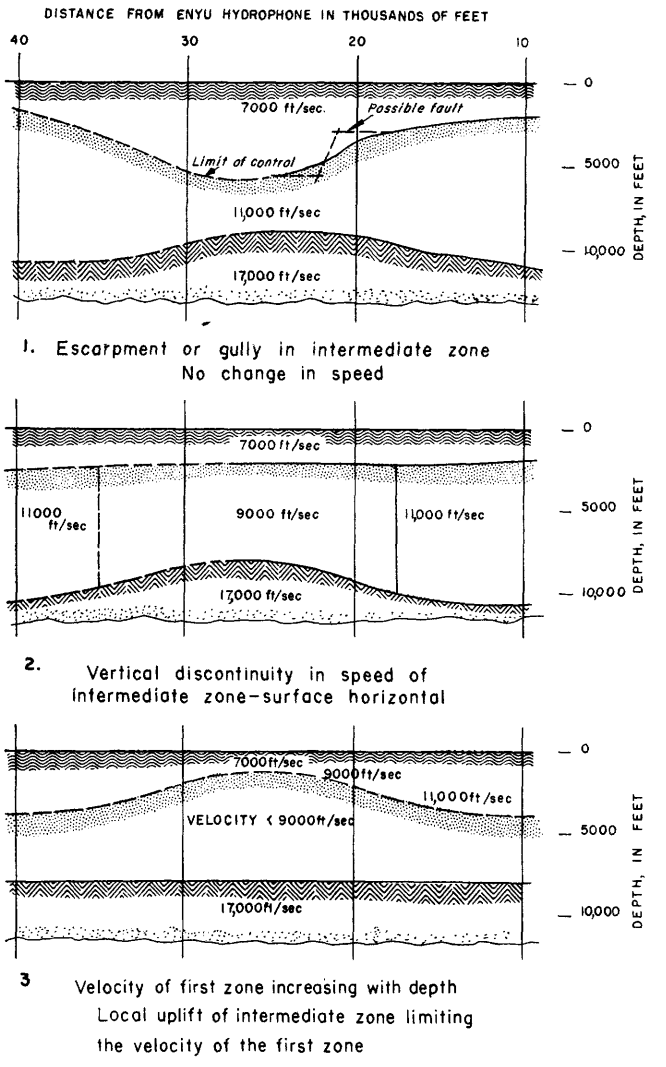


FIGURE 136.—Three alternative interpretations of anomaly in arrival times at eastern end of Chicerete-Enyu profile, see figure 130. Dotted lines show postulated configurations where control is missing.

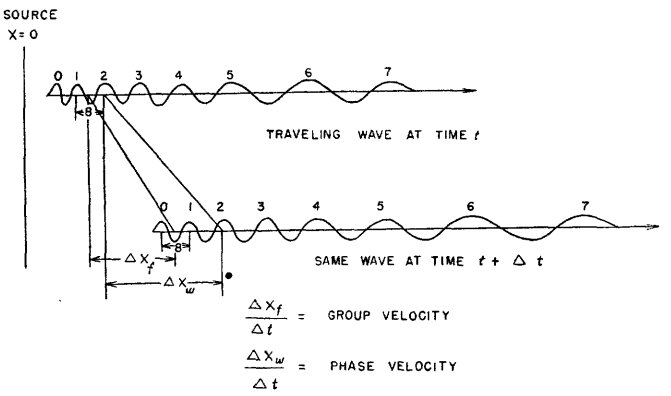


FIGURE 137.—Illustration of group and phase velocities.

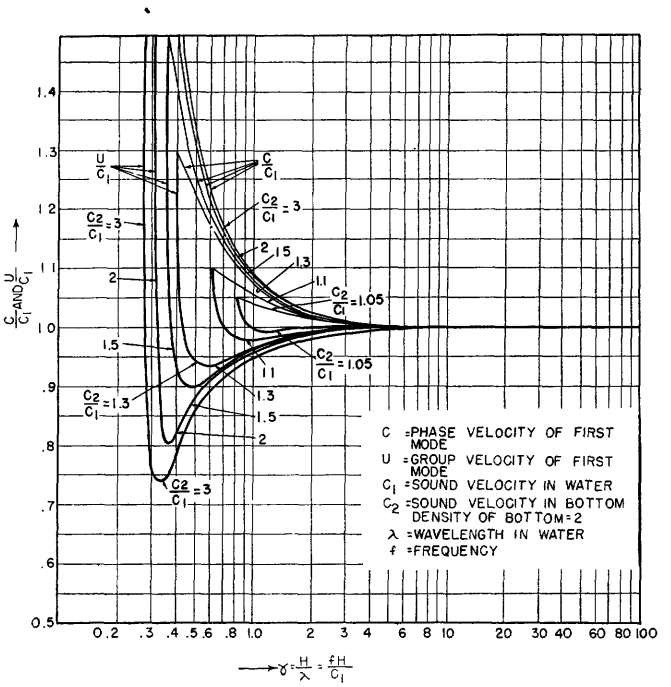


FIGURE 138.—Phase velocity and group velocity (of first mode).

propagated at a characteristic speed depending on frequency. This speed, known as the *group velocity, U,* is obtained directly from the record by dividing the shot-detector distance by the total travel time of the wave in question.

The phase velocity of a compressional explosion wave transmitted without damping through shallow water will vary inversely as the sine of the angle made with the vertical by the multiply reflected wave paths allowing maximum phase reinforcement for each frequency. This angle will be different for each wave length and for each allowed mode of transmission at this wave length. Thus, for any mode—usually only the first need be considered if the proper measurement techniques are employed—the phase velocity and group velocity will depend on the wave length, and the water waves will exhibit dispersion. For a given water depth, the precise form of the dispersion curve will depend only on the density of the bottom material and its elastic characteristics. It is thus possible to study the bottom structure from the dispersion of the compressional waves propagated through the overlying water layer.

Figure 2 [fig. 138, this report] shows a number of curves of $c$ and $U$ versus frequency, $f$, for a water layer with a speed of $c_1$ and a thickness $H$ underlain by a liquid bottom of speed $c_2$. These were calculated on the basis of Pekeris' normal mode theory. The frequencies are expressed in the dimensionless form $fH/c_1$, and the velocities in the form $c/c_1$ and $U/c_1$. Each curve represents a different $c_2/c_1$ ratio, covering the range from 1.05 to 3. If the upper medium is water with a sound velocity of 5,000 ft/sec and the lower medium is sedimentary rock (considered as a liquid), these curves, extending from $c_2=5{,}250$ fps to $c_2=15{,}000$ fps, should be valid for virtually all homogeneous bottom sediments, assumed to be liquid, for which the sound velocity is greater than that in water.

A significant feature of the group-velocity curves of figure 2 [fig. 138, this report] is the minimum observed in each. The higher the $c_2/c_1$ ratio the lower is the frequency at which this minimum occurs. Havelock (1924) shows that any maximum or minimum in the group-velocity versus frequency curve will result in a situation in which components having adjacent frequencies will travel at the same velocity and because of their reinforcement will give an amplitude maximum. The amplitude peak at the frequency of minimum-group velocity is

readily identified on most oscillograph records of shallow-water explosions and is called by Pekeris the *Airy wave*.

The first "water wave" to arrive after the initial ground wave should have, according to figure 2 [fig. 138, this report], a frequency approaching infinity; subsequent water waves should be of successively lower frequency. The water-wave arrivals, represented by the portion of the group-velocity curve to the right of the minimum, should be superimposed on the lower-frequency ground waves, represented by the portion of the curve left of the minimum and having a frequency which increases with time. At the minimum-group velocity the water wave and ground waves coincide and give rise to the Airy peak.

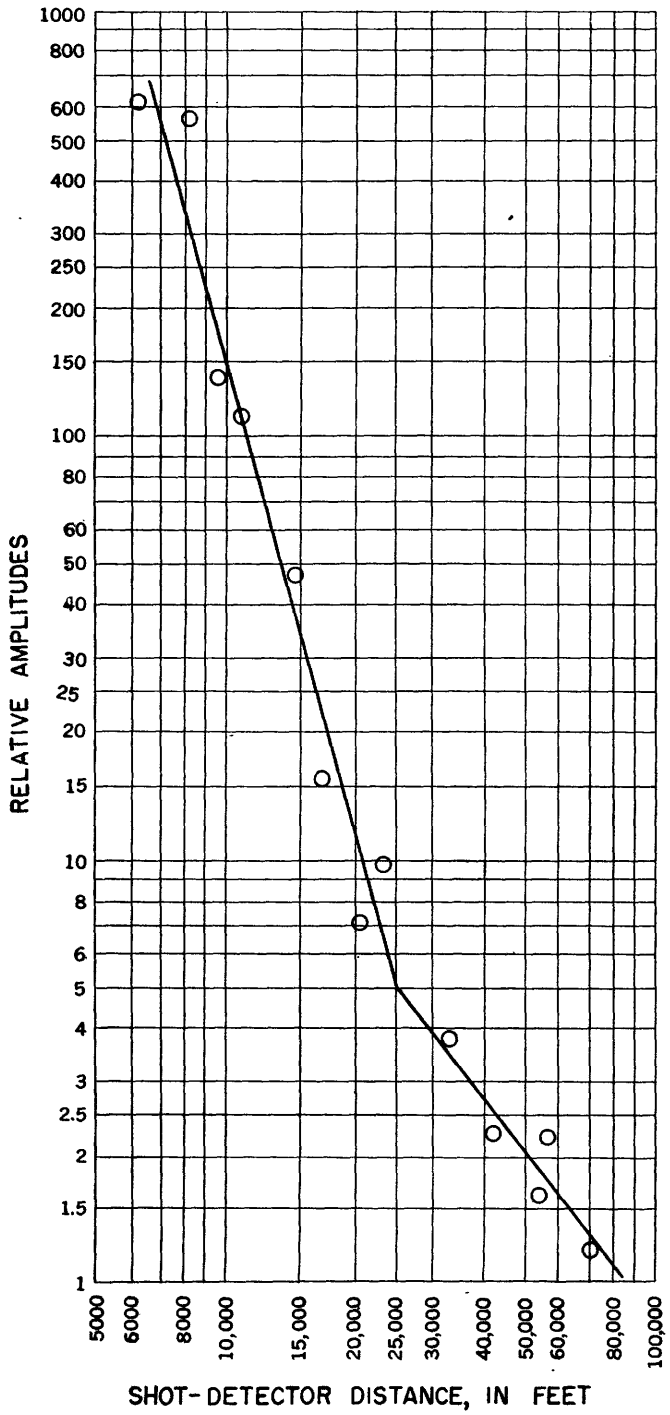


FIGURE 139.—Relative amplitudes of pressure versus distance from the shot. The pressure in the water around the hydrophone is generated by the seismic wave upon arrival after refraction through the subsurface beds.

Insofar as one can consider the unconsolidated bottom material in Bikini lagoon to have the elastic properties of a liquid as well as a uniform sound velocity greater than 5,000 fps, the speed of sound in it and, hence, its elastic properties should be deducible by comparing the observed group velocities with the theoretical curves of figure 2 [fig. 138, this report].

Dobrin's study of the data in the light of Pekeris' theory shows:

1. The "high frequency" waves, 50 cycles per second and higher, from the shots in shallow water near the lagoon's edge indicate that the speed of the seismic wave in the first 20 feet below the lagoon bottom averages about 5,250 fps. This speed increases to 6,500 fps at a depth of about 40 feet.

2. The Airy waves in all parts of the lagoon indicate a velocity of 6,500 fps to about 400 feet below the bottom.

These indications are in reasonable agreement with the velocity measurements made in the hole on Bikini island and with the refraction data. High-frequency waves from shots in the center of the lagoon give a dispersion pattern to which the Pekeris theory does not appear to apply. Dobrin attributes this discrepancy to a lateral variation in sedimentary composition of the top 100 feet between the edge and center of the lagoon, possibly a downward continuation of the surface change from sand to *Halimeda* debris observed by Emery (1948) on going toward the lagoon's center.

## DETERMINATION OF ABSORPTION COEFFICIENT

A byproduct of this investigation was a study of the attenuation of the elastic pulse in the 11,000 fps zone and in the 17,000 fps zone. Perkins (1952) has reported the results briefly. The pulse was assumed to be propagated in a cylindrical wave front horizontally through the bed corresponding to a particular section of the time-distance curve. The relative magnitudes of the pressure generated in the water by the compressional wave at each detector was determined. The magnitudes of the pressures transmitted by pulses of the same period are related by the equation

$$p_2 = p_1 \left(\frac{r_1}{r_2}\right) e^{-k(r_2 - r_1)}$$

in which

$r_1$ and $r_2$ = two distances at which the first-arriving pulses have been refracted horizontally through the same horizon;

$p_1$ and $p_2$=pressures at $r_1$ and $r_2$, respectively;
$k$=absorption coefficient of the medium through which the pulse was transmitted horizontally.

The value of $k$ for each zone was:

| Zone (seismic velocity, in ft/sec) | Geologic material | k per 1,000 feet [1] |
|---|---|---|
| 11,000 | calcareous (assumed) | 0.2 |
| 17,000 | igneous | .003 |

[1] For pulses of period 0.095 to 0.11 second.

The suggestion was made that the value of $k$ with the seismic velocity can be used to identify subsurface sediments from surface observations. A graph of the relative amplitudes versus distance is shown in figure 139.

The determination of $k$ and the seismic velocity in media similar to those above and which have had a similar history should aid in determining the nature of the two horizons in question until such time as a more direct determination is possible.

## GEOLOGIC INTERPRETATION

### POSSIBLE CONSTITUTIONS OF THE VELOCITY ZONES

Thus far there has been no attempt to identify or postulate the compositions of the three zones indicated by the seismic-refraction data. The 1947 borings have not made definite identification possible because of their limited depths and their location on Bikini island, at the atoll's edge instead of under the lagoon, where the refraction data apply. The well logs on the other hand give evidence which, combined with other indications, virtually specifies the nature of the uppermost zone and also provides us with a strong clue to the identity of the intermediate layer. Until a deeper or more ideally located hole is drilled, therefore, the internal constitution of the atoll can only be inferred from the available geological and geophysical evidence.

Cuttings from the 2,556-foot hole on Bikini island (Ladd and others, 1948) show only calcareous material from the surface to the bottom. The first 1,100 feet contains occasional hard streaks of limestone with loose calcareous sand in between. From 1,135 feet to the bottom, only loose sand (nearly all of Tertiary age) is encountered. Vertical seismic velocities measured in this hole to a depth of 1,800 feet fluctuated irregularly but showed definite trends when smoothed. In the first 1,000-foot interval velocities averaged about 8,000 fps although local values between successive detector positions were as high as 14,000 fps. Actually, velocities over intervals of 100 feet or so cannot be determined accurately, and the local fluctuations may indicate only the normal uncertainty in reading arrival times. However, since the detectors were opposite the known interfaces the fluctuations probably are real. In the remaining 800 feet the velocities were observed to increase quite uniformly from about 7,000 to 10,000 fps.

The refraction data indicate that the zone with a horizontal velocity of 7,000 fps extends from a depth of 2,000 or 3,000 feet upward to the lagoon bottom, since the time-distance segments representing it intercept the origin at zero time. Core samples several feet long (Emery, 1946) taken from the lagoon floor show that the bottom sediments over much of the lagoon consist largely of fragments of the calcareous alga *Halimeda*. Shallow-water sediments of the same lithologic type would be expected to continue downward from the lagoon bottom to the first seismic discontinuity.

*Halimeda* does not extend an appreciable distance below the surface. But all calcareous materials brought to the surface in the drilling are of kinds that would not have been laid down in water deeper than a few hundred feet. In this sense all are "shallow water" sediments as opposed to those ordinarily at the bottom of the deep sea. Small irregularities in the refraction arrival times from the uppermost zone as well as fluctuations in the vertical velocities observed in the well shooting suggest that some inhomogeneities exist in the elastic properties of these sediments.

The only observations in the literature on the velocity of sound in recent calcareous material were made by Ewing and others (1948) off Barbados and by Woollard and Ewing (1939) at Bermuda. Off Barbados they obtained a velocity of 5,620 fps in the uppermost layer and at Bermuda, 8,800 fps. The speeds at Barbados, Bermuda, and Bikini all lie within the range of 5,600 to 13,800 fps quoted by Birch (1942) for "soft" limestone.

The second zone, with an apparent horizontal seismic velocity of 11,000 fps, is the most difficult to identify. Its constitution, when established, will very probably provide the key to the atoll's origin and geologic history. If one extrapolates the observed interval velocities in the lower half of the 1,800-foot velocity log in the Bikini island boring, one would predict a speed of 11,000 fps at a depth of 2,000 feet. This is the velocity which, according to the refraction data, extends downward without increase (although it may decrease) for a considerable depth below an interface at 2,000–3,000 feet undersea. The most direct implication to be drawn from all the data taken together is that the calcareous deposits continue to the top of the 17,000 fps zone and that the 11,000 fps marker is the top of a zone in which the speed of seismic waves no longer increases with depth. Such a velocity distribution would suggest that the calcareous sand becomes increasingly compacted, cemented, and possibly replaced by dolomite down to a depth below which no further change is possible. The increase in compac-

tion and cementation appears to begin at 1,000 feet and the limiting depth would be 2,000 to 3,000 feet.

Upon receipt of the data from the vertical-velocity survey, some questions arose as to whether the seismic-refraction data, indicating discrete zones of constant velocity separated by surfaces of discontinuity, were compatible with the vertical-velocity log, which shows an increase of velocity with depth below 1,000 feet. A calculation was accordingly made to determine the time-distance curve that would be observed if the horizontal velocity varied with depth in the same way as the vertical velocity registered in the up-hole shooting. On the basis of the smoothed log, it was assumed that the horizontal velocity is 7,000 fps from the surface to 1,000 feet and that it increases downward for the next 1,000 feet at a uniform rate of 4 fps for each foot, so that at 2,000 feet it would be 11,000 fps, the value indicated by refraction for the first interface. Below this a uniform velocity of 11,000 fps was assumed. A calculation based on curved-path theory showed that all arrivals from the zone of increasing velocity would be masked by earlier direct-path arrivals through the 7,000 fps zone and also by arrivals along the top of the 11,000 fps zone. Hence the observed refraction data would not be contradicted by an increase of velocity with depth from 1,000 feet to the top of the intermediate layer. Such an assumption would require an increase of about 20 percent in the computed depth to the first interface and about 10 percent to the second, but it would not change the significant features of the refraction picture.

Since the suggested interpretation of the 11,000 fps zone as "shallow water" calcareous material in a limiting condition of compaction or cementation cannot be established as correct until a deep boring is put down, some alternative possibilities might be suggested. All such interpretations are necessarily speculative at this stage, and they are proposed mainly to point out the range of possibilities allowed by the geophysical observations.

In the Funafuti boring, dolomite was encountered at 600 feet, continuing to the bottom of the 1,114-foot hole. No dolomite, on the other hand, was found at Bikini down to 2,556 feet. It is not inconceivable that there is a thick dolomite zone under Bikini so deep that it was not reached by the drill.[1] If its top surface were 2,000 or 3,000 feet under the lagoon bottom it might well constitute the first seismic interface. Available literature (Birch, 1942) on the velocity of sound in dolomite indicates that it ranges from 16,000 to 19,600 fps. This is, to be sure, higher than the observed velocity of 11,000 fps, and it may indicate that any dolomite constitutes a relatively small proportion of the calcareous material at this depth. The previously suggested encrustation of higher velocity material at the top surface of the intermediate zone might represent a layer of greater dolomitization.

Professor R. A. Daly has suggested that the second zone might consist of volcanic materials such as pyroclastics. Revelle (1951) has reported the result of dredging on several guyots in the mid-Pacific. He found rounded basaltic pebbles, cobbles, and boulders at depths of 700 to 1,000 fathoms. In chapter A of this professional paper, which deals with the geology of Bikini Atoll, Emery, Tracey, and Ladd discuss the dredging and core sampling accomplished on the seaward slope of Enyu island. Olivine basalt was found at a depth of 1,000 fathoms, and pyroclastics were found at 1,150 fathoms. The 1946 aerial magnetic survey reported by Alldredge (chapter L) indicates several points where igneous rock comes relatively close to the surface. One of these locations is along the southern border of the atoll between Chieerete and Enyu islands. No data are available on seismic velocities in pyroclastics.

The geologic and magnetic data combined with the anomalous seismic data on the Chieerete–Enyu profile suggest that the third interpretation of the anomaly in arrival times in the Chieerete–Enyu profile (see p. 11) is the most reasonable at this time with the calcareous sediments extending down from the surface to about 3,000 feet and resting on volcanics.

Finally, there is the possibility that the zone consists of pelagic or other organic limestone deposited on an elevated igneous platform or an undersea peak under such conditions that it would not dissolve or be swept off by ocean currents. The 11,000 fps velocity is well within the range of previous measurements on limestone of such origin (Birch, 1942).

Identification of the 17,000 fps zone must also be based on circumstantial considerations. This velocity lies within the range that has been observed both in igneous rocks, such as granites and basalts, and in compact limestones. While it is conceivable that there might be a hard limestone layer at the base of the atoll, it would be very difficult to explain the considerable thickness that would be indicated for it by the 8-mile long segments representing it on the time-distance curves unless its velocity were greater than or identical to that of the basement. The 6,000-foot relief of its top surface would also be peculiar. It is more likely that the zone represents the igneous basement, which, under the part of the Pacific that lies east of the andesite line, is predominantly basaltic. This identification is essentially supported by the seismic measurements of Brockamp and Wölcken (1929) who obtained a velocity

[1] The writers are indebted to Professor W. H. Bucher for calling attention to this possibility.

of 18,300 fps for some known basalt formations in Germany.

### INDICATIONS OF SUBSIDENCE

If it is assumed that calcareous material deposited in water not more than a few hundred feet deep extends from the surface to the top of the 17,000 fps zone, one must conclude that there has been 7,000 to 13,000 feet of subsidence, or relative change in sea level, in the atoll's geologic history. The broad terrace in the northeast portion of the 17,000 fps surface suggests that the topographic relief of this surface is due to subaerial erosion. If this could be proved, we would know that the total subsidence must have been at least 13,000 feet. However, no such proof is possible at present.

If, on the other hand, the intermediate zone has some other constitution than compacted coral or algal sand, the almost certain identification of the uppermost zone as calcareous establishes a minimum subsidence of 2,000 to 3,000 feet.

The existence of a broad and probably igneous summit under the atoll about 6,500 feet below sea level is especially interesting in view of the announcement by Hess (1946) that fathometer surveys over a wide belt of the central Pacific have revealed the existence of 160 flat-topped truncated and beveled cones, which he calls "guyots," ranging in depth from 3,000 to 6,000 feet. Additional seamounts, or guyots, have subsequently been charted by Emery (1946). One of these adjoins Bikini Atoll on the northwest. Hess explained these as volcanic islands that sank too early in geological time or too rapidly for reef-building organisms to grow substantial accumulations during subsidence.

There is a possibility that the buried igneous mountain under Bikini Atoll coincides in geological origin with the nearby submerged truncated cones. Unfortunately the seismic survey could not give as precise data on the depth and shape of the mountain as the fathometer has given on the contours of the submerged cones, and comparisons are difficult. However, the basement surface under Bikini Atoll apparently has considerably more relief than the almost flat tops of Hess's guyots.

### INFERENCES REGARDING GEOLOGIC HISTORY OF BIKINI ATOLL

The geophysical data suggest several lines of speculation relative to the origin and geologic history of Bikini Atoll. Vaughan (1923) and Hobbs (1923) have pointed out the fallacy of assuming that a single theory can explain the origin of all coral reefs and atolls everywhere in the world, and it would certainly not be warranted to assume that all atolls have the composition indicated for Bikini Atoll.

In the present state of our knowledge, all theories regarding Bikini's geologic history must depend on the identity assumed for the 11,000 fps layer indicated by the refraction data. If, as seems logical, this layer consists of calcareous material, like that now being deposited, which has been compacted into a state of maximum consolidation, the atoll must have formed somewhat in the manner Darwin proposed, with a total subsidence of more than 2 miles. If the layer is presumed to be dolomitic, one can postulate essentially the same mechanism with the additional stipulation that conditions favored dolomitization of the reef limestone from the time of its initial deposition until a thickness was reached 2,000 to 3,000 feet less than the present thickness.

If one assumes that the intermediate zone is volcanic and consists of tuffs or pillow lavas, it is logical to propose an eruption from a submerged volcano of igneous products that emerged above sea level, forming a volcanic island something like Falcon Island today (Hoffmeister and Ladd, 1944). An island of such soft material would offer small resistance to wave cutting and, like Falcon Island, would soon be abraded to sea level. At this stage, shallow-water organisms would afix themselves to the platform's surface and upon subsidence would build up a calcareous layer several thousand feet thick.

If the intermediate layer should consist of pelagic or other deep-sea limestone, the mechanism becomes essentially a combination of the mechanism called for by the old Rein-Murray theory and that of Darwinian subsidence. Organic matter deposited on the surface of a deeply buried igneous platform builds up an increasing thickness of pelagic lime until its top is shallow enough for calcareous organisms such as corals and algae to take over. Subsidence would become the controlling factor at this point, and the present structure would be the result of a relative rise of several thousand feet in sea level. Banks, ridges, and other isolated topographic highs at depths as great as 400 fathoms off the California coast have been shown by Revelle and Shepard (1939) to have only a sparse and discontinuous veneer over rocky bottom. They ascribe this fact to the action of turbulence associated with intermittent bottom currents which suspends the sedimentary particles momentarily. This allows the component of gravity downslope eventually to remove the particles from the topographic high. If this process exists on mid-ocean banks, it is not likely that any appreciable amount of pelagic material could have accumulated on the initial platforms; this theory would thus not be tenable.

## SELECTED REFERENCES


Birch, Francis, ed., 1942, Handbook of physical constants: Geol. Soc. America Special Papers, no. 36, 325 p.

Brockamp, B., and Wölcken, K., 1929, Zeitschr. Geophysik, v. 5, p. 482.

Daly, R. A., 1915, The Glacial control theory of coral reefs: Am. Acad. Arts Sci. Proc., v. 51, p. 155–251.

Dana, J. D., 1853, On coral reefs and islands: 143 p. New York.

Darwin, C. L., 1842, The structure and distribution of coral reefs: London.

Davis, W. M., 1928, The coral reef problem: Am. Geog. Soc. Special Pub., no. 9.

Dobrin, M. B., 1950, Submarine geology of Bikini Lagoon as indicated by dispersion of water-borne explosion waves: Geol. Soc. America Bull., v. 61, p. 1091–1118.

——— 1951, Dispersion in seismic surface waves: Geophysics, v. 16, no. 1.

——— 1952, Introduction to geophysical prospecting: 435 p. New York, McGraw Hill.

Dobrin, M. B., Perkins, Beauregard, Jr., and Snavely, B. L., 1949, Subsurface constitution of Bikini Atoll as indicated by a seismic refraction survey: Geol. Soc. America Bull., v. 60, p. 807–828.

Emery, K. O., 1946, Submarine geology of Bikini Atoll (Abstract): Geol. Soc. America Bull., v. 57, p. 1191.

Ewing, Maurice, Pekeris, C. L., and Worzel, J. L., 1948, Propagation of sound in the ocean: Geol. Soc. America Mem. 27, 205 p.

Gardner, L. W., 1939, An areal plan of mapping subsurface structure by refraction shooting: Geophysics, v. 4, p. 247–259.

Heiland, C. A., 1940, Geophysical exploration: New York, Prentice-Hall, Inc.

Hess, H. H., 1946, Drowned ancient islands of the Pacific basin: Am. Jour. Sci., v. 244, p. 772–791.

Hobbs, W. H., 1923, Reef formations as an index of mountain building processes: Pan-Pacific Sci. Cong. Proc., Australia, v. 2, p. 1128–1131.

Hoffmeister, J. E., and Ladd, H. S., 1944, The antecedent platform theory: Jour. Geology, v. 6, p. 388–401.

Jones, J. H., 1934, A seismic method of mapping anticlinal structures: World Petroleum Congress Proc., Pt. 1 (1934).

Kuenen, Ph. H., 1947, Two problems of marine geology—atolls and canyons: K. Nederl. Akad. Wetensch. Verh. (Tweede Sectie) D1. XLIII, p. 1–69.

Kuwahara, S., 1939, Velocity of sound in sea water and calculation of the velocity in sonic sounding: Hydrographic Rev. (Monaco), v. 16, p. 123–140.

Ladd, H. S., and Hoffmeister, J. E., 1936, A criticism of the glacial-control theory: Jour. Geology, v. 44, p. 74–92.

Ladd, H. S., Tracey, J. I., and Lill, C. G., 1948, Drilling on Bikini Atoll, Marshall Islands: Science, v. 107, p. 51–55.

Matsuyama, Motonori, 1918, Determination of the second derivatives of the gravitational potential on the Jaluit Atoll: College of Science, Mem., Kyoto, v. 13, p. 17–68.

Nettleton, L. L., 1940, Geophysical prospecting for oil: 444 p., New York, McGraw-Hill.

Perkins, Beuaregard, Jr., 1952, Attenuation of seismic waves: Geophysics, v. 27, no. 2, p. 411.

Revelle, Roger, 1947, Bikini revisited (Abstract): Science, v. 106, p. 512–513.

——— 1951, Paleoecology and deep sea exploration: Committee on Treatise on Marine Ecology and Paleoecology, 11th Ann. Rept., Natl. Research Council, December 1951.

Revelle, Roger, and Shepard, F. P., 1939, Recent marine sediments: Am. Assoc. Petroleum Geologists, Symposium, edited by P. D. Trask, p. 245–280.

Royal Society of London, 1904, The Atoll of Funafuti: Rept. Coral Comm. of the Royal Society.

Skeats, E. W., 1918, The coral reef problem and the evidence of the Funafuti boring: Am. Jour. Sci., 4th ser., v. 45, p. 81–90.

Snavely, B. L., Baresford, R., Clarkson, H. N., Erickson, K. W., White, G., and Atanasoff, J. V., 1947, Use of a water coupled microphone system for seismic surveying (Abstract): Geophysics, v. 12, p. 500.

Stearns, Harold, 1946, An integration of coral reef hypotheses: Am. Jour. Sci., v. 244, p. 245–262.

Vaughan, T. Wayland, 1923, Coral reefs and submerged platforms: Pan-Pacific Sci. Cong. Proc., Australia, v. 2, p. 1128–1131.

Woollard, G. P., and Ewing, Maurice, 1939, Structural geology of the Bermuda Islands: Nature, v. 143, p. 898.

# INDEX

# Seismic-Refraction Studies of Bikini and Kwajalein Atolls

*By* RUSSELL W. RAITT

With a section on Coordination of Seismic Data, Bikini Atoll
*By* BEAUREGARD PERKINS, Jr.

GEOLOGICAL SURVEY PROFESSIONAL PAPER 260-K


UNITED STATES GOVERNMENT PRINTING OFFICE, WASHINGTON : 1954

# CONTENTS



# ILLUSTRATIONS

# BIKINI AND NEARBY ATOLLS, MARSHALL ISLANDS

## SEISMIC-REFRACTION STUDIES OF BIKINI AND KWAJALEIN ATOLLS AND SYLVANIA GUYOT, 1950

By RUSSELL W. RAITT [1]


### ABSTRACT

Seismic-refraction studies made at Bikini Atoll, Sylvania Guyot, and Kwajalein Atoll on the joint University of California–U. S. Navy Electronics Laboratory Mid-Pacific Expedition of 1950 expanded the scope of the original 1946 studies to include a section across Sylvania Guyot and several deepwater sections extending from Bikini Atoll. Also Bikini Lagoon was surveyed in much greater detail, with particular emphasis on more complete control with reversed profiles. In addition, one short section was obtained at Kwajalein Atoll.

It was found that the seismic velocities beneath Bikini Lagoon vary laterally as well as with depth. They can be grouped into six more or less well defined layers averaging approximately 2.5, 3, 4, 5.5, 6.5, and 8 kmps. The first four were observed only in the lagoon profiles, and the remaining two were found only in deep water.

From sections taken on Sylvania Guyot and the flanks of Bikini Atoll near regions where samples of volcanic rock were obtained from the sea bottom, it was concluded that the third layer, of about 4 kmps seismic velocity, represents volcanic rock. Its estimated depth under Bikini Lagoon ranges from 600 m to 2,100 m and averages about 1,300 m. One short section at the south end of Kwajalein Lagoon shows somewhat greater depths of the third layer than that at Bikini Atoll but the lagoon coverage was insufficient to demonstrate that Kwajalein differs significantly from Bikini.

Indications were found that the 6.5 kmps layer is deeper under Bikini Atoll than under the surrounding deep sea. If real, this local depression is unlikely to be greater than 3 km.


### INTRODUCTION

The seismic-refraction studies of 1950 in the Marshal Islands took place during the period September 29 to October 9. They formed a concluding phase of the seismic program of the joint University of California–U. S. Navy Electronics Laboratory Mid-Pacific Expedition (Revelle, foreword of chapter A, Professional Paper 260).

The previous seismic-refraction survey of Bikini in 1946 (Dobrin, Perkins and Snavely, 1949) indicated the existence of at least three layers, with velocities of the order of 7,000 fps (2.1 kmps), 11,000 fps (3.4 kmps), and 17,000 fps (5.2 kmps), respectively. The first layer, extending to a depth of 2,000 ft to 3,000 ft (0.6 to 0.9 km) was inferred to consist of calcareous lagoon and reef deposits on the basis of drilling to 2,556 ft on Bikini island in 1947.

The zone with a velocity of 17,000 fps was inferred to represent igneous basement. Its depth was indicated to be 7,000 ft to 13,000 ft (2.1 to 4.0 km). The second zone, with a velocity of 11,000 fps, was more difficult to identify. Available circumstantial evidence suggested that it was calcareous material similar to the first zone with a higher velocity caused by increasing compaction and cementation with depth. However, the possibility that it was volcanic material could not be excluded.

In planning the seismic operations within Bikini Lagoon the spacing of stations was chosen to attain an optimum degree of reversed control on the second zone. The results of the 1946 survey were very helpful in this planning.

In addition to the operations within Bikini Lagoon, an approximately equal effort was expended on operations outside the Lagoon, on Sylvania Guyot and extending down the flanks of Bikini Atoll into deep water. This work had two major objectives: (1) to seek clues for the identification of the second zone by means of outcrops and (2) to determine the relationship of the subsurface structure of Bikini Atoll and Sylvania Guyot to the structure of the deepwater region surrounding it.

A trip to Kwajalein Atoll for supplies gave an opportunity, on October 1, 1950, for one day of seismic observations in the southeast end of Kwajalein Lagoon. Although there had been no previous work on this atoll to guide this operation the principles applied to the Bikini Lagoon operation were successfully followed at Kwajalein Atoll.

[1] Scripps Institution of Oceanography, University of California.

NOTE.—Contribution from the Scripps Institution of Oceanography New Series No. 723.

## ACKNOWLEDGEMENTS

Seismic-refraction operations at sea, thousands of miles from the home base, required careful planning and the cooperation of many people, whose help is gratefully acknowledged.

The work reported on was sponsored by the Bureau of Ships and the Office of Naval Research, the Institute of Geophysics of the University of California, and the U. S. Geological Survey.

Dr. Roger R. Revelle, director of Scripps Institution of Oceanography, and leader of the 1950 Mid-Pacific Expedition, was responsible for initiating the project. His infectious enthusiasm and inspiring leadership were essential to its success.

All shots were fired from USS EPCE(R)–857, whose captain, Lt. Comdr. D. J. McMillan, and officers and crew skillfully executed the difficult navigation required among the coral knolls and reefs of Bikini and Kwajalein Atolls. Major credit for the successful reception of the weak refraction signals is due to the sympathetic cooperation of Mr. James L. Faughn, captain of the receiving ship, the M. V. *Horizon*, and the officers and crew.

The friendly help of the commanding officer of Kwajalein Naval Station and his staff in supplying explosives, provisions, and fuel to the expedition was greatly appreciated.

Mr. Daniel K. Gibson supervised the shooting operations, assisted by Chief Gunner's Mate Albert Obregon, who was responsible for firing the shots. Mr. Arthur D. Raff was responsible for the receiving-equipment installation and for acquiring the vast quantity of supplies and spare parts required in its operation. In recording the seismic waves on the M. V. *Horizon* the author was assisted by Mr. T. Wayne Runyan and Mr. Jeffery D. Frautschy. The travel time data were read, plotted, and analyzed by Miss Gloria J. Slack and Miss Gwendolyn A. Roy.

Helpful discussion and criticism have been received from B. Perkins, Carl Eckart, R. S. Dietz, H. V. Menard, E. M. Hamilton, R. F. Dill, and T. A. Magness, who have read this manuscript in rough form.

## OPERATING PROCEDURE

The plan of operation for the Bikini area and for Kwajalein Atoll is shown in figures 140 and 141. Points designated by letters represent receiving stations occupied by the receiving vessel, the M. V. *Horizon*, of Scripps Institution of Oceanography. At all stations within Bikini and Kwajalein Lagoons, the *Horizon* was at anchor. At all other stations the *Horizon* was either lying to or under way slowly to maintain position. Seismic shots were fired by U.S.S. EPCE(R)–857 along the solid black lines shown in figures 140 and 141. For the profiles outside the lagoons standard speed while firing was 12 knots. Inside the lagoons the risk of navigation among coral knolls required a slower speed, usually 8 knots.

With the exception of twenty 20-pound demolition charges of tetrytol obtained from Kwajalein Naval Station, all charges were made up with one-half pound TNT demolition blocks. They were fired with slow burning fuse cut to fire about a minute after ignition. Standard charge sizes of 1, 4, 20, and 50 pounds were used. The time of firing was recorded by picking up the direct blast on the firing ship's echo sounder and transmitting it by radio to the receiving ship where it was recorded by the oscillograph used to record the seismic waves.

The refracted ground waves and the direct water-borne waves were picked up by three pressure-sensitive crystal hydrophones capable of responding to sound frequencies as low as three or four cycles per second. The hydrophones were supported by buoys at a depth of 120 feet. They trailed out from the receiving ship separated by intervals of about 300 feet. It was desirable, but not always possible, to lay the line of hydrophones in the direction of the line of shots in order to obtain a rough estimate of wave velocity from a single shot. However, even when wind and current caused the hydrophone spread to make a large angle with the line of shots, the use of three separate pickups gave a great advantage in identifying a weak refracted wave in the presence of noise.

Signals from each hydrophone were recorded on a Miller oscillograph in three rather broad frequency bands centered roughly at 10, 100, and 1,000 cycles per second. Frequencies of the refracted ground wave were generally of the order of 5 to 10 cycles per second and were received only on the lowest frequency channel. The higher frequency channels recorded the water-borne waves used to determine distances between shots and hydrophones.

Timing lines were flashed on the oscillograph record at 0.01 second intervals with a slotted disc driven by a fork-controlled synchronous motor. The timing accuracy was controlled with a break-second chronometer which was checked daily with WWV time signals. Travel times of both water-borne and refracted seismic waves were read to 0.01 second. The sharp onset of refracted waves of near shots permitted the beginning to be read to this degree of precision. However, the more distant shots frequently had very gradual beginnings and the error of reading the instant of first arrival of these shots is several hundredths of a second. Figure 142 gives samples of records at various ranges inside and outside of Bikini Lagoon.

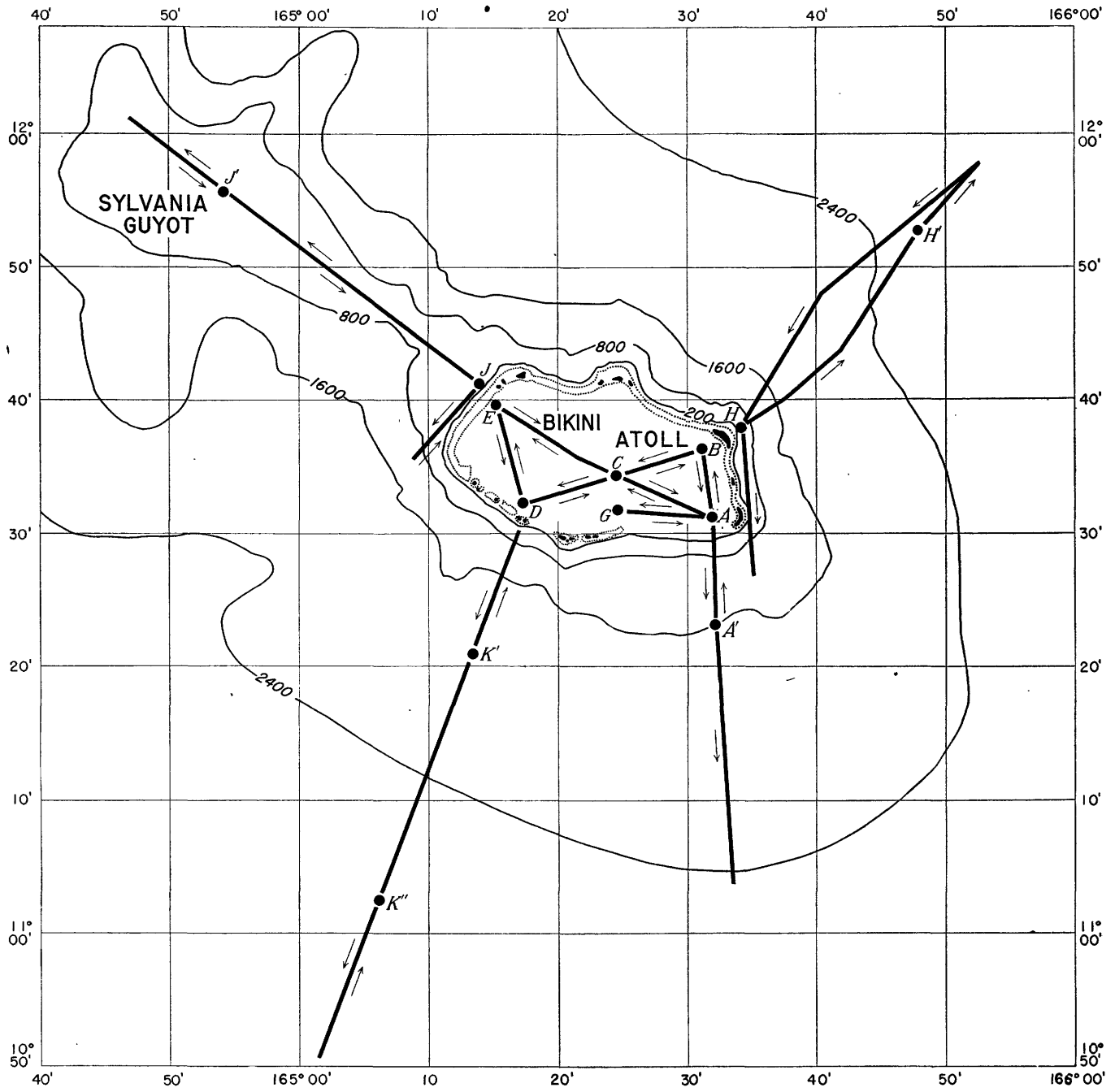


FIGURE 140.—Plan of operations in the Bikini area. Depth contours are given in fathoms.

For determining the shot-hydrophone distance from the travel time of the water-borne sound, the velocity tables of Kuwahara (1939) were used. The temperature of 29° C and salinity of 34.5 parts per thousand gave a velocity of 1.54 kmps, which was used for all the distance determinations.

## THEORY OF INTERPRETATION OF SEISMIC-REFRACTION OBSERVATIONS

Travel-time data for seismic waves rarely yield a unique picture of the subsurface structure. Not only is it difficult to determine the nature of subsurface rocks from measurements of seismic-wave velocity, it is also in many cases impossible to obtain a unique solution for subsurface velocity as a function of depth and position, from travel-time data alone. In most situations it is possible to set up a model of subsurface velocities consistent with the curves of observed travel time. This model may resemble the true structure to a greater or lesser degree dependent on the local conditions and on the control achieved in shooting operations.

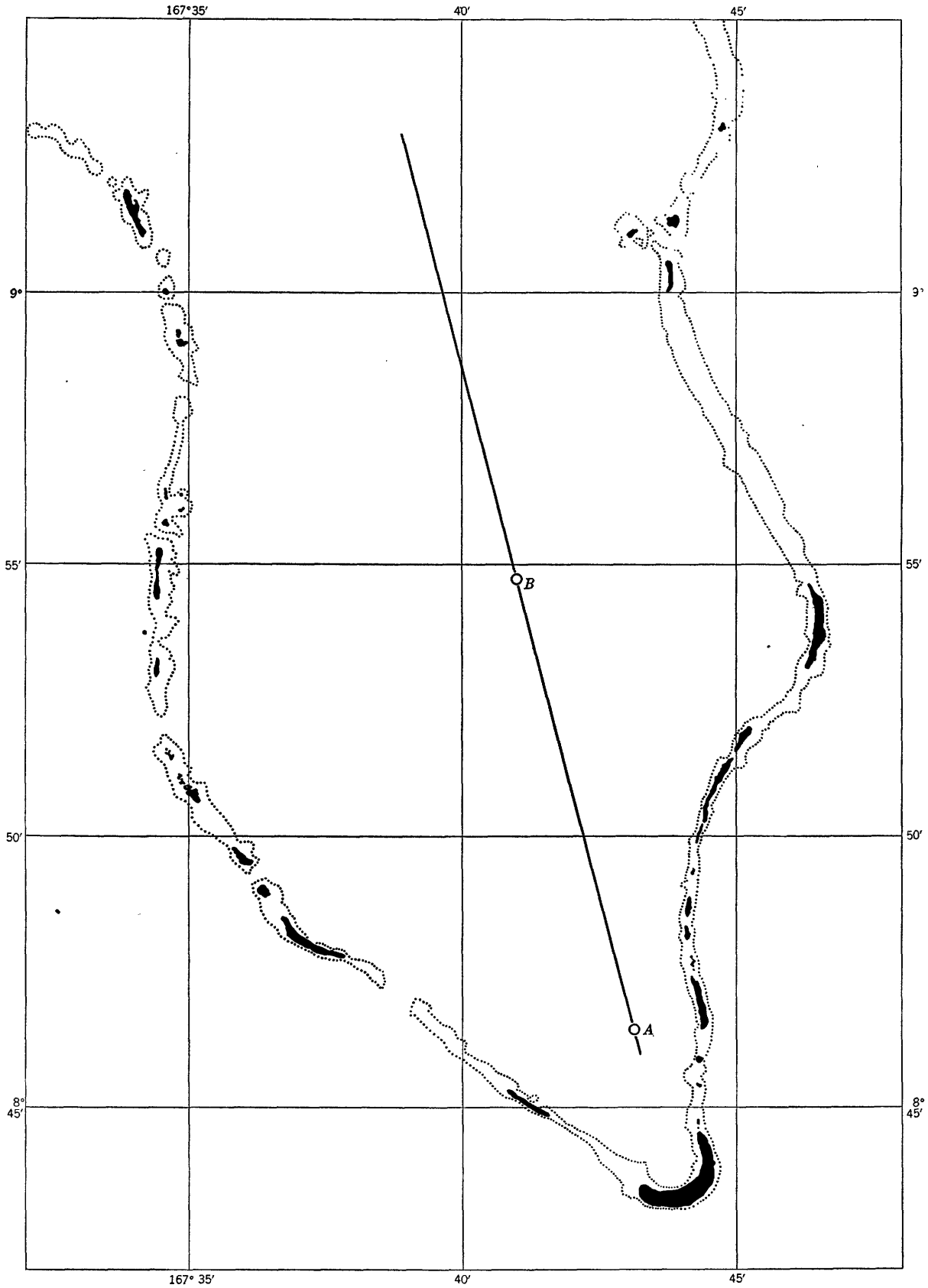


FIGURE 141.—Plan of operations in Kwajalein Lagoon.

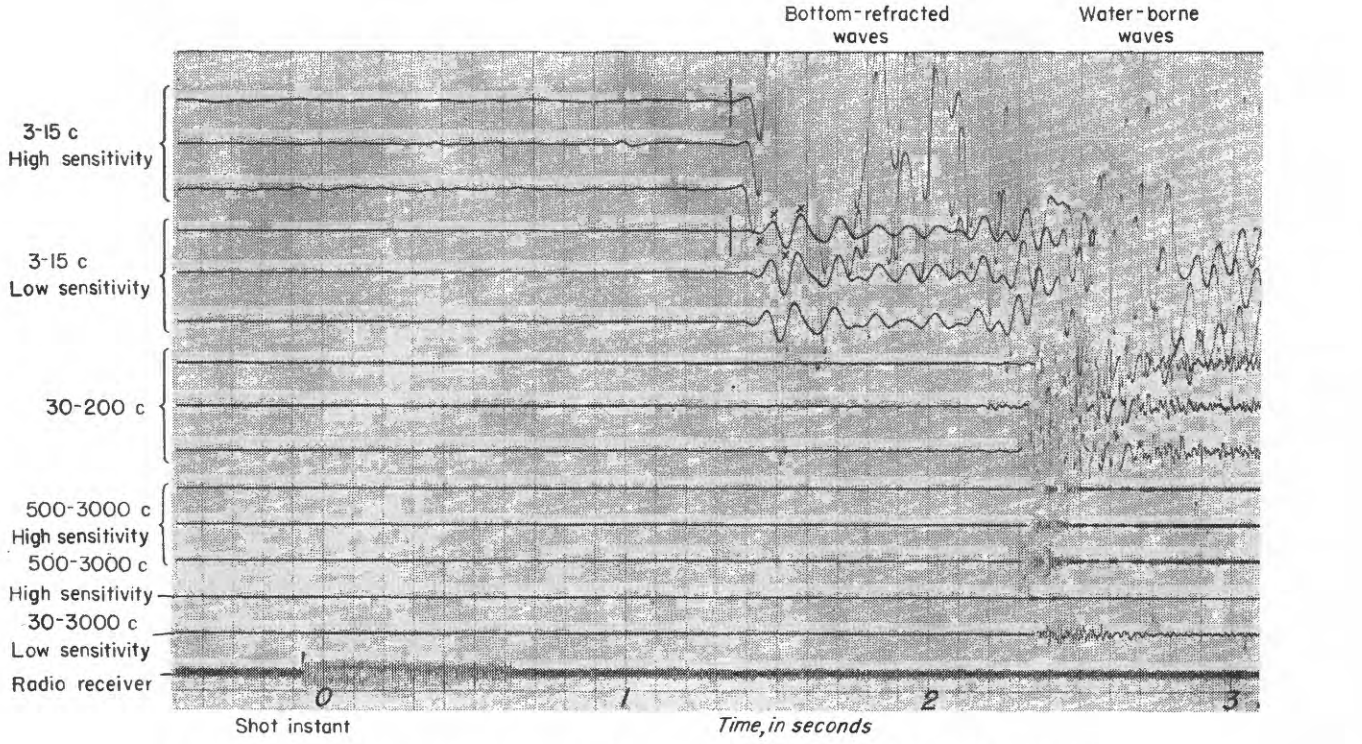


FIGURE 142.—Oscillograms illustrating bottom-refracted waves and water-borne waves. In the lower three oscillograms only the first arrivals of the bottom-refracted waves are shown.

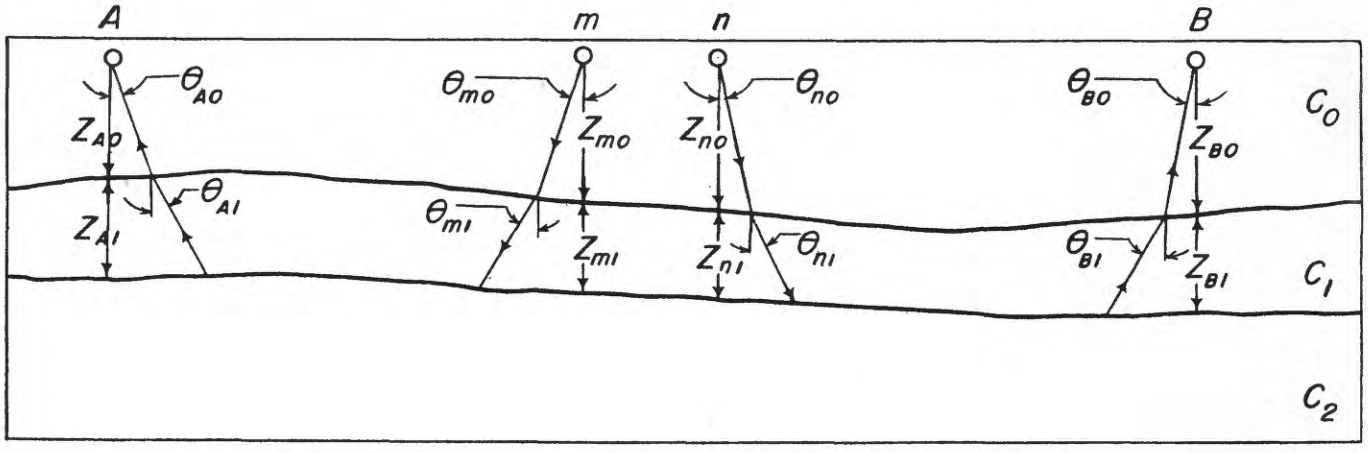


FIGURE 143.—Model of subsurface structure assumed for interpretation of the travel-time plots

The model adopted in the present survey is the conventional one, consisting of successive layers of constant velocity, with each deeper layer having an appreciably higher velocity than the one above it. This model and the interpretation methods involved in its use, have been widely discussed in the literature and in geophysics textbooks (Nettleton, 1940; Heiland, 1940); however, as the procedures used have varied somewhat, a brief discussion of the methods employed in this paper is in order.

Figure 143 illustrates a subsurface section consisting of three layers, with velocities $c_0$, $c_1$, and $c_2$, respectively. In seismic work at sea the upper layer is water. For the example illustrated, the velocities $c_1$ and $c_2$ are two and four times as great, respectively, as the water velocity, $c_0$. Two receiving stations, $A$ and $B$, and two shot points, $m$ and $n$, are shown. Sound rays are shown refracted through the third layer. The travel time, $T_{Am}$, from $m$ to $A$ is given by

$$T_{Am}=\frac{X_{Am}}{c_2}+\frac{z_{A0}\cos\Theta_{A0}}{c_0}+\frac{z_{m0}\cos\Theta_{m0}}{c_0}+\frac{z_{A1}\cos\Theta_{A1}}{c_1}+\frac{z_{m1}\cos\Theta_{m1}}{c_1}, \tag{1}$$

where $X_{Am}$ is the horizontal distance from shot to hydrophone and the $z$'s and $\theta$'s have the meaning shown in figure 143. A similar equation is obtained for travel time between $n$ and $B$. The term $(T_{Am}-X_{Am}/c_2)$ is called the "intercept time," (Gardner, 1939). The four remaining terms of equation (1) are called "delay times" and are designated $\tau_{A0}$, $\tau_{m0}$, $\tau_{A1}$, and $\tau_{m1}$, respectively.

In the typically deep Pacific Ocean, where the depths are of the order of 4 to 5 km, the second and third terms of equation (1), the "water delays", are each of the order of 3 seconds and are generally much larger than the delays pertaining to subsurface structure. Hence, when the topography is irregular the form of the travel-time plot is usually determined by bottom topography to a greater extent than by the underlying structure. These water delays are analogous to the familiar "weathering corrections" of seismic surveying on land. The first step in the interpretation of the data is to subtract them from the observed travel times. The resultant travel-time data, corrected for water delay, effectively represent the travel times that would have been observed if the shots and detectors had been placed on the sea bottom directly under the shot and detector positions.

In the profiles recorded in Bikini and Kwajalein Lagoons, the hydrophones and shots were placed close to the bottom, the water-delay corrections are very small, and the errors in the correction are negligible. In deep water, where the bottom is flat, the depth of shot point and receiver and the angles of incidence at the surface can be measured with precision, and the error of the water-delay correction is of the order of 0.01 second. Where the bottom slopes steeply and is irregular, such as on the flanks of Bikini Atoll, the error is greater, and can be of the order of 0.1 second or more.

After correction for water delay the corrected travel times $T'_{Am}$ and $T'_{Bn}$ are

$$T'_{Am}=\frac{X_{Am}}{c_2}+\tau_{A1}+\tau_{m1}$$

$$T'_{Bn}=\frac{X_{Bn}}{c_2}+\tau_{B1}+\tau_{n1}, \tag{2}$$

The velocity $c_2$ can be determined from the slopes of the reverse travel-time distance profiles received at $A$ and $B$ from shots in the central region between $A$ and $B$. For, if shot points $m$ and $n$ are placed at the same point, $dz_{n1}/dX_{Bn}=-(dz_{m1}/dX_{Am})$ and

$$\frac{\frac{dT'_{Am}}{dX_{Am}}+\frac{dT'_{Bn}}{dX_{Bn}}}{2}=\frac{1}{c_2}+\frac{(\cos\Theta_{m1}-\cos\Theta_{n1})\left(\frac{dz_{m1}}{dX_{Am}}\right)}{c_1}. \tag{3}$$

For gently sloping structures $(dz/dX)$ is small and $\cos\Theta_{m1}$ is nearly equal to $\cos\Theta_{n1}$. Hence, to a sufficient degree of approximation for nearly all cases

$$c_2=\frac{2}{\frac{dT'_{Am}}{dX_{Am}}+\frac{dT'_{Bn}}{dX_{Bn}}}. \tag{4}$$

Also, when shots $m$ and $n$ are at the same point, $\tau_{m1}$ and $\tau_{n1}$ are nearly equal and may be considered so as a first approximation. If the travel time from $A$ to $B$ can be measured by placing a shot at $B$ and receiving it at $A$ or vice versa then the delay times at $A$, $m$ and $B$ are determined by three measured intercept times,

$$T'_{Am}-\frac{X_{Am}}{c_2}=\tau_{A1}+\tau_{m1}$$

$$T'_{Bn}-\frac{X_{Bn}}{c_2}=\tau_{B1}+\tau_{m1}$$

$$T'_{AB}-\frac{X_{AB}}{c_2}=\tau_{A1}+\tau_{B1}. \tag{5}$$

Solution of these three equations gives the values of $\tau_{A1}$, $\tau_{m1}$ and $\tau_{B1}$.

The layer thicknesses $z_{A1}$, $z_{m1}$, and $z_{B1}$ are given to a first approximation by assuming that $\Theta_{A1}$, $\Theta_{m1}$, $\Theta_{n1}$ and $\Theta_{B1}$ are all equal to the critical refraction angle

$\sin^{-1}(c_1/c_2)$. With this approximation,

$$z_{A1}=\frac{c_1\tau_{A1}}{\left[1-\left(\frac{c_1}{c_2}\right)^2\right]^{\frac{1}{2}}}$$

$$z_{m1}=\frac{c_1\tau_{m1}}{\left[1-\left(\frac{c_1}{c_2}\right)^2\right]^{\frac{1}{2}}}$$

$$z_{B1}=\frac{c_1\tau_{B1}}{\left[1-\left(\frac{c_1}{c_2}\right)^2\right]^{\frac{1}{2}}} \qquad (6)$$

In the interpretation of travel times of waves through the $c_3$ layer, of higher velocity beneath the $c_2$ layer, corrections for delay in the $c_1$ layer are made in the same manner as for the water-delay correction previously described. These corrected times are then effectively those that would be observed if shots and receivers were placed on the $c_1/c_2$ interface directly beneath their actual positions. This requires knowledge of the velocity and thickness of the $c_1$ layer under all sections of the profile where penetration to the $c_3$ layer is achieved. The process outlined can be repeated indefinitely in principle. The practical difficulties and cumulative errors are severe if a large number of layers with small velocity contrast between them are present.

## TRAVEL-TIME PLOTS

The observed travel times of the bottom-refracted waves, corrected for water delay, are plotted in figures 144 to 155. For the sections outside Bikini Atoll, where there is a great variation of bottom depth, the bottom-depth profiles are shown directly below the travel-time data.

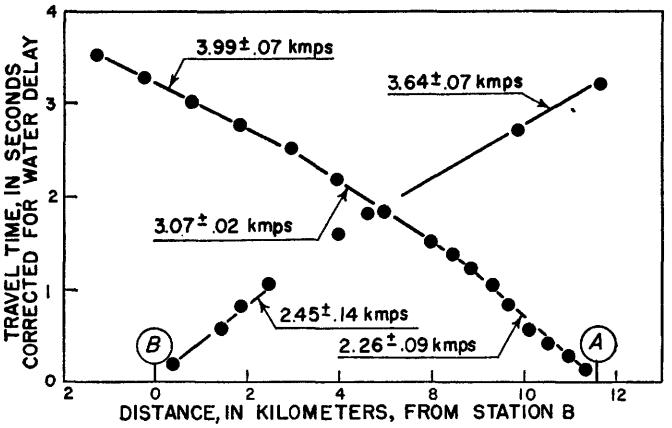


FIGURE 144.—Travel-time plots for section through stations *A* and *B*, Bikini Lagoon.

It is seen that in most of the profiles the travel-time curves can be represented by segments of straight lines. The lines drawn on the plot have been fitted by least squares to the indicated points, and the apparent velocity and standard error of its estimate are shown for each segment. Although the values of apparent velocity cover a wide range of magnitude there is a tendency to group around values of the order of 2.5, 3, 4, 5.5, 6.5, and 8 kmps, the last value being represented by a single determination at the outer end of the *K*-line southwest of the Bikini Atoll. It therefore appears that at least six velocity layers are involved in the overall structure. The first four were observed in the lagoon profiles and the last two were identified only outside Bikini Atoll.

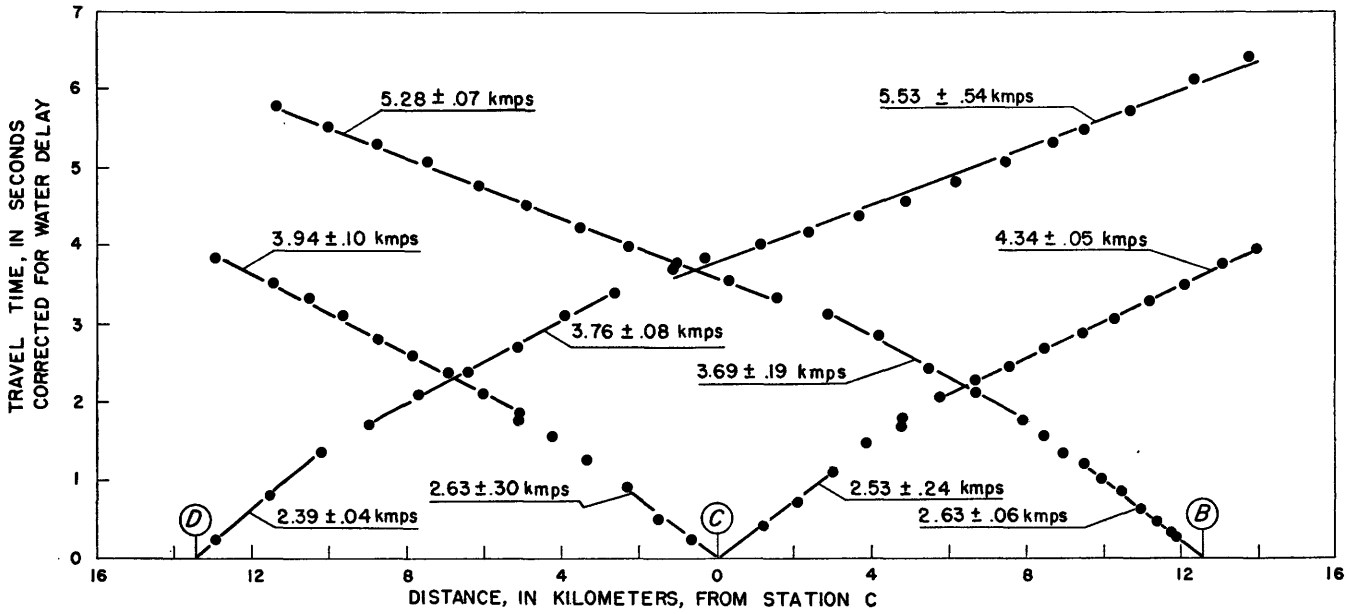


FIGURE 145.—Travel-time plots for section through stations *B*, *C*, and *D*, Bikini Lagoon.

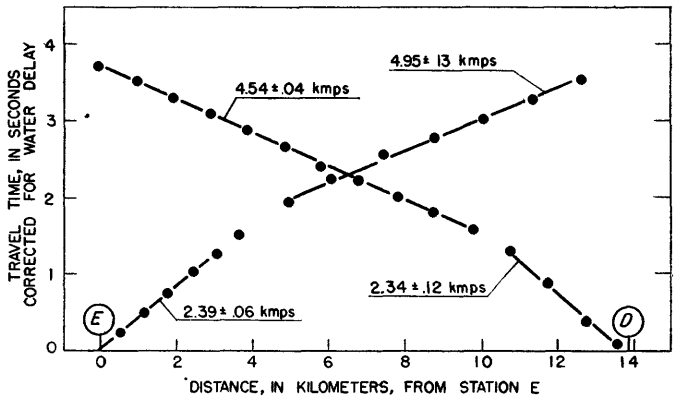


FIGURE 146.—Travel-time plots for section through stations *D* and *E*, Bikini Lagoon.

## VELOCITIES

Not all the travel-time data can be used for velocity determination. Except for the initial segment of the lagoon profiles where the seismic waves were propagated through the topmost layer, the apparent velocities can be used to determine "true" velocities of the deep formations only when paired with reversed profiles in the manner of equation (4). Even though most of the lines in Bikini Lagoon, depicted in figure 140, were traversed three times by the firing ship, the distance over any one layer in which true reverse control was established was necessarily a small fraction of the whole.

## FIRST LAYER

Observed only in Bikini and Kwajalein Lagoons, the velocity of the first layer was determined by using only the data of the first 3 kilometers of each profile. The waves penetrating the deeper, higher velocity layers are first observed at ranges beyond 3 kilometers; this insures that a systematic error will not be introduced by including some of these higher velocity data. Results for Bikini Lagoon are shown in table 1 and for Kwajalein Lagoon in table 2.

TABLE 1.—*First-layer velocities in Bikini Lagoon*

| Station | Direction | Number of shots | Velocity (kmps) | Intercept (sec) | Harmonic mean velocity (kmps) | RMS (residuals in sec) |
|---|---|---|---|---|---|---|
| A | N | 8 | 2.26±0.09 | −0.034±0.034 | ---------- | 0.05 |
| A | S | 6 | 2.68±.16 | .069±.042 | ---------- | .05 |
| A | W | 4 | 2.34±.14 | −.018±.050 | ---------- | .05 |
| A | NW | 4 | 2.50±.24 | .015±.060 | 2.43 | .07 |
| B | S | 4 | 2.45±.14 | .034±.038 | ---------- | .03 |
| B | SW | 7 | 2.63±.06 | .062±.015 | 2.53 | .02 |
| C | SW | 3 | 2.63±.30 | −.006±.072 | ---------- | .05 |
| C | NE | 3 | 2.53±.24 | −.080±.082 | ---------- | .05 |
| C | SE | 3 | 2.51±.37 | −.054±.113 | ---------- | .08 |
| C | NW | 3 | 2.80±.19 | −.019±.052 | 2.60 | .03 |
| D | NE | 3 | 2.39±.04 | −.002±.016 | ---------- | .01 |
| D | N | 4 | 2.34±.12 | −.014±.043 | 2.36 | .05 |
| E | S | 5 | 2.39±.06 | .025±.019 | ---------- | .02 |
| E | SE | 7 | 2.36±.03 | .036±.027 | 2.38 | .01 |
| G | E | 5 | 2.41±.20 | −.023±.065 | 2.41 | .08 |

TABLE 2.—*First-layer velocities in Kwajalein Lagoon*

| Station | Direction | Number of shots | Velocity (kmps) | Intercept (sec) | RMS (residuals in sec) |
|---|---|---|---|---|---|
| A | N | 7 | 2.34±0.09 | 0.018±0.030 | 0.04 |
| B | N | 5 | 2.50±.15 | .039±.043 | .04 |
| B | S | 5 | 2.45±.12 | .042±.037 | .04 |

A characteristic feature of all profiles is the large scatter from linearity. The magnitudes of the residuals are much greater than the value of 0.01 sec expected at short range if the bottom were homogeneous. How-

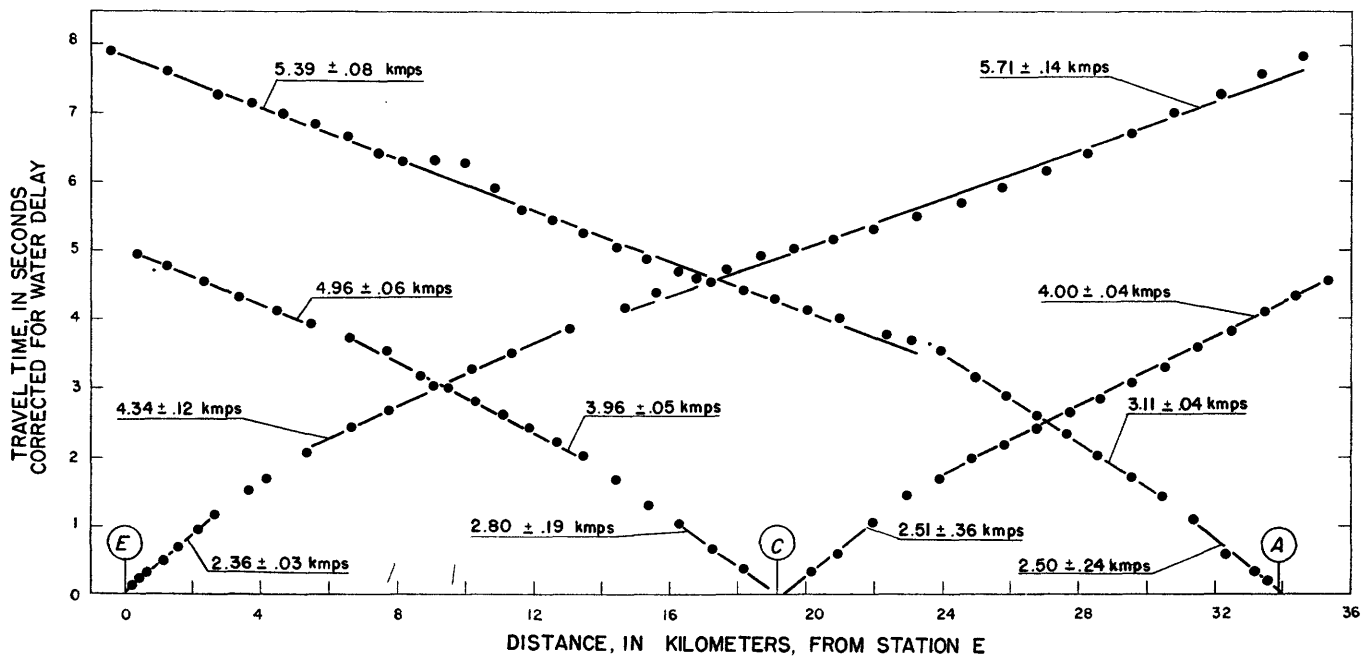


FIGURE 147.—Travel-time plots for section through stations *E*, *C*, and *A*, Bikini Lagoon.

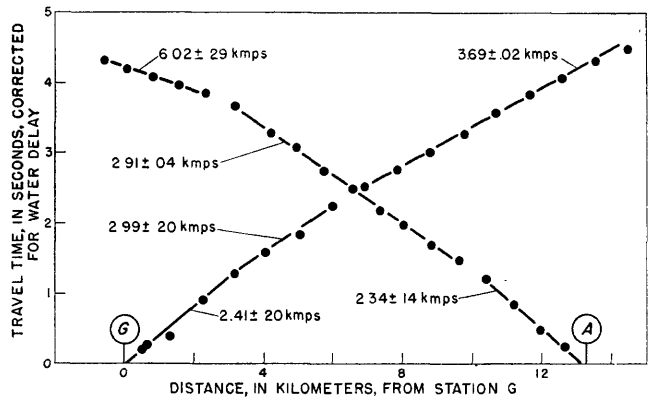


FIGURE 148.—Travel-time plots for section through stations *A* and *G*, Bikini Lagoon.

ever, they appear reasonable for a bottom formed of irregularly distributed regions of differing seismic velocity. This structure is also indicated by the irregular bottom topography, the presence of numerous coral knolls (Emery, 1948), and by the drilling under Bikini island (Ladd and others, 1948).

The highest mean velocity of any of the six stations in Bikini Lagoon was observed at station *C*, the one nearest the center of the lagoon. This effect may indicate a systematic increase of velocity from the periphery to the center. However, it is so small compared to the general variability that it may not be real. Hence, there does not appear to be any strong evidence for systematic variation of velocity of the first layer with position. The best estimate of its average velocity was taken to be the average for the six positions weighted equally. This value is 2.45 kmps. It agrees within experimental error with the up-hole times measured in the hole drilled under Bikini island (Perkins and Lill, 1948). The velocities in Kwajalein Lagoon, tabulated in table 2, do not differ significantly from the Bikini Lagoon values.

Intercepts, with few exceptions, differ from zero by less than the standard errors. There is no positive evidence that a layer with a velocity significantly less than 2.45 kmps forms the floor of the lagoon. Failure to observe a significant intercept indicates that the 2.0 kmps (6,500 fps) layer indicated in the first survey (Dobrin, 1950) has an average thickness less than 50 m. A layer having these properties would give an intercept of 0.03 sec.

## SECOND AND THIRD LAYERS

Velocities determined by equation (4) from the seven reversed profile pairs, *A–G; A–B; B–C; C–D; C–E; D–E;* and *C–A*, figures 144 to 148, ranged from 3.10 kmps for *A–G* to 4.74 kmps for *D–E*. It is concluded that velocities beneath the first layer vary with position as well as depth and that velocities 3.10 kmps and 4.74 kmps probably represent two different layers.

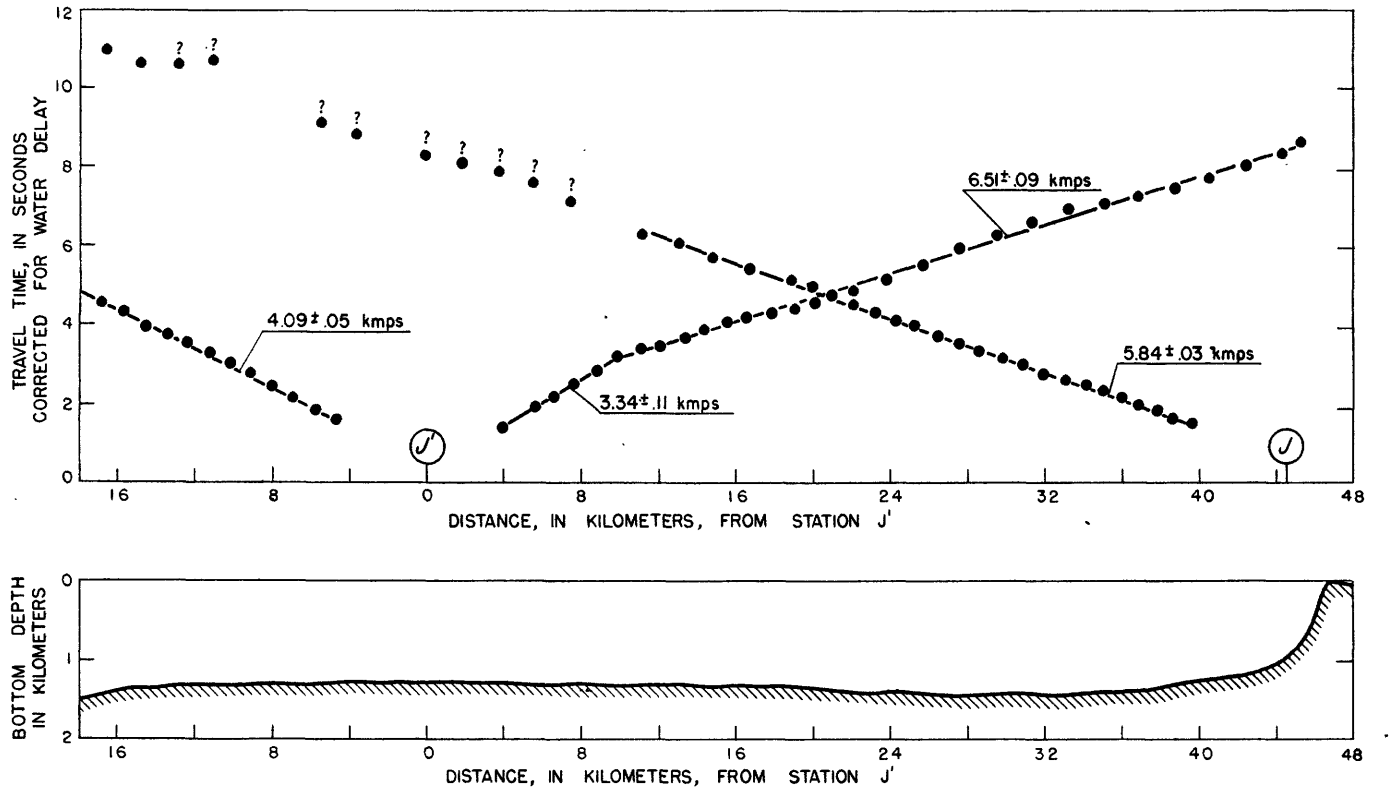


FIGURE 149.—Travel-time plots for section through stations *J* and *J'*, Sylvania Guyot.

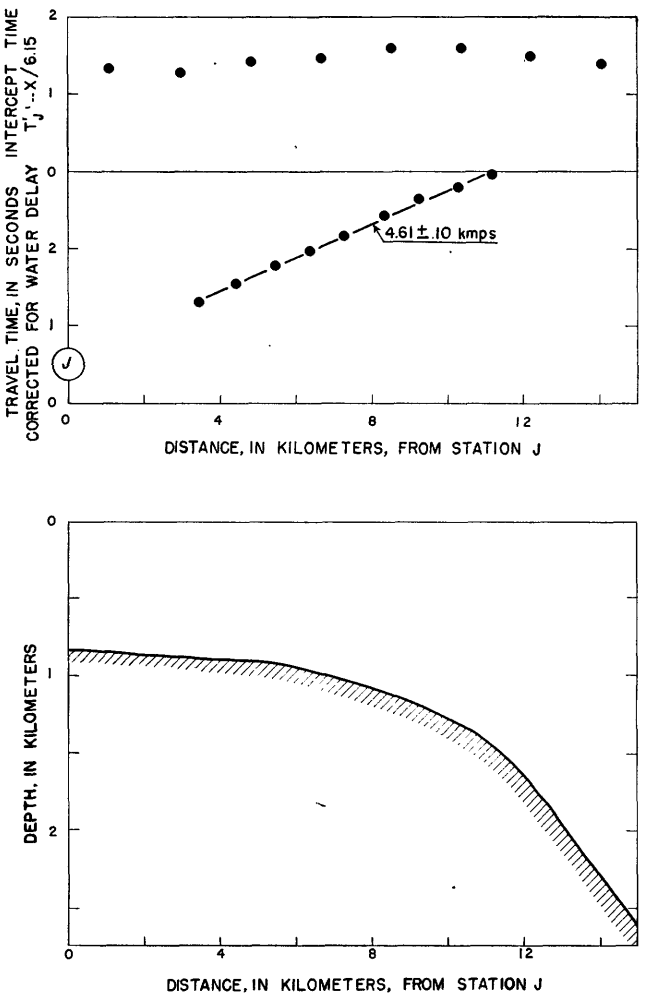


FIGURE 150.—Travel-time plots for profile extending southwest of Bikini station *J* and received at stations *J* and *J'*. The points in the upper part of the figure represent intercept times $T'_J - X/6.15$ at station *J'*.

This presents a difficulty of interpretation that was also encountered by the first survey (Dobrin and others, 1949), in which an unreversed profile in the *A–G* region also showed an anomalously low apparent velocity. Although the problem presented does not have a unique solution for the available data, the solution which appears to be the simplest and most reasonable, while at the same time consistent with the travel-time data, requires two layers to include the velocity range 3.10 kmps to 4.74 kmps. The upper one, designated the second layer, is well expressed only in the reversed-profile pair *A–G* which is used to determine its velocity, 3.10 kmps. The third layer is expressed in the second segments of the reversed-profile pairs *B–C; C–D; D–E; E–C*. In these profiles the wave refracted through the second layer is suppressed entirely by the prior arrival of the waves through the third layer, or its presence is indicated only as a short transition between the first and second principal segments of the travel-time curves. The velocities of the third layer determined from these four reversed-profile pairs are: *B–C*, 3.98 kmps; *C–D*, 3.84 kmps; *D–E*, 4.74 kmps; *E–C*, 4.13 kmps. The two remaining reversed pairs, *A–B* and *A–C*, were not used for velocity determinations of the second or third layer, because of ambiguity of travel paths for these profiles.

### FOURTH LAYER

Each of the long profile pairs *B–D* and *E–A* of figures 145 and 147 have outer segments whose apparent velocities average around 5.5 kmps. They are assumed to represent waves refracted through the fourth layer. Systematic departures of the travel time from the straight lines determined by least squares occasionally amount to about 0.2 to 0.3 sec. This is not an unexpected result, for it could be attributed to variations of velocity and thickness of the material above the fourth layer. A more serious anomaly is the fact that the fourth-layer velocity, determined by equation (4) in the overlap region of E–A reversed profile, varies with position along the profile. Hence, it was felt to be unsafe to base the determination of the fourth-layer velocity on the small overlapping central portion of A–E reversed-profile pair. A compromise solution adopted was to apply equation (4) to the two long segments at the ends of the reversed pair A–E. This yielded the value 5.54 kmps, which was assumed for the fourth layer throughout Bikini and Kwajalein Lagoons.

The long reversed profile pair, *J–J'*, figure 149, extending over Sylvania Guyot northwest of Bikini Atoll gives a velocity of 6.15 kmps, a value significantly greater than 5.54 kmps, but perhaps not enough greater to be regarded as a different material. Comparison of reversed slopes at individual points along the profiles shows that here too velocity varies with position. The systematic difference between the Bikini and Sylvania velocities is no greater than the differences indicated along this one section and does not necessarily indicate that the fourth layer is significantly different in the two areas.

### FIFTH LAYER

In the deep-water profiles, *K'–K''*, *A–A'*, and *H–H'*, figures 151, 152, and 153, principal segments have apparent velocities of the order of 6.5 kmps, a value which indicates that this layer corresponds to that observed at all 15 deep-water areas studied in the deep Pacific Ocean basin, a layer which has an average velocity of about 6.7 kmps (Raitt, 1951). Its velocity in the Bikini area was determined from the reversed-profile pair *K'–K''* to be 6.53 kmps.

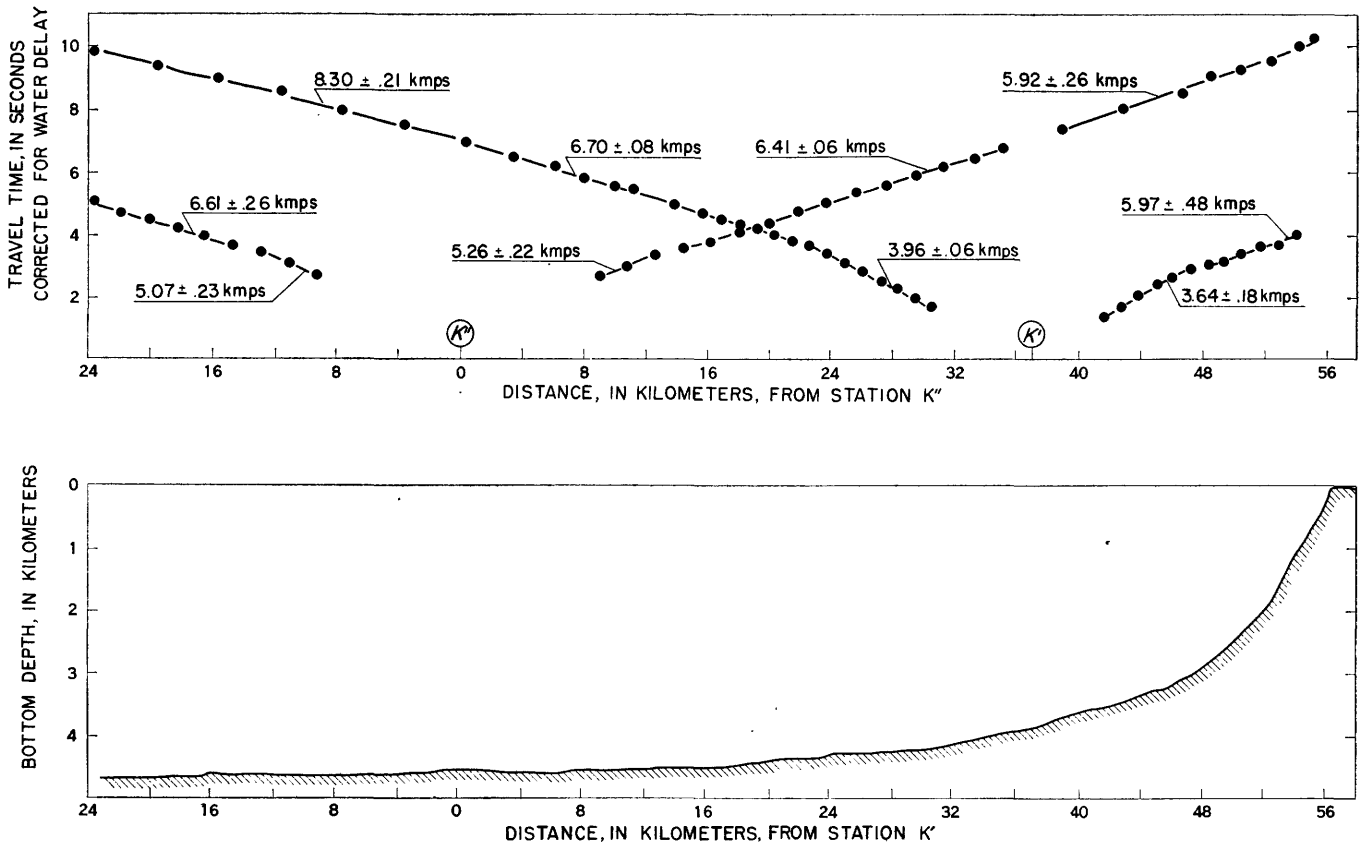


FIGURE 151.—Travel-time plots for section through stations $K'$ and $K''$ southwest of Bikini Atoll.

### SIXTH LAYER

The outer segment of the 60-km profile extending southwest of $K'$ through $K''$ has an apparent velocity of $8.30 \pm 0.21$ kmps. Although a reversed profile for this segment was not obtained, the fact that the short profile from station $K''$ over the same area gives an apparent velocity of 6.61 kmps shows that this high velocity cannot represent a steep upward slope of the 6.53 kmps layer. Correction for the gentle slope indicated by the 6.61 kmps velocity yields a value of 8.2 km/sec for the sixth layer velocity. This agrees with values observed elsewhere in the Pacific Ocean (Raitt, 1951), and corresponds to the velocities found at the Mohorovičić discontinuity at the base of the earth's crust (Gutenberg and others, 1951).

## STRUCTURE

### INTERPRETATION

Depths to interfaces between the six velocity layers have been determined, using the procedure outlined in the previous section on the theory of interpretation. They are presented in figures 156 to 159, in the form of subsurface cross sections. Figure 156 represents a section extending the length of the Sylvania-Bikini axis, through stations J', J, E, C, and A. The section on figure 157 extends across Bikini Atoll from southwest to northeast and runs through stations K'', K', D, C, B, H, and H'. Figure 158 extends southerly from Bikini Lagoon through stations B, A, and A' into deep water south of Bikini Atoll. It is the only section having profiles crossing the edge of the atoll from the lagoon to deep water and vice versa. Figure 159 represents the short section observed in Kwajalein Lagoon.

In each figure the stippled portions of the interfaces represent sections along which shots have been received with velocities corresponding to strata just below the stippled interface. The dashed interfaces have been assumed in order to calculate the depth to deeper strata.

The velocities used in calculating the layer thicknesses are shown on the sections. In sections where the velocity was not directly measured, assumed values based on apparent velocities and measurements of the same strata elsewhere were used. Wherever this was done, the assumed values are enclosed in parentheses.

For example, at station $K'$ the initial segment represents the material at or near the bottom surface. Its velocity, determined by averaging the two profiles, was determined to be 3.79 kmps, a value corresponding to that of the third layer. In the other deep-water

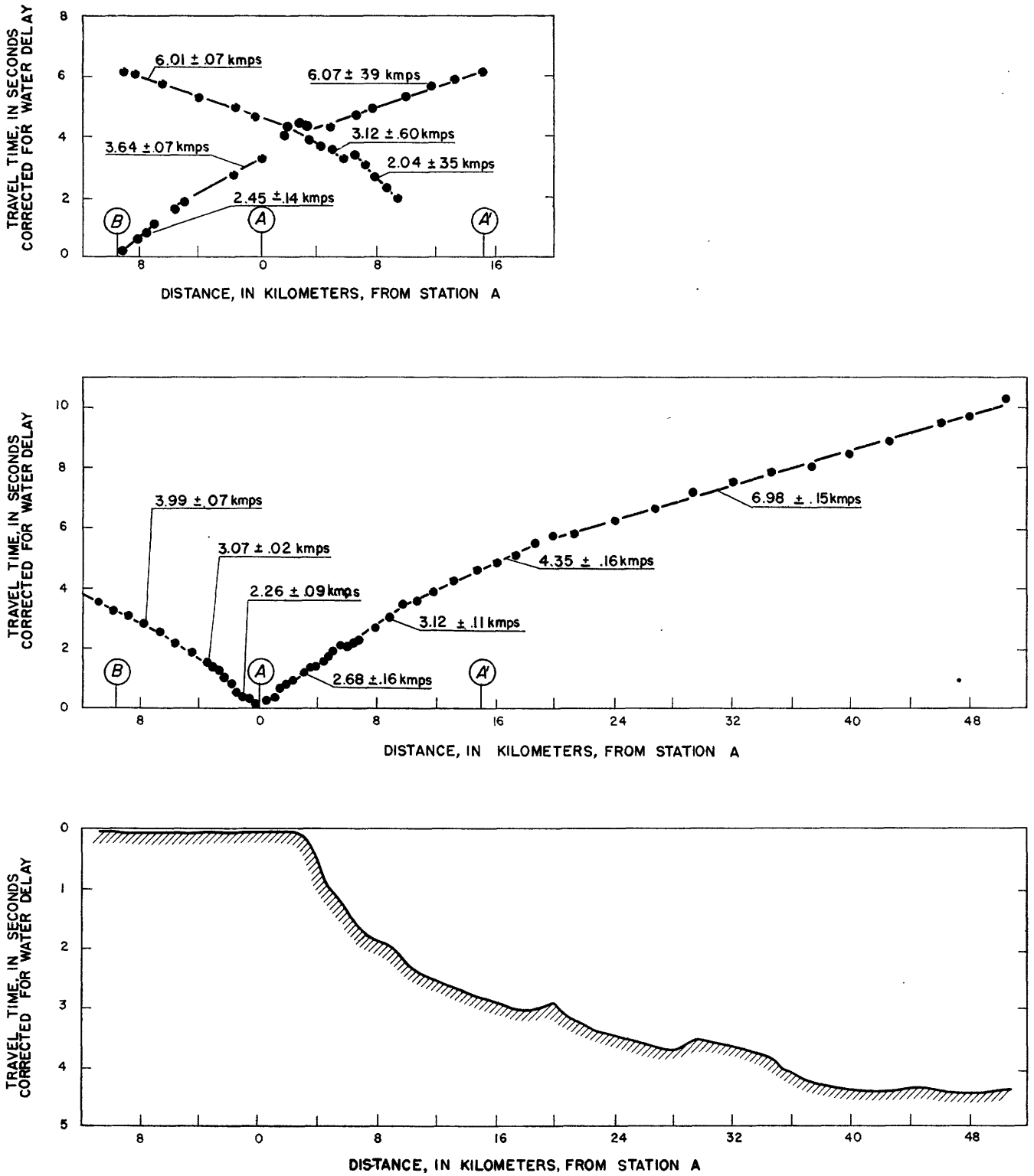


FIGURE 152.—Travel-time plots for section through stations *B*, *A*, and *A'*, extending from Bikini Lagoon into deep water south of the atoll. The data previously shown in figure 144 are repeated for comparison.

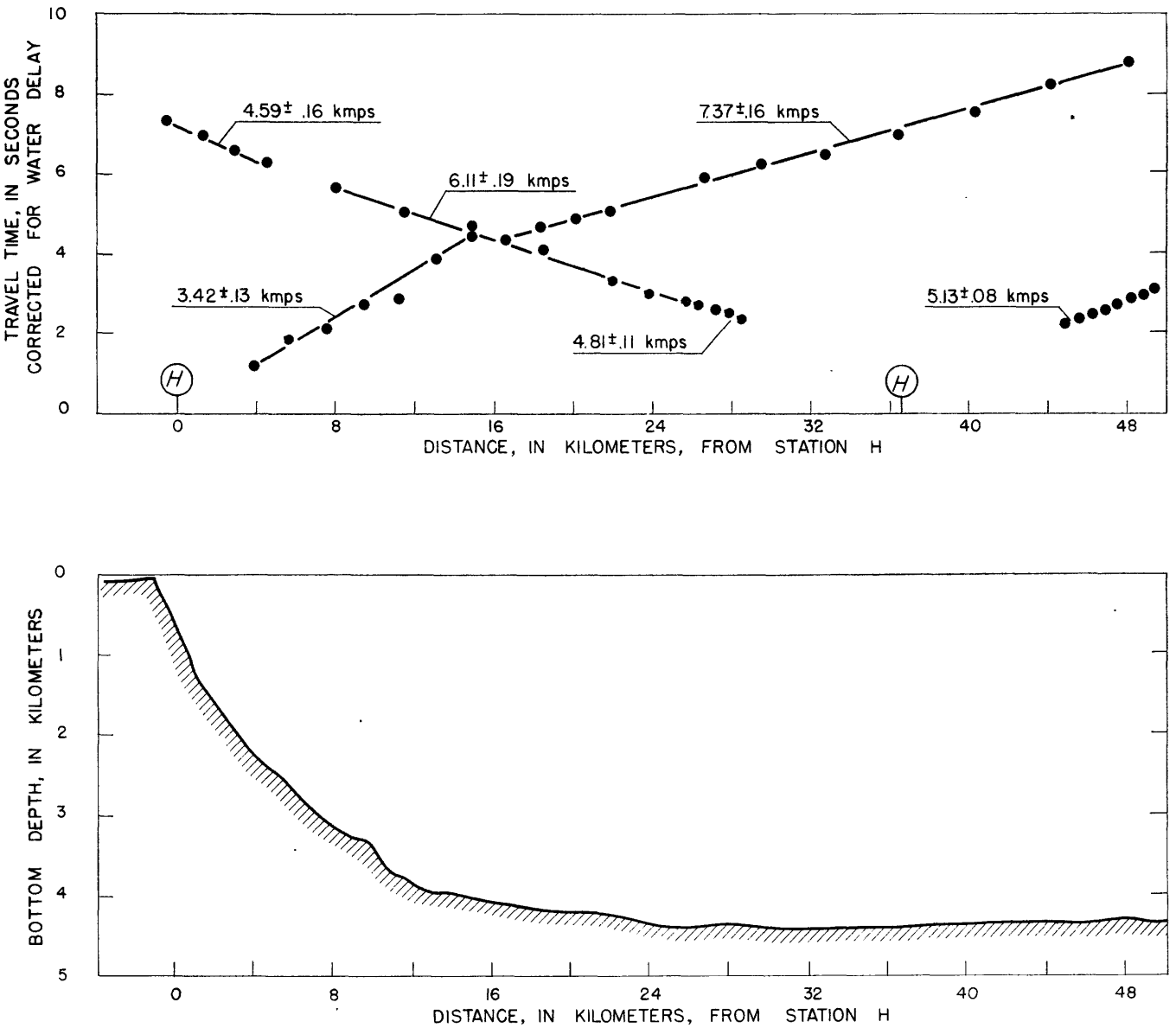


FIGURE 153.—Travel-time plots for section through stations $H$ and $H'$ northeast of Bikini Atoll.

cross sections, however, the velocity of the layer exposed at the bottom was not determined. Hence, 3.79 kmps was assumed for the upper layer of the lower slopes of the atoll in profiles $H$—$H'$ and $A$—$A'$.

In deep water well away from Bikini Atoll, where the bottom is flat, sediment is being deposited and the velocity is lower. The value 3.0 kmps was assumed to be reasonable in this area for the average value of the upper layer.

Owing to the fragmentary nature of the subsurface control, the horizontal variation of velocity, and the great changes of depth in the subsurface structure, the cross sections shown are necessarily highly schematic. No attempt was made to compute depths shot by shot for each of the 617 shots of the survey. Depths were computed at the receiving station and at a few control points between stations. Interfaces between between these points were then sketched in with reference to the travel-time data. This procedure yields a hypothetical structure whose calculated travel times agree on the average within about 0.1 sec with the observed travel time. It tends to give some smoothing of the interfaces because there is no way of separating the relative effects of velocity changes and topographic roughness in producing minor irregularities of travel time. However, this does not mean that the seismic interpretation always tends to show a reduction in the magnitude of the relief. An illustration of the reverse is the sharp change of depth to the fourth layer between stations $E$ and $J$, which is probably an interpretation

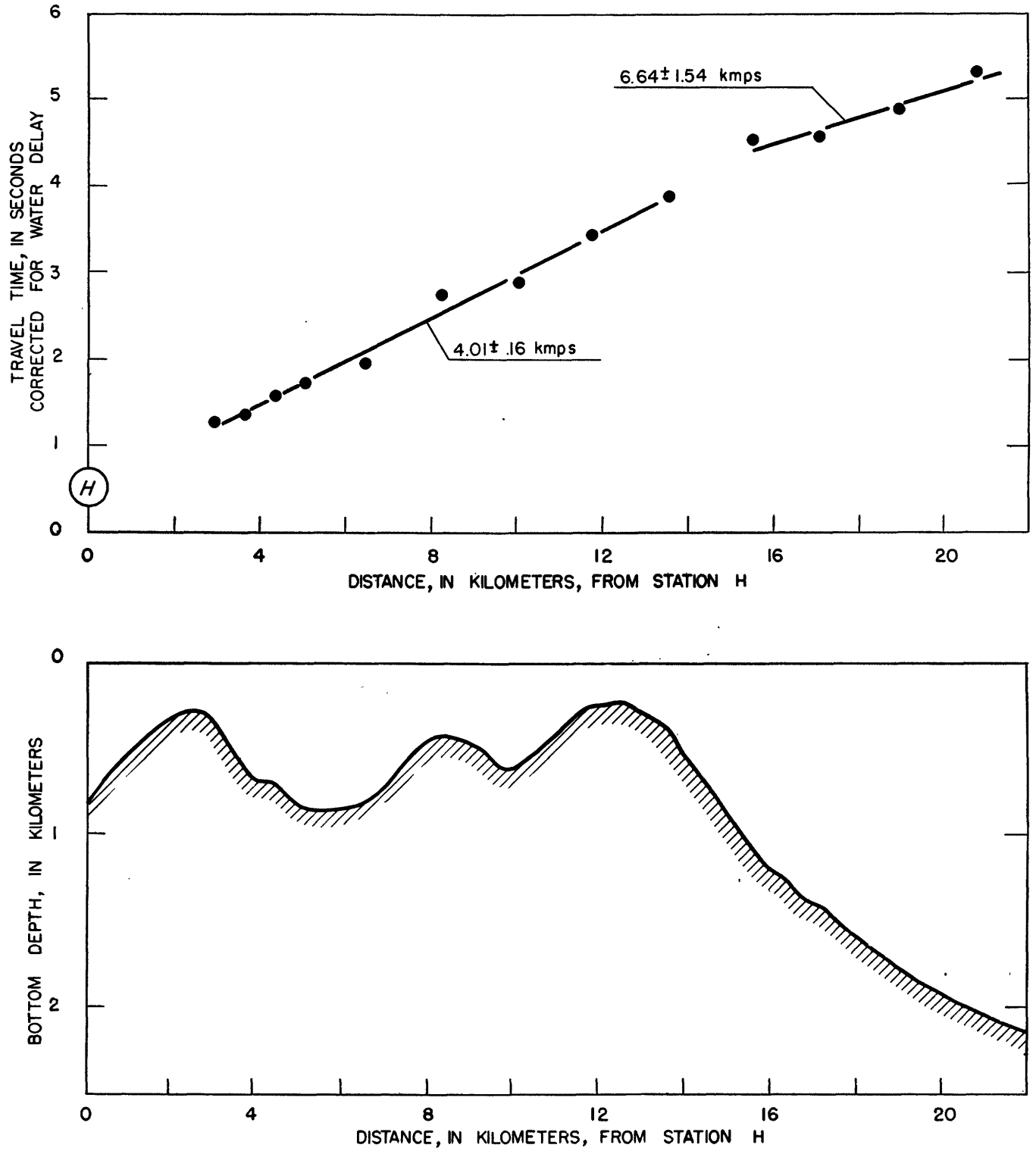


FIGURE 154.—Travel-time plot for section extending south from station *H* along the eastern side of Bikini Atoll.

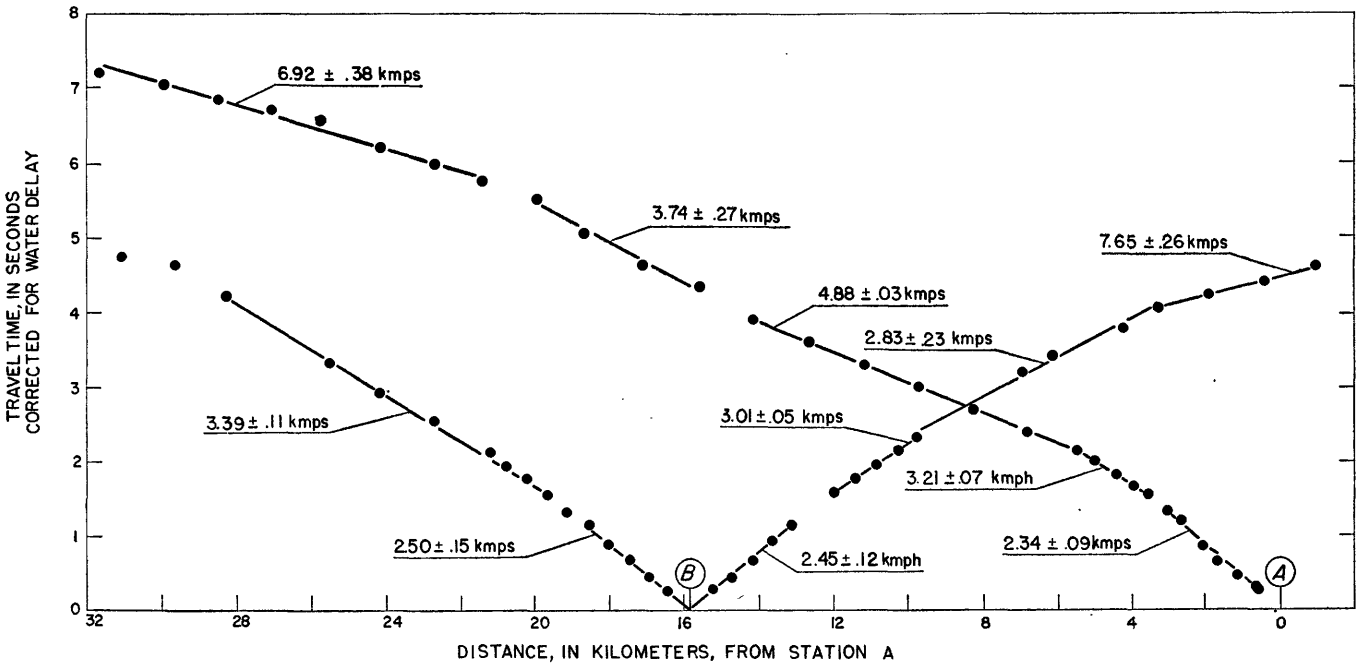


FIGURE 155.—Travel-time plots for section through stations *A* and *B*, Kwajalein Atoll.

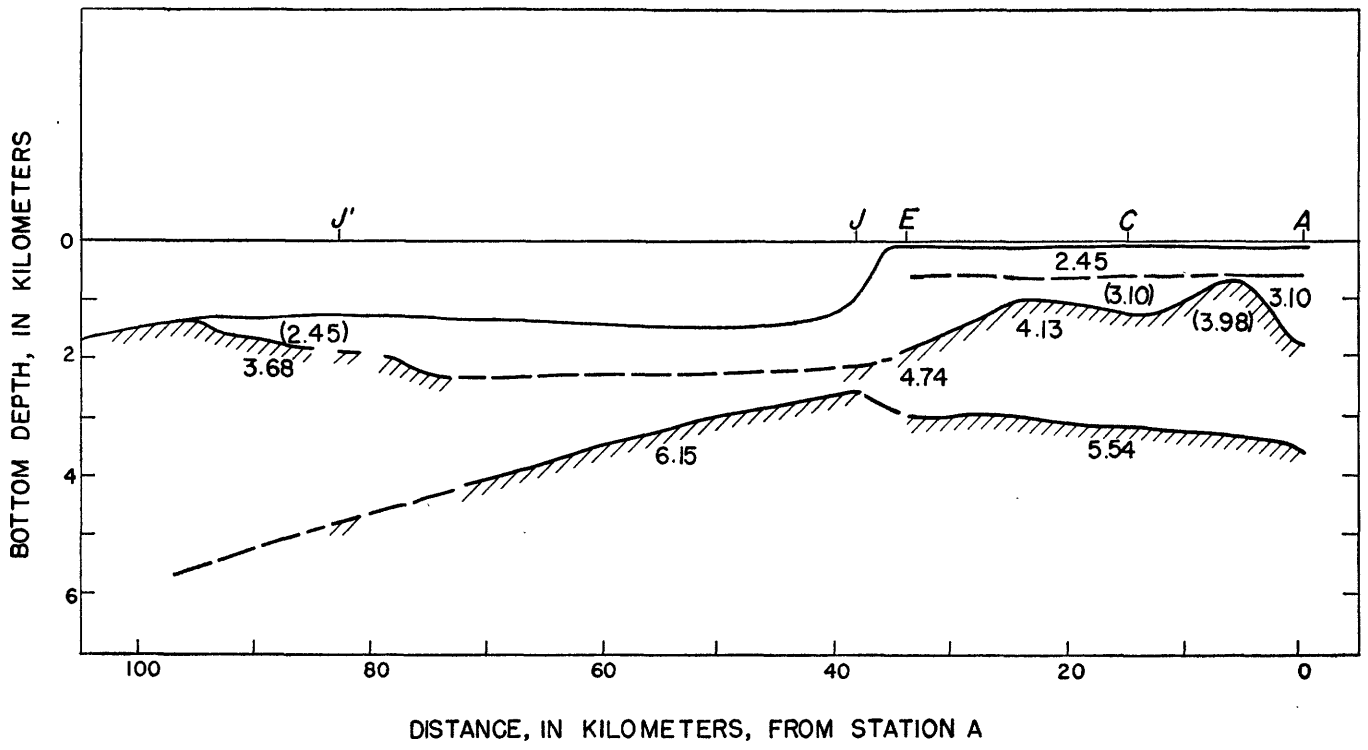


FIGURE 156.—Hypothetical cross section of Sylvania Guyot and Bikini Atoll through stations *J'*, *J*, *E*, *C*, and *A*.

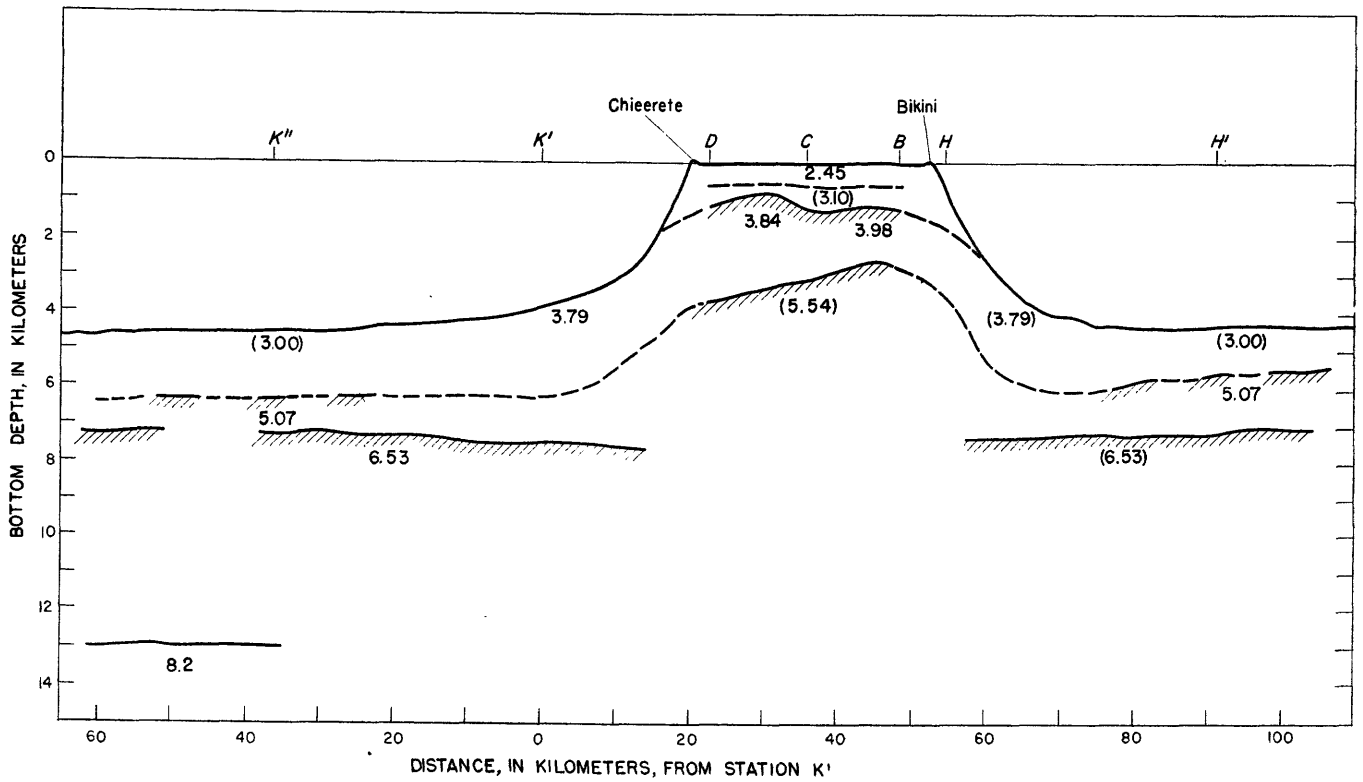


FIGURE 157.—Hypothetical cross section across Bikini Atoll through stations $K''$, $K'$, $D$, $C$, $B$, $H$, and $H'$.

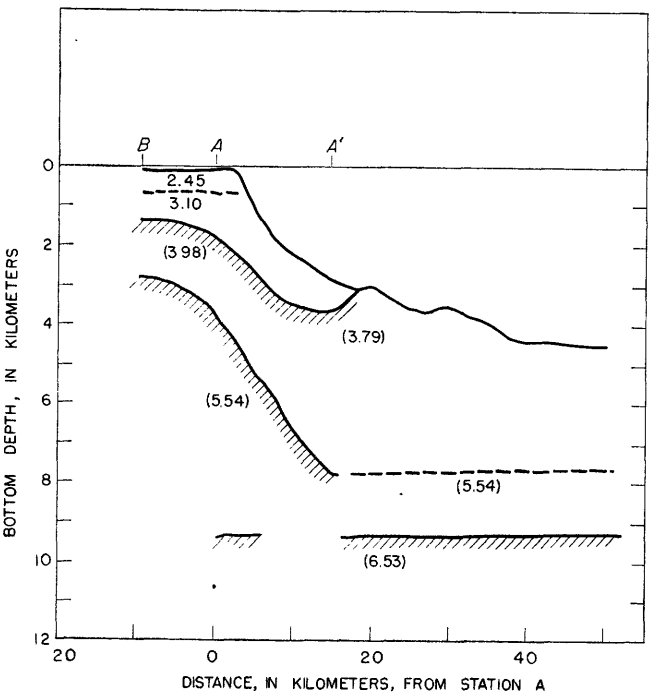


FIGURE 158.—Hypothetical cross section from Bikini Lagoon south through stations $B$, $A$, and $A'$.

error caused by the arbitrary change of assumed velocity between stations $E$ and $J$.

## ERRORS OF INTERPRETATION

Although it is clear that other structure sections differing from those of figures 156 to 159 may agree reasonably well with the travel-time data, it is not clear how great a permitted variation from these sections can be. There are many factors affecting the error of depth of measurement and they operate in varying degree in different regions of the survey. In general, they can be lumped into three categories: (1) errors of measurement of the travel time, (2) errors of velocity, and (3) errors in the interpretation of the path traveled by the refracted wave.

Errors in category (1) have been discussed in previous sections and are rarely greater than 0.10 sec. Errors in category (2) depend not only on the accuracy of the velocities of the material through which the waves can travel but also on the path length. Hence, they are greater for distant shots and deep layers and may amount effectively to several tenths of seconds, particularly for cases having poor velocity control.

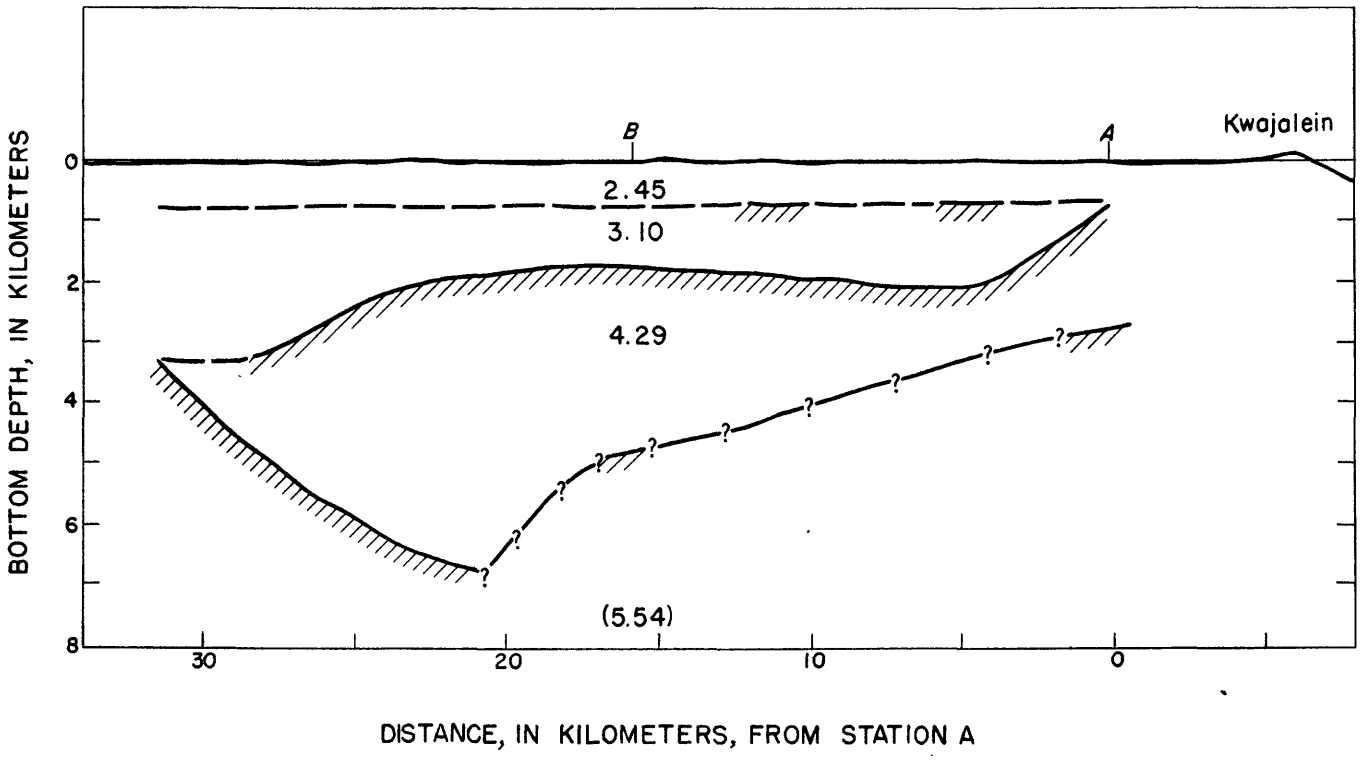


FIGURE 159.—Hypothetical cross section of Kwajalein Lagoon through stations *A* and *B*.

Category (3) is the most difficult to specify because it involves departures of the true structure from the assumed model in a manner which cannot be determined from travel-time data alone. It is probably least important for the Bikini Lagoon profiles, where the detailed shot pattern provides the most complete control.

The greatest uncertainty in this category occurs in those portions of the three deep-water cross sections *A–A'*, *K'–K''*, and *H–H'* which lie under the steep flanks of Bikini Atoll. Travel-time data are insufficient to determine the continuity of interfaces between the lagoon and deep water outside. This is to a great extent a fundamental indeterminancy in this complex type of structure, which is far from the "ideal" simple situation required for a unique solution (Nettleton, 1940, p. 255). In addition, it is aggravated by sparse velocity control.

Although the nebulous character of the errors in category (3) renders a precise statement impracticable, reasonable estimates of the depth errors would allow the order of 100 m to 200 m for the shallower strata under Bikini and Kwajalein Lagoons and as much as 3 km for the 6.53 kmps layer under the flanks of Bikini Atoll. In the relatively horizontal structures in deep water far from Bikini Atoll and in the deep layers beneath Bikini Lagoon and Sylvania Guyot the depths may be in error by the order of ½ km to 1 km.

## DISCUSSION

Even though many details are missing and much of the picture is subject to considerable uncertainty, most of the major features of the subsurface structure of Bikini Atoll and Sylvania Guyot are shown by the seismic cross sections. The geological significance of all of these features requires detailed study of the palaeontology and petrology of the bottom samples and the deep boring in the Bikini area and throughout the Marshall Islands as well. Other pertinent geophysical data such as the magnetic studies of Aldredge and Dichtel (1949) should also be considered.

The coordination of this great and complex quantity of observations is beyond the scope of this report and has been treated elsewhere (Emery, Tracey, and Ladd, 1954). However, it is appropriate to close with a discussion of the most significant contributions of the 1950 seismic studies to this problem. These involve two principal aspects: (1) the form of the ancient volcano now buried by calcareous deposits and (2) the local distortion of the crust accompanying the formation of a guyot and an atoll.

Regarding the first aspect, it now appears probable that the third layer, whose velocity is of the order of 4 kmps, represents volcanic rock. There are little data in the literature (Birch, 1942; Gutenberg, 1951) to support this conclusion. Some data on basalt

(Brockamp and Wolcken, 1929) give 5.6 kmps, which is about that observed for the fourth layer. However, this probably represents plateau basalt, whose elastic moduli are expected to be higher than for lavas and pyroclastic deposits forming a volcano. That velocities of volcanic rock of Pacific islands are variable and of the order of 4 kmps is shown by unpublished observations by the writer in shallow water off the northeast coast of Hawaii Island. Reversed profiles in this area indicated that velocities of the upper layers are variable and of the order of 3 to 4 kmps. Velocities of the order of 6 kmps were found only at depths of at least 2 km. Similar results were found at Guadalupe Island, a recent extinct volcano off the coast of Mexico.

Two seismic refraction studies have been made near Bermuda, an island which a deep boring has shown to be composed of volcanic rock below about 250 ft subsea (Pirsson and Vaughan, 1913; Pirsson, 1914; Sayles, 1931). Seismic velocity determined by Woollard and Ewing (1934) was 4.9 kmps and by Gaskell and Swallow (1951) was 4.1 kmps.

Furthermore the variability of velocity observed for the third layer is quite reasonably explained in terms of the great variability of physical structure of the various types of rock emitted in volcanic eruption. On the other hand, the variations in velocity and topography in the third layer are unreasonable for a structure formed of an orderly succession of calcareous shallow-water deposits similar to those now being laid down in view of the absence of any systematic variation of velocity of the first layer in Bikini Lagoon.

Direct evidence for the identification of the third layer as volcanic is found in the presence of volcanic rocks on Sylvania Guyot and on the southern slopes of Bikini Atoll, (Emery, Tracey, and Ladd, 1954). In both areas the seismic data indicate that the third layer crops out. However, on the guyot the outcrop is indicated only at the northwest end. Although velocity control is incomplete much of the guyot appears to be covered with a layer of undertermined velocity significantly less than 3.68 km/sec. This layer may be largely composed of calcareous sand, but it may also contain a high proportion of volcanic sand and gravel similar to that found below the calcareous deposits in the deep boring of Bermuda Island.

Beneath Bikini Lagoon the depth of the third layer averages about 1.3 km, closely approximating the average depth of Sylvania Guyot. Its relief is considerable, being of the order of 1½ km from greatest to least calculated depth. The highest point determined in the survey was found about two-thirds of the distance from station $C$ to station $A$ where its estimated depth is 0.6 km. At the periphery of the lagoon the depths are systematically greater. Although no depth determinations were made under the islands of Bikini Atoll rough estimates from interpolation on the $K''$ to $H'$ cross sections of figure 157 indicates that the depth under Chieerete and Bikini islands is about 1.5 km.

The short section under Kwajalein Lagoon shown in figure 159 exhibits the same principal features as the Bikini sections. Although minor differences are apparent there is no basis for concluding that Kwajalein differs significantly in subsurface structure from Bikini.

Regarding the second major aspect—the local depression of the crust beneath Bikini—the sections of the profile of greatest interest are also those having the greatest error of depth determination—that is, the sections running from deep water to the lagoon. Hence, any conclusion concerning them must be qualified by this uncertainty.

If it is assumed that prior to the beginning of the volcanic eruption the fifth layer, of 6.53 kmps velocity, was approximately flat in the Bikini region, then the eruption should be accompanied by a down-warping of the crust in order to fill the void that would otherwise be created by the withdrawal of the material erupted. The magnitude of the depression of the crust will depend on such factors as the densities of the volcanic rock and of the magma from which it is derived, the degree of isostatic compensation, and the depth from which the erupting rock is derived. One of the key problems in the study of the mechanics of volcanic eruption and the related problem of the yielding of the earth's crust, is to know whether or not this depression takes place locally under the volcano or is regionally distributed (see, for example, Daly, 1942; Vening Meinesz, 1941; Woollard, 1951).

From the illustrated cross sections the evidence appears to favor a depression of the 6.53 kmps layer. It is only slightly indicated in the $H$–$H'$ and $K'$–$K''$ profiles, and amounts to about 2½ km for the $A$–$A'$ section. This is of the same order of magnitude as the estimated-depth error and can hardly be regarded as significant without further work supporting it. Hence, it is concluded that if there is a local depression of the crust it is less than 3 km.

## SELECTED REFERENCES

Alldredge, L. R. and Dichtel, W. J., 1949, Interpretation of Bikini magnetic data: Am. Geophys. Un. Trans. v. 30. p. 831–835.

Birch, Francis [Editor], 1942, Handbook of physical constants: Geol. Soc. America Special Papers, no. 36.

Brokamp, B., and Wolcken, K., 1929, Zietschr fürs Geophysik: v. 5, no. 34, p. 163–171.

Daly, R. A., 1942, The floor of the ocean: p. 62 ff, Univ. of North Carolina Press.

Dobrin, Milton B., 1950, Submarine geology of Bikini Lagoon as indicated by dispersion of water-borne explosion waves: Geol. Soc. Am. Bull. v. 61., p. 1091–1118.

Dobrin, M. B., Perkins, Beauregard, Jr., and Snavely, B. L., 1949, Subsurface constitution of Bikini Atoll as indicated by a seismic-refraction survey: Geol. Soc. Am. Bull. v. 60, p. 807–828.

Emery, K. O., 1948, Submarine geology of Bikini Atoll: Geol. Soc. Am. Bull., v. 59, p. 855–860.

Emery, K. O., Tracey, J. I., Jr., and Ladd, H. S., 1954, Bikini and nearby atoll; Part 1: U. S. Geol. Survey Professional Paper 260–A.

Gardner, L. W., 1939, An areal plan of mapping subsurface structure by refraction shooting: Geophys., v. 4, p. 247–259.

Gaskell, T. F., and Swallow, J. C., 1951, Seismic refraction experiments in the North Atlantic: Nature, v. 167, p. 723–724.

Gutenberg, Beno and others, 1951, Internal constitution of the earth: 2d ed., New York, Dover Pub., Inc.

Heiland, C. A., 1940, Geophysical exploration, New York, Prentice-Hall.

Kuwahara, S., 1939, Velocity of sound in sea water and calculation of the velocity in sonic sounding. Hydrographic Rev. (Monaco), vol. 16., p. 123–140.

Ladd, H. S., Tracey, J. I., and Lill, G. G., 1948, Drilling on Bikini Atoll, Marshall Islands. Science Vol. 107. p. 51–55.

Nettleton, L. L., 1940, Geophysical prospecting for oil. New York, McGraw-Hill.

Perkins, Beauregard, Jr., and Gordon G. Lill, 1948, Velocity studies on Bikini island: Office of Naval Research, Monthly Res. Rept., p. 13–17, July 1.

Pirsson, L. V., and Vaughan, T. W., 1913, A deep boring on Bermuda Island. Am. Jour. Sci. v. 36, p. 70–71.

Pirsson, L. V., 1914, Geology of Bermuda Island. I. The igneous platform. II. Petrology of the lavas: Am. Jour. Sci., vol. 38, p. 189–344.

Raitt, R. W., 1951, Seismic refraction studies of the Pacific Ocean basin. Paper delivered at Annual Meeting, Seismol. Soc. America, March 23 and 24.

Sayles, Robert W., 1931, Bermuda during the ice age: Am. Acad. Arts. and Sci. Proc., v. 66, p. 381–467.

Vening Meinesz, F. A., 1941, Gravity over the Hawaiian Archipelago and over the Madeira area: Nederl. Acad. Wetensch. Proc., v. 44.

Woollard, George P., 1951, A gravity reconnaissance of the Island of Oahu: Am. Geophys. Union. Trans., v. 32, p. 358–368.

Woollard, George P., and Ewing, Maurice, 1939, Structural Geology of the Bermuda Island: Nature, v. 143, p. 898.

## COORDINATION OF SEISMIC DATA, BIKINI ATOLL

By Beauregard Perkins, Jr.

The two seismic surveys of Bikini Atoll differed greatly in character. The survey of 1946, which was reconnaisance, provided velocity information of the various horizons at only a few points. It was without reverse control except on one profile and then only for the deepest horizon. The 1950 survey, on the other hand, provided excellent velocity control and added much detail to the subsurface picture. The first survey provided velocity information of the first and second zone at only two points in the lagoon, one at Enyu island and the second at Yurochi island. Of these two locations only the first corresponds in location to profiles of the second survey. The first survey being so sketchy, several pictures of the subsurface could be fitted to the data, and actually three possible pictures were proposed. Only general features of the results of the two surveys can be expected to match.

The following general features are shown by both surveys:

a. A surface zone of uniform thickness.
b. The basement (velocity 5.54 kmps) rises from Enyu toward the northwest.
c. An anomalous velocity situation exists in the southeast corner of the lagoon.

In the vicinity of Enyu island where the velocity in zones 1 and 2 were determined in both surveys, the agreement was very good. In the first survey along the Enyu-Chieerete profile the velocity of the second zone was 2.74 kmps.

This is in good agreement with 2.95 kmps, the average of the velocities of the second zone, shown in figure 148, in the second survey, or in reasonable agreement with Raitt's calculated value of 3.10 kmps. The velocity of 3.35 kmps for the second zone near Enyu on the Enyu-Namu profile in the first survey agrees with the velocity of 3.35 kmps for the same zone along profile A–B and compares favorably with the velocity of 3.56 kmps along profile *A–C* in the second survey.

The velocities determined inside the lagoon in the two surveys were:

| Zone | Velocities in kmps— | | Nature of zone |
|---|---|---|---|
| | 1st survey | 2d survey | |
| First | 2.1 | 2.45 | Calcareous. |
| Second | 2.74 | 2.95 | Assumed calcareous. |
| | 3.35 | 3.35 | |
| Third | | 3.56 | Assumed volcanic material. |
| | | 4.15 | |
| | | 4.74 | |
| Fourth | 5.2 | 5.54 | Assumed basement. |

Velocities of 3.56 kmps to 4.74 kmps were not detected in the first survey. The value 5.2 kmps for the deepest horizon of the first paper is probably the average of the velocities of the third and fourth zones as defined by Raitt.

An areal plot (figure 160) of Raitt's average velocity of the third zone within the lagoon shows an increase in velocity from the southeast corner of the lagoon toward the north and west. This indicates a change in elastic properties of the material composing this third zone from southeast to northwest. The magnetic map (Alldredge, L. R., and Dichtel, W. J., 1949, Interpretation of Bikini magnetic data: Am. Geophys. Union Trans., v. 30, p. 831–835) shows sharply defined areas of various degrees of intensity. The intensities

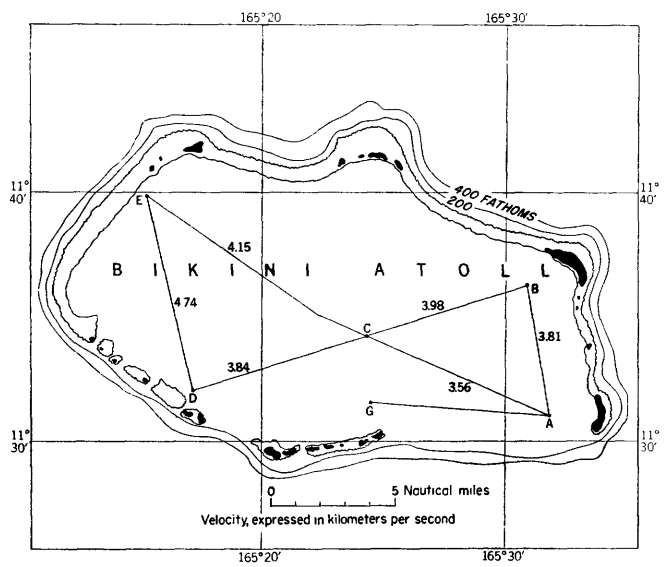


FIGURE 160.—Variation of true velocity in third zone showing gradual increase from southeast to northwest. Average velocities calculated from profiles of second survey.

increase to the north and west in a similar fashion to the velocities. This is probably due to a change in magnetic properties of the rock, since the relief of the top of the third zone does not match the sharp changes

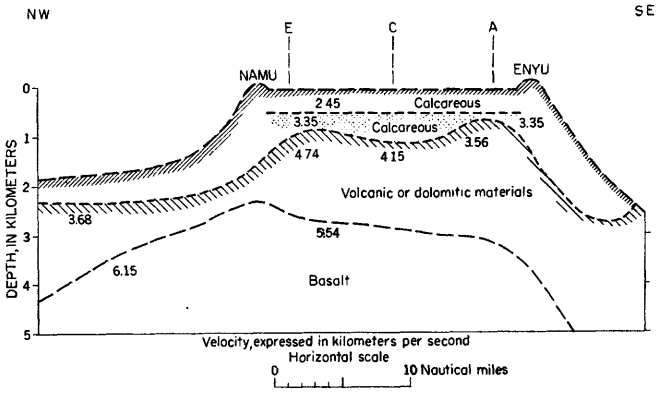


FIGURE 161.—Cross section of Bikini Atoll showing zones of different seismic velocity and the change in velocity in the third zone from the vicinity of Enyu on the southeast to the vicinity of Namu on the northwest, based on data of first and second surveys.

indicated by the magnetic map. These changes indicate the possibility of the third zone being composed of volcanic material. The possibility of this zone being composed of dolomitized limestone cannot be ruled out, however, since the velocity change can be due to different degrees of dolomitization and the magnetic changes may be due to conditions in the basement. Figure 161 is a cross section of Bikini Atoll which incorporates all the above features.

# INDEX

# Magnetic Structure of Bikini Atoll

*By* L. R. ALLDREDGE, FRED KELLER, Jr., *and* W. J. DICHTEL

## Bikini and Nearby Atolls, Marshall Islands

GEOLOGICAL SURVEY PROFESSIONAL PAPER 260–L


UNITED STATES GOVERNMENT PRINTING OFFICE, WASHINGTON : 1954

# CONTENTS



# ILLUSTRATIONS

# BIKINI AND NEARBY ATOLLS, MARSHALL ISLANDS

## MAGNETIC STRUCTURE OF BIKINI ATOLL

By L. R. Alldredge, Fred Keller, Jr., and W. J. Dichtel

ABSTRACT

The magnetic total field intensity was surveyed, at an altitude of 1,500 feet above Bikini and the adjacent guyot. The resulting contour map shows a broad negative anomaly of 750 gammas over Bikini Atoll, with several superimposed more localized anomalies. Study based on a magnetic model indicates that basement material rises to within 5,000 feet of sea level approximately 1 mile to the northeast of Bikini island. The model assumes uniform susceptibility and zero permanent magnetization and conforms to known seismic profiles of the basement.

### INTRODUCTION

During June, July, and August of 1947, the Office of Naval Research, the U. S. Geological Survey, the Naval Ordnance Laboratory, and the U. S. Naval Air Modification Unit at Johnsville, Pa., cooperated on a large-scale magnetic survey (Alldredge and Keller, 1949) in which 31,000 miles were flown and 8,300 miles of magnetic traverse were completed. Nearly 1,700 miles were flown in obtaining a detailed magnetic map of Bikini Atoll and the adjacent guyot area in the Marshall Islands using Kwajalein Atoll as the operating base.

It is of interest to review earlier magnetic work of a similar nature done on the Atoll of Funafuti (Creak, 1904).

### INSTRUMENTATION

The survey aircraft was an amphibious PBY–5A equipped with an orienting total-field magnetometer developed by the Naval Ordnance Laboratory and the Bell Telephone Laboratories during the War (Felch and others, 1947). The magnetometer sensitive unit was housed in a fixed tail cone extending about 4 feet aft of the trailing edge of the rudder.

The magnetometer sensitive unit utilizes permalloy cores which are driven into saturation with a driving current of 1,000 cycles per second. The second harmonic voltage induced in the coil is proportional to the magnetic field along the core axis. The sensitive unit consists of three such elements mounted mutually perpendicularly in a gimbal mechanism. Two of these elements are used as orientators to keep the third element, the detector, in line with the magnetic-field vector. The magnetometer measures changes in the total magnetic field about an undertermined zero line. The zero line is steady with time except for a slow drift which depends upon the temperature and the gradual decay of a battery which partially nulls the magnetic field to be measured. The intensity observed is automatically charted by a recording milliammeter.

The magnetometer is capable of measuring changes as small as 1 gamma in the mangetic field while airborne. During this survey, however, the anomalies encountered were so large that a reduced sensitivity was required. The sensitivity used was such that a change of 500 gammas would produce a full-scale deflection of the recording meter. In precise surveys such as the one over Bikini Atoll a base line is crossed every 15 minutes or less to permit correction for drift errors.

### FIELD DATA

A detailed survey was made over Bikini and the guyot that adjoins it on the northwest. Eleven north-trending and eight east-trending survey lines, spaced 2 miles apart were flown across Bikini Atoll. Most of the lines were continued approximately 10 miles seaward beyond the coral reefs. Figure 162 shows the resulting detailed contour map. A few minor positive peaks are seen to occur within a broad negative anomaly of approximately 750 gammas. This type of anomaly would be produced by a broad guyot with rather irregular surface features in the basement.

Figure 163 shows a total-field magnetic-contour map of Bikini Atoll and its adjacent guyot. The ground control for the survey over the guyot was not accurate enough to maintain the 50-gamma contour interval of figure 162. The entire area was flown using dead reckoning with check points taken on Bikini Atoll before and after the survey. These check points were approximately 8 hours apart.

Note.—L. R. Alldredge, U. S. Naval Ordnance Laboratory, White Oak, Md.; Fred Keller, Jr., U. S. Geological Survey, now at U. S. Naval Air Development Center, Johnsville, Pa.; and W. J. Dichtel, U. S. Naval Ordnance Laboratory, White Oak, Md.

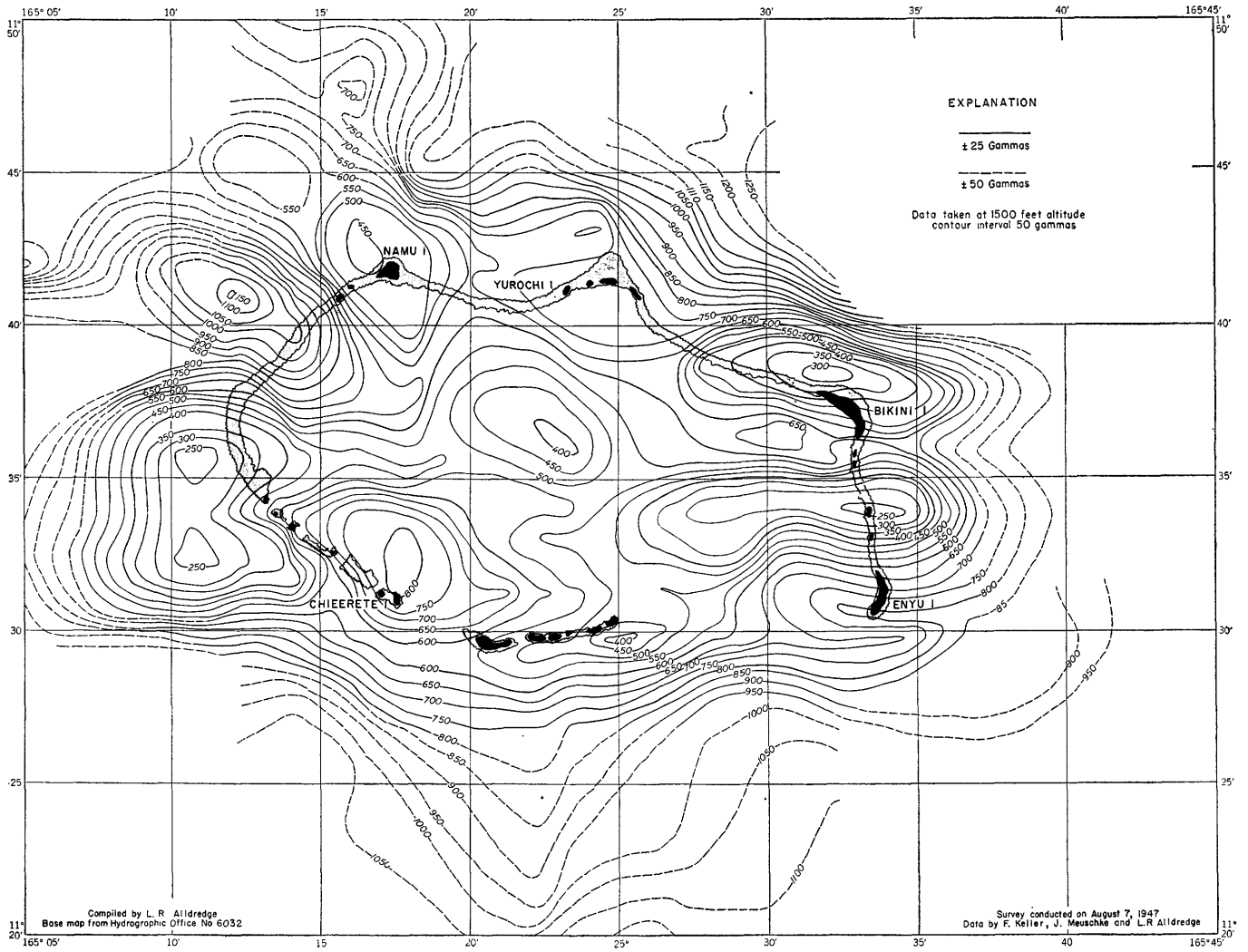


FIGURE 162.—Total intensity anomaly contour map of Bikini Atoll. Data taken at 1,500 feet altitude.

## METHOD OF INTERPRETING RESULTS

[Based closely on the description given by Alldredge and Dichtel (1949)]

As is well known, there are an infinite number of different configurations of magnetic materials which could account for the observed data given in figure 162. In spite of this ambiguity some useful ideas, based upon a few elementary assumptions, may arise from determining a possible magnetic substructure. Model techniques can profitably be employed in such a study.

It is realized that randomly oriented permanent magnetization and variations in susceptibility account for large anomalies in many places throughout the earth, and there is no assurance that these factors are not important in the case of Pacific atolls. A model which admits these variables and which matches the observed magnetic data could be built; in fact, any number of such models could be built. Complicated models of this type would yield substructures which would be very difficult to interpret. To simplify the problem it was decided to assume zero permanent magnetization and uniform susceptibility. Such a simple model must have topographic relief to account for the observed data. The property of these simple assumptions can be judged only after the predictions of such a model are checked by other geophysical methods.

It was assumed that a smooth basement surface where Bikini Atoll now stands would result in a uniform magnetic field of 345 milligauss with a dip angle of $+13.5°$ and a declination of 5° E. This is the present average field. This uniform field was applied to the model using a 20-foot three-dimensional coil system with the model placed in the center. Bikini Atoll is very near the geomagnetic equator having a geomagnetic latitude of approximately 6.5° N. The north-trending total-field gradient is less than 3 gamma per mile and was therefore neglected.

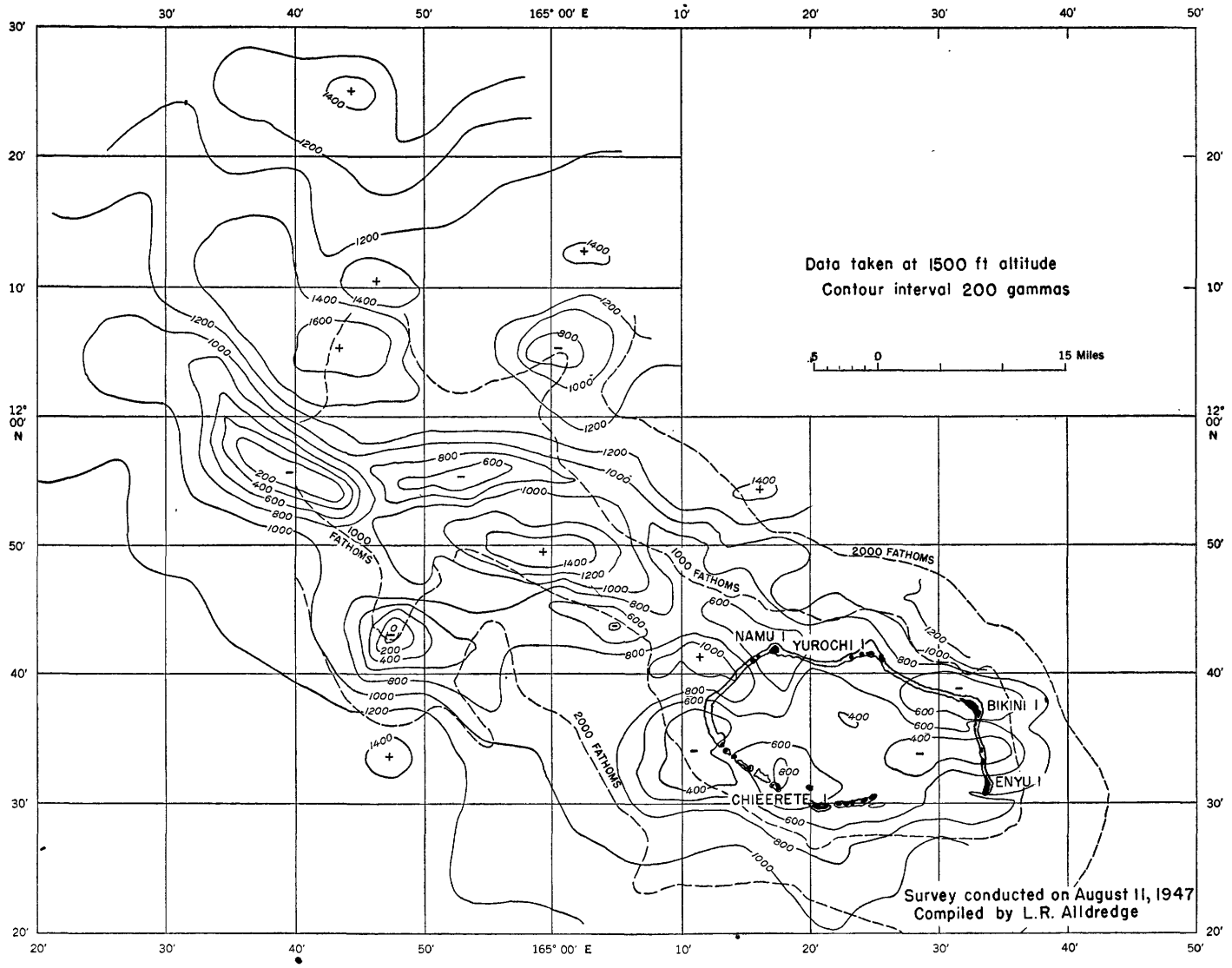


FIGURE 163.—Total intensity anomaly contour map of Bikini Atoll and its adjacent guyot. Data taken at 1,500 feet altitude.

A mixture of foundry clay, ground magnetite, linseed oil, and glycerine was used for the model material. For the base of the model very little glycerine was used. As the oil dried out, an unyielding base was formed to support the upper part of the model. Glycerine was mixed with the clay used on the top part of the model so it would remain soft for later reshaping. Before construction of the model, the clay mixture was thoroughly demagnetized by applying an alternating field of diminishing amplitude in zero background field.

The magnetic potential V $(x, y, z)$ at points outside the magnetic material is given by

$$V(x, y, z)=\int\left(\vec{I}(x', y', z')\cdot\frac{\vec{r}}{r^3}\right)dv \qquad (1)$$

where $\vec{I}$ is the magnetic moment per unit volume, $\vec{r}$ is the vector between $x, y, z$ and $x', y', z'$ and the integral extends over the entire volume occupied by the magnetic material. Since zero permanent magnetization has been assumed, the magnetic moment per unit volume will all result from induced magnetization when a uniform magnetizing field $Ho$ is applied to the model. We may write $\vec{I}=k\vec{H}$, where $k$ is the magnetic susceptibility and $\vec{H}$ is the actual field applied to each volume element. Since $k$ has been assumed uniform throughout the model, (1) may be written

$$V=k\int\left(\vec{H}\cdot\frac{\vec{r}}{r^3}\right)dv \qquad (2)$$

It is now evident that the value of $k$ can change the magnitude of the potential and the resulting potential gradient but can have no effect on the shape of the resulting field—that is, the location of maximum and

minimum. The shape of the resulting field will depend on $\vec{H}$ and the boundaries of the magnetic material. These last two factors are not independent as $\vec{H}$ depends not only upon the applied field $\vec{H}o$ but also upon the demagnetizing factor which depends on the geometry of the magnetic material.

With all the simplifying assumptions we have made there may still be an infinite number of different configurations of magnetic material which can account for the known shape of the magnetic-countour map shown in figure 162. Fortunately, in the problem under consideration something is known about the boundary conditions. During Operations Crossroads at Bikini Atoll several seismic profiles were obtained across Bikini Lagoon (Dobrin, Perkins and Snavely, 1949) which indicated three distinct layers. The top of the deepest layer extended downward from 7,000 to 13,000 feet below sea level, and it has been assumed that this is the basalt layer. To some extent this boundary information limits the ambiguity inherent in (2) and permits a better determination of the substructure within the original simplifying assumptions of the zero permanent magnetization and uniform susceptibility.

The choice of $k$ is not critical, as has been shown. The general shape of the substructure can be determined using any value of $k$, which can then be adjusted to obtain the correct magnitude.

To determine a likely value of $k$ it was noted that the susceptibilities of various magnetic minerals and rocks are given (Chapman and Bartels, 1940) as basalt (Northumberland), $k=0.0002$ to 0.01; mean of 45 dolorites and basalts from the British Isles, $k=0.0026$; lava from Mount Etna, $k=0.008$.

In addition a simple calculation was made assuming that the general features of figure 162 were caused by a uniformly magnetized sphere. The data on figure 162 do not go to seaward far enough to establish definitely the location of the fringe peaks. It is estimated, however, that they occur approximately 30 miles apart for a north-trending profile line over the center of the lagoon. Using this value for the separation in the peaks, assuming that the basement material rises to within 7,000 ft. of sea level on the basis of the seismic work, substituting 34,000 gamma as the applied field, and putting in 700 gamma as the magnitude of the central negative peak (see fig. 162), a value of 0.008 for $k$ was obtained. This value was used throughout the model work. No readjustment of $k$ was required after the general shape of the substructure was determined. This value of $k$ was obtained by adding the proper amount of magnetite to the clay.

The model technique described above avoids the erroneous assumption of uniform magnetization which is common to many methods where magnetic fields are synthesized mathematically by adding uniformly magnetized sections of material.

The resulting magnetic anomaly caused by the model was recorded using a miniature magnetometer carried at the proper height above the model by an automatic traverse system. This procedure yields a magnetic-contour map which can be compared with the original magnetic data.

The miniature magnetometer used in the model work was capable of measuring only a single magnetic component, whereas the original data were taken using an orienting total-field detector. The anomalous field of Bikini Atoll has a small value when compared to the earth's field. At Bikini Atoll only the component of the anomaly in the direction of the earth's field produces an appreciable effect on a total-field magnetometer. For this reason a single component magnetometer may be used in the model work as long as its detection axis is maintained in the direction of the earth's field, as was done in this work.

The miniature magnetometer has a sensitive core element approximately five-eighths of an inch long. For the scale used, this represents approximately 2,500 feet. The field indicated by the magnetometer is roughly the average field in this distance, which tends to decrease both negative and positive peak values. This averaging process is not serious as can be judged from figure 162. The miniature magnetometer system is accurate to only $\pm 50$ gamma.

Sinclair (1948) has given a rather complete discussion of the relationship required between a full-scale system and a model. In this model work all linear dimensions were scaled, and susceptibility of the model was adjusted to be equal to that of the full-scale object. Under these conditions equal fields applied to the object and model produce the same magnetic states, and the resulting model field, when measured at the scaled distance, is equal to that of the object.

The size of the model was limited by the dimensions of the large coil system used to apply the field found at Bikini Atoll, and by the limitations of the automatic traverse system used to carry the magnetometer over the model. Two nautical miles on the atoll were made equivalent to 3 inches on the model. The model-scale factor was therefore approximately 1/48,640.

The general ocean depth in the area surrounding Bikini Atoll is 2,500 fathoms. The plywood board upon which the model was constructed represented this depth below sea level. Copper nails were driven into the plywood board so that their heads indicated the proper depth below sea level of the upper surface of the

basement material as indicated by the siesmic data. Magnetic clay was then placed on the board and molded flush with the heads of the copper nails. In regions void of seismic data, the clay was formed roughly into peaks where figure 162 indicates magnetic lows and into depressions where magnetic highs are indicated.

A survey with the magnetometer showed where the model data differed from the full-scale data. Suggested changes were made, always keeping the seismic profiles invariant in an attempt to obtain a model which would reproduce the full-scale data.

It was soon found that in the first model the seismic and magnetic data were incompatible if the uniform susceptibility assumption was to be retained. There was no way to account for the general decrease in magnetic field in moving from Yurochi island toward Enyu island without violating the seismic data in this region. Not desiring to abandon the uniform susceptibility assumption, since to do so would make any contour predictions about the basement in regions not covered by the seismic data impossible, another solution was sought.

The above incompatibility of data was removed by adding an equivalent 7,000-foot thick slab of the magnetic clay to the underside of the model. By cutting a rather steep side on the eastern end of the south side of the mound and gradually sloping the clay on all the other edges, the magnetic data were matched without violating the seismic profile lines.

This new model is equivalent to assuming that the general basement underlying the ocean floor begins a little more than a mile beneath the present ocean floor.

## INTERPRETATION OF RESULTS

[Based closely on the description given by Alldredge and Dichtel (1949)]

Figure 164 shows the magnetic contours resulting from the final model. A basement relief (topographic) map of the final model is shown in figure 165. In most places the magnetic-contour lines of the model agree

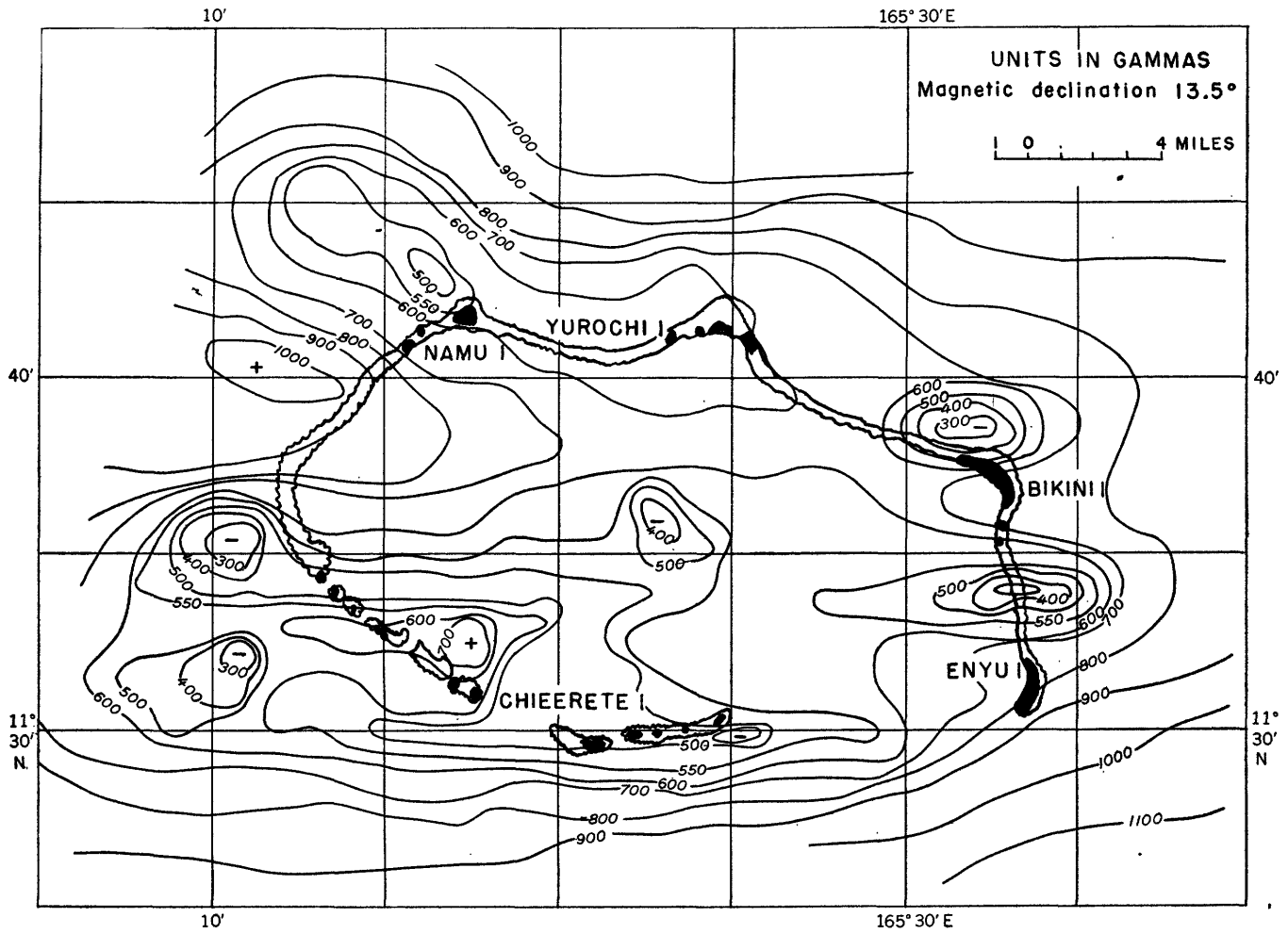


FIGURE 164.—Total magnetic intensity contour map of model of Bikini Atoll. Data taken at 1,500 feet altitude.

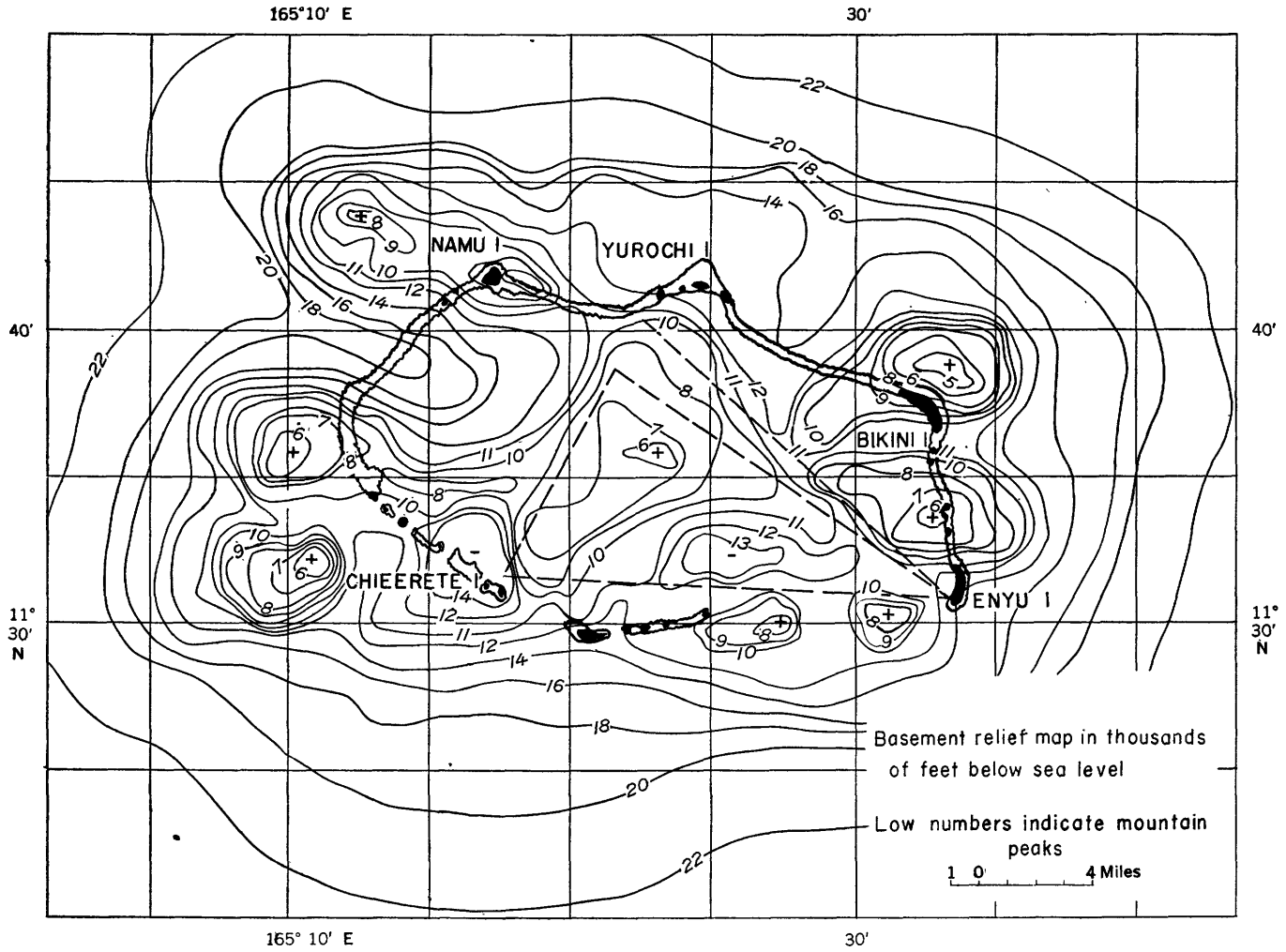


FIGURE 165.—Basement relief map of model of Bikini Atoll, contours in thousands of feet below sea level. Low numbers indicate mountain peaks.

quite well with the original magnetic anomaly map (fig. 162). The fact that this model shows a string of topographic highs around the atoll fringes with major peaks near each island adds strength to the simple assumption of uniform susceptibility. The only place where this is not true is near Chieerete island where a topographic low is shown.

The model predicts that the basement rises to its highest peak approximately 1 mile to the northeast of Bikini island. At this point the basement is only 5,000 feet below sea level. The water over this peak is 3,000 feet deep leaving only 2,000 feet of nonmagnetic material. The model predicts 8,000 feet to the basement at the northeast edge of Bikini island.

On high peaks, such as occur northeast of Bikini island and to the north of Enyu island, changes in model height of one-fourth of an inch (1,000 feet) could easily be detected magnetically. In the center of the large flat area between Yurochi and Enyu islands changes in height of three-eighths of an inch (1,500 feet) were barely detectable magnetically. As would be expected, the depth resolution was even less precise in craters such as the one to the northeast of Chieerete island.

The general location of the seismic profile lines are indicated by dashed lines in figure 165. The seismic control did not, however, extend along the entire length of the dashed lines. The magnetic fit as shown was obtained by following the seismic data carefully except in the region of Chieerete island. Over a small area in this region model depths were 2,000 feet deeper than those shown by the seismic data. This deviation from the seismic data permitted a better magnetic fit. The authors (Dobrin, Perkins and Snavely, 1949) of the original seismic work point out that their conclusions might be in error by as much as 1,500 feet on the basement. The large crater northeast of Chieerete island was necessary to match the magnetic data. The depth of the crater was found to make little difference so long as it was made greater than 14,000 feet. The exceedingly steep sides were necessary to match the magnetic data to the north of the crater.

Since the clay was tapered off to zero thickness on all sides of the model, neither the magnetic nor the topographic maps would be expected to be accurate near the northwest corner of the atoll where a guyot is known to connect with the atoll.

The magnetic-contour map of the guyot adjacent to Bikini Atoll showed a greater magnetic low than Bikini atoll itself. If these same model techniques were extended into this region it is quite sure that the measurement of the basement would rise to the full height of the guyot (4,000 ft. below sea level).

## LITERATURE CITED

Alldredge, L. R. and Dichtel, W. J., 1949, Interpretation of Bikini magnetic data: Am. Geophys. Union Trans., v. 30, p. 831–835.

Alldredge, L. R. and Keller, Fred, Jr., 1949, Preliminary report on magnetic anomalies between Adak, Alaska, and Kwajalein, Marshall Islands: Am. Geophys. Union Trans., v. 30, p. 494–500.

Chapman, S., and Bartels, V., 1940, Geomagnetism: Oxford, Clarendon Press.

Creak, E. W., 1904, The Atoll of Funafuti, Report of the Coral Reef Committee, Royal Soc. London, p. 33–39, 64.

Dobrin, M. B., Perkins, B., Jr., and Snavely, B. L., 1949, Subsurface constitution of Bikini Atoll as indicated by a seismic-refraction survey: Geol. Soc. America Bull., v. 60, p. 807–828.

Felch, E. P. and others, 1947, Air-borne magnetometers: Elec. Eng., v. 66, pp. 680–685.

Sinclair, G., 1948, Theory of models of electromagnetic systems: Inst. Radio Eng. Proc., v. 36, p. 1364–1370.